

**University of Southampton**  
**Faculty of Medicine, Health and Biological Sciences**  
**School of Medicine**

**Optimization of Radioimmunotherapy  
for non-Hodgkin's Lymphoma**

by

**Yong Du**

Thesis for the degree of Doctor of Philosophy

August 2005

# UNIVERSITY OF SOUTHAMPTON

## ABSTRACT

FACULTY OF MEDICINE, HEALTH AND BIOLOGICAL SCIENCES

### Doctor of Philosophy

## **Optimization of Radioimmunotherapy for non-Hodgkin's Lymphoma**

By Yong Du

Non-Hodgkin's lymphoma (NHL) is the fifth and sixth most common malignancy in females and males, respectively. Whilst many patients with indolent NHL can achieve clinical remission to first-line chemotherapy and/or radiotherapy, most will relapse. Current treatment options for relapsing patients are limited since most patients become resistant to repeated chemotherapy. Death usually occurs within 10 years of diagnosis. Overall, these disappointing results have not changed significantly in a quarter of a century and clearly advocate the urgent priority to research into potential new therapeutic approaches into this diverse and increasingly prevalent group of human tumours.

Radioimmunotherapy (RIT) has emerged as a new form of effective treatment for this disease. In this form of treatment, radionuclide-labelled monoclonal antibodies (mAbs) are able to deliver selective systemic irradiation by recognising tumour-associated antigens. Most recently, the use of RIT with radiolabelled anti-CD20 antibodies in patients with B-cell lymphoma has resulted in extremely high rates of durable complete remissions. However, the optimal approach and mechanisms of action of successful RIT remain poorly understood.

The work described in this thesis has focused on clarifying some of the important determinants and mechanisms of effective RIT using syngeneic murine B-cell lymphoma models. The *in vivo* irradiation delivery capabilities of a panel of mAbs against mouse B cell antigens were determined by bisdistribution studies using Medical Internal Radiation Dosimetry formula and the intracellular signalling induction capabilities of these mAbs were measured by Western Blot. By comparing the radiation dosimetry with the RIT therapeutic effects of these mAbs, it has been revealed that successful RIT requires the combination of targeted irradiation and mAb mediated intracellular signalling transduction. Furthermore, by visualizing the different patterns of intratumoural distribution of intravenously administered mAbs using immunohistochemistry technique, the RIT performances of radiolabelled mAbs were found linked to microscopic dosimetry. This discovery has further confirmed that the radiation dosimetry plays critical role in the success of RIT and revealed that the conventional dosimetry methods which assume the homogeneous intratumoural distribution of radiolabelled mAb could substantially underestimate the radiation dose delivered to the tumour by RIT.

# **Optimization of Radioimmunotherapy for non-Hodgkin's Lymphoma**

## **Table of Contents**

<b>Table of Contents</b> .....	i
<b>List of Table</b> .....	vi
<b>List of Figures</b> .....	vii
<b>Author's Declaration</b> .....	ix
<b>Acknowledgements</b> .....	x
<b>Abbreviations</b> .....	xi
<b>Chapter 1 Introduction</b> .....	1
1.1 Non-Hodgkin's Lymphoma .....	2
1.2 Current Treatment for Non-Hodgkin's Lymphomas .....	6
1.3 The Emerging Role of Monoclonal Antibody Therapy for NHL.....	7
1.4 The Principles of Radioimmunotherapy .....	9
1.4.1 The Choose of Target Antigen .....	10
1.4.2 The Evolution of RIT .....	11
1.4.3 The Selection of Radionuclide for RIT .....	16
1.5. Clinical Progress of Radioimmunotherapy for NHL .....	20
1.5.1 Non-Myeloablative RIT .....	20
1.5.2 Myeloablative RIT.....	27
1.5.3 Non-Haemetological Toxicities of RIT.....	28

<b>1.6. Ongoing Issues in Radioimmunotherapy .....</b>	29
1.6.1 Dosimetry and Radiation Dose Response in RIT .....	30
1.6.2 Pre-dosing in RIT .....	33
1.6.3 Radiation Dose-Rate-Effect in RIT of NHL .....	38
1.6.4 The mAb Mediated Cytotoxicity in RIT .....	40
<b>1.7. The Contribution of Experimental Radioimmunotherapy.....</b>	42
1.7.1 The Use of Animal Models in Radioimmunotherapy .....	42
1.7.2 Approaches to Improve the Therapeutic Index of RIT .....	45
1.7.3 Attempts to Understand the Determinants of Successful RIT of NHL .....	46
<b>Optimization of RIT for NHL.....</b>	50
<b>Aims of Current Project.....</b>	50
<b>Chapter 2 Materials and Methods.....</b>	51
2.1 Animals and Cell Lines .....	51
2.2 Antibodies and Radioiodination .....	52
2.3 Immunoreactivity of Radiolabelled mAb .....	55
2.4 Measure of Surface Antigen by Immunofluorescence .....	56
2.5 In Vitro Cytotoxicity Assessment of mAb: CDC and ADCC Assays.....	57
2.6 Biodistribution Studies and Organ Dosimetry Estimation .....	58
2.7 RIT Experiments Using Murine Lymphoma Models.....	59
2.8 Immunohistochemistry Localisation of Intravenously Administered mAb within the RIT Target Organ – the Spleen .....	60

2.9 Hematological Toxicity of RIT .....	61
2.10 Phosphotyrosine Detection by Western Blot.....	62
2.11 Immunoprecipitation Analysis for Tyrosine Phosphorylation of Syk.....	63
<b>Chapter 3 Developing Radioimmunotherapy Animal Models .....</b>	<b>64</b>
<b>3.1 Introduction .....</b>	<b>64</b>
<b>3.2 Materilas and Methods .....</b>	<b>65</b>
<b>3.3 Results.....</b>	<b>67</b>
3.3.1 The Establishment of Optimal Radio-iodine Labelling Technique.....	67
3.3.2 Biodistribution and Organ Dosimetry of Radiolabelled mAb.....	75
3.3.3 Biodistribution and Organ Dosimetry of Radiolabelled mAb in Advanced Stage Tumour .....	78
3.3.4 Impact of Pre-dose on the Biodistribution and Organ Dosimetry of Radiolabelled mAb .....	83
<b>3.4 Discussion .....</b>	<b>88</b>
<b>3.5 Conclusions .....</b>	<b>92</b>
<b>Chapter 4 Determinants of Successful Clearance of Tumour in Radioimmunotherapy of B-cell Lymphoma .....</b>	<b>93</b>
<b>4.1 Introduction .....</b>	<b>93</b>
<b>4.2 Materilas and Methods .....</b>	<b>94</b>
4.2.1 Animal Models .....	94
4.2.2 Antibodies and Radioiodination .....	95
4.2.3 Radioimmunotherapy .....	95
4.2.4 Haematological Toxicity of RIT .....	96

4.2.5 Phosphotyrosine Detection by Western Blot.....	96
4.2.6 Immunoprecipitation Analysis for Tyrosine Phosphorylation of Syk.....	97
<b>4.3 Results.....</b>	<b>97</b>
4.3.1 Radiation Dose Delivered by RIT Does Not Correlate with Survival .....	97
4.3.2 RIT of BCL <sub>1</sub> Lymphoma with Serial Doses of <sup>131</sup> I Labelled Anti-MHCII....	100
4.3.3 A Radiation Dose Response Exists for RIT of Lymphoma in the Presence of anti-Id mAb .....	102
4.3.4 The Impact of Pre-dose on RIT with <sup>131</sup> I labelled anti-MHCII mAb .....	104
4.3.5 Anti-CD19 Improves Survival in Combination with <sup>131</sup> I-anti-MHCII RIT ...	106
4.3.6 Anti- Id and anti-CD19 mAb Induce Direct Cell Surface Mediated Signalling ..	108
4.3.7 Haematological Toxicity of Therapeutic RIT Using <sup>131</sup> I-anti-MHCII mAb ..	111
<b>4.4 Discussion .....</b>	<b>113</b>
<b>4.5 Conclusions .....</b>	<b>118</b>
<b>Chapter 5 The Microscopic Intratumoural Distribution of <sup>131</sup>I Labelled mAb is Critical to Successful RIT of B-cell Lymphoma.....</b>	<b>119</b>
<b>5.1 Introduction .....</b>	<b>119</b>
<b>5.2 Materilas and Methods .....</b>	<b>122</b>
<b>5.3 Results.....</b>	<b>123</b>
5.3.1 Binding of Radioiodinated anti-CD45 mAb to the Surface of BCL <sub>1</sub> Cells....	123
5.3.2 Complement and Antibody Dependent Cellular Cytotoxicity of BCL <sub>1</sub> Cells	126
5.3.3 Anti-CD45 mAb Demonstrated High Radiation Delivery Capability in Conventional Biodistribution Assays.....	130
5.3.4 Anti-CD45 RIT Fails to Produce Long Term Survival .....	134

5.3.5 Intratumoural Localisation of mAb in RIT of BCL <sub>1</sub> Lymphoma.....	136
5.3.6 Long Term Survival is Achievable with Increased Doses of <sup>131</sup> I Labelled anti-CD45 mAb in RIT .....	141
<b>5.4 Discussion .....</b>	<b>145</b>
<b>5.5 Conclusions .....</b>	<b>148</b>
<b>Chapter 6 Summary and Conclusions.....</b>	<b>149</b>
<b>Appendix.....</b>	<b>153</b>
<b>References .....</b>	<b>158</b>

## List of Tables

Table 1.1 The Word Health Organization classification scheme for non-Hodgkin's lymphoma	4
Table 1.2 The Ann Arbor Staging System for NHL	5
Table 1.3 The characteristics of an ideal target antigen	11
Table 1.4 Physical Characteristics of Radionuclides Used in RIT	17
Table 1.5 Bexxar <sup>TM</sup> ( <sup>131</sup> I-Tositumomab) Therapeutic Regimen	21
Table 1.6 Characteristics of <sup>131</sup> I tositumomab (Bexxar <sup>TM</sup> ) and <sup>90</sup> Y ibritumomab tiuxetan (Zevalin <sup>TM</sup> )	26
Table 1.7 Pre-dose Schedules for Zevalin <sup>TM</sup> and Bexxar <sup>TM</sup> RIT Regimens	36
Table 2.1 Anti-mouse monoclonal antibodies used in this work	54
Table 3.1 Internal radiation dosimetry of RIT treated mice	77
Table 3.2 Internal radiation dosimetry of advanced tumour in comparison with early stage tumour	82
Table 3.3 Impact of pre-dose on the internal radiation dosimetry in comparison with those without pre-dose	86
Table 5.1 Internal radiation dosimetry of RIT treated mice with early stage tumour	133

## List of Figures

Figure 3.1 Labelling efficiency of Chloramine-T, Iodogen-Beads and NBS iodination methods	68
Figure 3.2 HPLC analysis of $^{131}\text{I}$ labelled Rituximab	70
Figure 3.3 Immunoreactivity of serial doses of $^{131}\text{I}$ labelled Rituximab as measured by human lymphoma cell line Daudi cell binding activity	71
Figure 3.4 Immunoreactivity assay of rat-anti-mouse mAb on BCL <sub>1</sub> cells	72
Figure 3.5 Binding curves of radioiodinated rat-anti-mouse mAbs on BCL <sub>1</sub> cells	74
Figure 3.6 Biodistribution of $^{125}\text{I}$ labelled mAb in BCL <sub>1</sub> tumour inoculated mice	76
Figure 3.7 The development of BCL <sub>1</sub> tumour in the spleen of BALB/c mice	80
Figure 3.8 Comparison biodistribution of $^{125}\text{I}$ labelled mAb in early stage and advanced stage BCL <sub>1</sub> tumour models	81
Figure 3.9 Influence of pre-dose on biodistribution of radiolabelled anti-MHCII mAb in early stage and advanced stage BCL <sub>1</sub> tumour models	84
Figure 3.10 Influence of pre-dose on biodistribution of radiolabelled anti-Id mAb in advanced stage BCL <sub>1</sub> tumour models	87
Figure 4.1 RIT of BCL <sub>1</sub> lymphoma showed that radiation dose delivered by RIT does not correlate with animal survival	99
Figure 4.2 RIT of BLC <sub>1</sub> lymphoma with serial doses of $^{131}\text{I}$ -anti-MHCII	101
Figure 4.3 Dose response of RIT in BCL <sub>1</sub> and A31 B-cell lymphoma models	103
Figure 4.4 The impact of pre-dose on RIT with $^{131}\text{I}$ -anti-MHCII mAb in BCL <sub>1</sub> lymphoma model	105
Figure 4.5 Anti-CD19 improved survival in combination with $^{131}\text{I}$ labelled anti-MHCII mAb in the BCL <sub>1</sub> lymphoma model	107
Figure 4.6 Measurement of intracellular signalling	110
Figure 4.7 Haematological toxicity of RIT with $^{131}\text{I}$ labelled anti-MHCII mAb	112

Figure 5.1 Immunoreactivity assay of rat-anti-mouse mAb on BCL <sub>1</sub> cells	124
Figure 5.2 Binding curve of rat-anti-mouse mAb on BCL <sub>1</sub> cells	125
Figure 5.3 Complement dependent cytotoxicity of BCL <sub>1</sub> cells	127
Figure 5.4 Antibody dependent cell-mediated cytotoxicity of BCL <sub>1</sub> cells	129
Figure 5.5 Biodistribution of radiolabelled mAb in BCL <sub>1</sub> tumour models	131
Figure 5.6 RIT comparing the therapeutic effect of <sup>131</sup> I labelled anti-CD45 and anti-MHCII mAb in BCL <sub>1</sub> lymphoma model	135
Figure 5.7 Immunohistochemistry study revealed the micro-distribution of intravenously administered mAb in BCL <sub>1</sub> lymphoma	138
Figure 5.8 Immunohistochemistry of advanced stage BCL <sub>1</sub> lymphoma	140
Figure 5.9 Long term survival is achievable with double dose (37.0MBq) <sup>131</sup> I labelled anti-CD45 mAb in RIT in BCL <sub>1</sub> lymphoma	142
Figure 5.10 Radiation dosimetry plays critical role in the success of RIT in BCL <sub>1</sub> lymphoma	144

## **ACKNOWLEDGEMENTS**

I would like to thank all the people in the Director's Group at the Tenovus Research Laboratory for their technical help and friendly accompany particularly, Jamie, Mike and Andrey who had worked with me shoulder to shoulder within the Targeted Radiotherapy Group and made my days there so enjoyable and memorable. I would also like to thank Richard for his excellent help with the administration of radiolabelled monoclonal antibodies and his interesting discussion about the "past" Barclays' premier league.

Special thanks go to Prof. Tim Illidge, my supervisor, for his unique role in providing me with the opportunity to join his group to pursue my interest in radioimmunotherapy and for his constructive instructing throughout this project. His support has been invaluable, and unreserved on a daily basis, since the very beginning.

I would also like to thank Prof. Peter Johnson, my supervisor, for his insightful instructions, for his very kind encouraging and generous help throughout these years.

I am also indebted to the administrative members of the Cancer Sciences Division both past and present, especially Mrs. Sue Oglesby, Mrs. Rahila Arain and Mr. Paul Reeve.

Finally I thank my wife, Yan, my parents and my daughter for their trust and never failing support.

\* Financial support was provided by Cancer Research UK.

## Abbreviations

Ab	Antibody
Ag	antigen
ADCC	antibody dependent cellular cytotoxicity
ASCT	autologous stem cell transplantation
BCR	B-cell receptor
CD	cluster of differentiation
CDC	complement dependent cytotoxicity
CHOP	cyclophosphamide, doxorubicin, vincristine, prednisone
CR	complete remission
DAB	diaminobenzidine tetrahydrochloride
EBRT	external beam radiation therapy
FACS	fluorescence activated cell sorter
FDA	Food and Drug Administration (United States of America)
G <sub>1</sub>	first phase of cell cycle
G <sub>2</sub> /M	second phase of cell cycle/mitosis
GMA	glycol methacrylate
Gy	Gray
HACA	human anti-chimeric antibody
HAMA	human anti-mouse antibody
HDR	high dose rate
HLA	human leukocyte antigen
HPLC	high performance liquid chromatography

Id	idiotype
IgG	immunoglobulin G
IHC	immunohistochemistry
ITLC	instant thin layer chromatography
kDa	kiloDaltons
LDR	low dose rate
MBq	million Becquerel
MHC	major histocompatibility complex
MIRD	medical internal radiation dose
mAb	monoclonal antibody
NHL	non-Hodgkin's lymphoma
PBS	phosphate buffered saline
PI	propipidium iodide
PR	partial remission
PTP	protein tyrosine phosphatase
RID	radioimmunodetection
RIT	radioimmunotherapy
S – phase	chromosome synthesis phase of cell cycle
scFv	single chain Fv
SD	standard deviation
SPECT	single photon emission computed tomography
TBS	Tris buffered saline

## Chapter 1 Introduction

Non-Hodgkin's lymphomas (NHL) form a heterogeneous group of lymphoid malignancies which range from indolent, "low grade" to the extremely aggressive "high grade" malignancies. NHL are usually widespread at the time of diagnosis and this is especially so in the case of the "low grade" or indolent lymphomas. Patients with advanced low grade lymphomas remain incurable and their survival has not been improved since the introduction of chemotherapy in the early 1960's (Horning 2003). Despite the sensitivity of most lymphomas to initial therapy with chemotherapy or radiotherapy, conventional chemotherapy and radiotherapy cure approximately one third of patients who develop aggressive NHL, but the majority of patients with advanced low grade NHL eventually relapse and die of their disease. There is therefore an urgent need to develop alternative treatment strategies (Press 2003).

Following the advent of monoclonal antibody (mAb) technology in the 1970's (Kohler and Milstein 1975) there has been a great expectation that mAb would provide effective targeted therapy for cancer. Over the past three decades, extensive investigations have been undertaken to evaluate the therapeutic potential of a wide spectrum of mAb recognizing different tumour specific or tumour associated antigens. In 1997, the approval of Rituximab, an anti-CD20 mAb by the United States Food and Drug Administration (US FDA) was a milestone in the immunotherapy of NHL. This mAb has subsequently been applied to the therapy of various kinds of B-cell malignancies (Avivi, Robinson et al. 2003). The single agent response rates of Rituximab however remain rather modest, with overall response rates of about 50% and complete response rates usually in single figures (McLaughlin 2001; Coiffier 2005). However the different mechanisms of action and non-overlapping toxicity has enabled mAb to be combined with other therapy modalities such as chemotherapy to greatly improve response rates and Rituximab is now being evaluated as integrated into many treatment pathways for both indolent and aggressive NHL in combination with conventional chemotherapy (Press, Leonard et al. 2001; Thieblemont and Coiffier 2002; Coiffier 2005).

Radioimmunotherapy (RIT) is a conceptually appealing approach for cancer treatment because the conjugation of radioisotope to mAb as part of RIT enables the additional delivery of targeted radiotherapy and thus enhance the specific cytotoxic effects. Over the last few years this approach has demonstrated superior clinical responses to unlabelled mAb (Witzig, Gordon et al. 2002; Davis, Kaminski et al. 2004). A variety of different mAbs, delivery schedules, radioisotopes, and doses of radioactivity have been used in RIT and have resulted in impressive durable partial and complete responses in the treatment of non-Hodgkin's lymphomas (NHL) (Press, Leonard et al. 2001; Witzig, Gordon et al. 2002; Kaminski, Tuck et al. 2005). It now seems highly likely that RIT will play a significant role in the treatment of some NHL following the US FDA approval of <sup>90</sup>Y-Ibritumomab tiuxetan and <sup>131</sup>I-Tositumomab (Connors 2005).

Despite these clinical successes the mechanisms of action involved in the clearance of tumour by RIT remains poorly understood (DeNardo, DeNardo et al. 1998; Illidge, Cragg et al. 1999; Horning 2003).

The work described in this thesis has been aimed at elucidating more of the mechanisms of action of RIT, and increasing our understanding between the interaction of mAb with irradiation in the treatment of NHL. It is hoped that this would provide new insights into the future optimization of clinical RIT application. Starting from some of the aspects of the biology of NHL, the current deficiencies in treatment and indeed the justification for exploring new therapeutic avenues will be outlined. The scientific basis of RIT and then the recent progress as well as the remaining problems in RIT will then be reviewed.

## **1.1 Non-Hodgkin's Lymphoma**

In 1832, Thomas Hodgkin described a Hodgkin's disease (characterized by the growth of Reed-Sternberg cells) which was the first malignant lymphoma recognized (Aisenberg 2000). Hodgkin's disease is just one circumscribed entity of malignant lymphoma and all other types of malignant lymphomas subsequently became non-

Hodgkin's lymphomas (NHL), among which 85% are B-cell lymphomas (Armitage and Weisenburger 1998).

NHL represents a group of lymphoid malignancies that traverse a broad clinical spectrum ranging from very indolent illnesses with a long natural history such as low grade follicular lymphoma to very aggressive "high grade" but curable diseases such as Burkitt's lymphoma (Fisher 2003). NHL is largely a disease of older adults, with peak incidence occurs in individuals greater than 60 years of age (the average diagnosis age is 60). It is the fifth and sixth most common malignancy in females and males, respectively, and the NHL are responsible for 4% of all cancers and 4% of cancer deaths seen in the United States (Wingo, Tong et al. 1995). The incidence of NHL has been continuously on the rise over the past 25 years and the reasons for this are largely unknown. Data collected from the Survival, Epidemiology, and End Results (SEER) project demonstrated a 2-fold rise in incidence (8/100,000 to 16/100,000) between 1973 and 1995, whereas a majority of 85% of NHL are B-lymphocytes origin while T-lymphocytes, Natural Killer cells or unknown cell type origins form the rest 15% (Wingo, Ries et al. 1998; Weir, Thun et al. 2003). Although observational data have demonstrated an association between NHL and several toxic exposures, immune defects, or infectious diseases, however the cause of NHL in most individuals is unknown.

The recognition and description of the very heterogeneous lymphoma types has evolved over many years. In the twentieth century, with the accumulation of pathological and histological knowledge, various schemes of classification were introduced (Fisher, Miller et al. 1998). Currently, the "World Health Organization Classification Scheme for Non-Hodgkin's Lymphoma" (Table 1.1) (Armitage and Weisenburger 1998; Harris, Jaffe et al. 1999) is widely accepted and a scheme is shown in Table 1.1. The Ann Arbor classification is still used for the staging of lymphoma and is summarized in Table 1.2 (Hiddemann, Longo et al. 1996).

**Table 1.1. World Health Organization Classification Scheme for Non-Hodgkin's Lymphoma**

B-cell Neoplasms	Frequency(%)
<i>Precursor B-cell Neoplasms</i>	
Precursor B-lymphoblastic leukemia/lymphoma	2-3%
<i>Mature B-cell Neoplasms</i>	
B-cell chronic lymphocytic leukemia/small lymphocytic lymphoma	7%
B-cell prolymphocytic leukemia	
Lymphoplasmacytic lymphoma	1.5%
Splenic marginal zone B-cell lymphoma ( $\pm$ villous lymphocytes)	<1%
Hairy cell leukemia	
Plasma cell myeloma/plasmacytoma	
Extranodal marginal zone B-cell lymphoma of MALT type	10%
Nodal marginal zone B-cell lymphoma ( $\pm$ monocytoid B cells)	1-3%
Follicular lymphoma	22-24%
Mantle-cell lymphoma	5-7%
Diffuse large B-cell lymphoma	31%
Mediastinal large B-cell lymphoma	
Primary effusion lymphoma	
Burkitt's lymphoma	2%
<b>T-cell and NK-cell Neoplasms</b>	
<i>Precursor T-cell Neoplasms</i>	
Precursor T-lymphoblastic lymphoma/leukemia	2-3%
<i>Mature T-cell Neoplasms</i>	
T-cell prolymphocytic leukemia	
T-cell granular lymphocytic leukemia	
Aggressive NK-cell leukemia	
Adult T-cell lymphoma/leukemia (HTLV-1 +)	
Extranodal NK/T-cell lymphoma, nasal type	
Enteropathy-type T-cell lymphoma	
Hepatosplenic gamma-delta T-cell lymphoma	
Subcutaneous panniculitis-like T-cell lymphoma	
Mycosis fungoides/Sezary syndrome	
Anaplastic large-cell lymphoma, T/null cell, primary cutaneous type	
Anaplastic large-cell lymphoma, T/null cell, primary systemic type	2%
Peripheral T-cell lymphoma, not otherwise characterized	
Angioimmunoblastic T-cell lymphoma	1-2%

HTLV-1, human T-cell leukemia virus 1; MALT, mucosa-associated lymphoid tissue; NK, natural killer

**Table 1.2. The Ann Arbor Staging System for NHL**

<b>Stage</b>	<b>Anatomic Description</b>
Stage I	Involvement of a single lymph node region (I) or a single extralymphatic organ or site (IE)
Stage II	Involvement of 2 or more lymph node regions on the same side of the diaphragm (II) or localized involvement of an extralymphatic organ or site (IIE)
Stage III	Involvement of lymph node regions on both sides of the diaphragm without (III) or with (IIIE) localized involvement of an extralymphatic organ or site
Stage IV	Diffuse involvement of $\geq 1$ extralymphatic organ or site, with or without lymphatic involvement

Use of the letter "A" after the stage description denotes the absence of systemic symptoms (unexplained fevers  $> 38^\circ \text{C}$ , drenching night sweats, weight loss of  $\geq 10\%$  of body weight over previous 6 months). Use of the letter "B" after the stage description denotes the presence of systemic symptoms.

## 1.2 Current Treatment for Non-Hodgkin's Lymphomas

Radiation therapy of NHL has been used for nearly 100 years, and drug therapy has become available with the discovery of cytotoxic agents in last 40 years (Fisher 2000). Generally, NHL are sensitive to treatments with chemotherapy or radiotherapy, and in contrast to most solid tumours NHL are extremely radiosensitive. However, conventional cancer therapies do not cure the majority of patients with NHL. This is particularly true in nearly half of patients with the indolent low-grade and follicular forms of NHL.

Indolent lymphomas which largely comprise follicular lymphomas rarely present with early-stage, localised form of disease (stage I or II). For the 10% that do, radiation therapy has become the established treatment. Approximately 50% of patients treated in this fashion will remain free of disease after 10 years follow-up.

The majority of patients (more than 90%) with low-grade NHL however present with disseminated disease at diagnosis and, have been considered incurable with standard-dose cytotoxic agents and their survival has not been improved since the early 1960's (Fisher and Oken 1995; Horning 2003). For patients with follicular lymphoma the prognosis is traditionally thought to be good with many series reporting 5-year survivals in the order of 60-80%. However this population has a continual decline in survival over the years, so that by 15 years, they fare worse than patients do with diffuse large B-cell lymphoma. A reflection of this substantial long-term mortality and the inadequacies of current therapies is the wide range of treatment policies. Because earlier or more aggressive approaches do not appear to improve long-term survival, approaches have included "watch and wait" for asymptomatic patients and treatments for patients with significant symptoms or evidence of organ dysfunction have included oral single alkylating agents, anthracycline-based combination regimens, fludarabine based regimens and more recently combining chemotherapy with Rituximab (Marcus 2005).

None of these approaches have produced curative results. These patients typically undergo several treatments over a disease course that may last a decade, with numerous remissions and relapses before they ultimately die of the disease (Fisher 2003; Connors 2005).

Since the introduction of anthracycline-containing combination chemotherapy regimens in the 1970s, aggressive NHL has been considered a curable disease (DeVita, Canellos et al. 1975). CHOP chemotherapy (Cyclophosphamide, Doxorubicin, Vincristine, Prednisone) was considered the gold standard treatment for diffuse large B-cell lymphoma (DLBC), largely on the basis of a randomized trial showing no benefit in disease-free or overall survival for more intensified chemotherapy regimens (Fisher, Gaynor et al. 1993). However, CHOP is curative in only fewer than 50% of patients, and numerous clinical trials have been carried out to find a treatment regimen that can increase the cure rate in aggressive NHL (Fisher 2003; Coiffier 2004). Very recently, consistent improvement over CHOP chemotherapy in the treatment of aggressive NHL has been demonstrated with the addition of the chimeric anti-CD20 mAb Rituximab (R-CHOP) and this immunochemotherapy regimen has now become the standard of care for patients with advanced stage DLBC (Coiffier, Lepage et al. 2002; Coiffier 2004), although some groups are investigating the merits of intensified chemotherapy regimens (Pfreundschuh, Trumper et al. 2004; Pfreundschuh, Trumper et al. 2004). High-dose chemotherapy with autologous stem cell transplantation (ASCT) is the standard treatment for younger patients with aggressive NHL who relapse or are refractory to CHOP (Fisher 2003; Coiffier 2004).

### **1.3 The Emerging Role of Monoclonal Antibody Therapy for NHL**

Despite the sensitivity of most lymphomas to initial therapy with chemotherapy or radiotherapy, few patients with low-grade lymphomas, or relapses of any type of lymphoma, can be cured with current conventional approaches. The majority of patients with advanced NHL eventually relapse and die. Although most conventional cytotoxic

agents take advantage of the relatively faster growth fraction of malignant cells, the obvious limitation of conventional cytotoxic agents is their inability to selectively target malignant cells only and therefore, the severe life-threatening normal tissue damage is thought to severely compromise the possibility of achieving tumouricidal doses and ultimately cure (Fisher 2003).

The discovery of mAb technology sparked great expectation that targeted therapy would be forthcoming for many human diseases. The overriding factor that determines the importance of mAb is their specificity. The acquired immune system has evolved a unique ability to generate highly specific antibody molecules that allow recognition of almost any foreign substance, whether it is a protein, a carbohydrate or even a synthesized chemical. Antibodies are generated by a complex process in which host gene segments are arranged randomly into functional genes allowing the generation of potentially limitless different specificities. Once the immune response is triggered, usually by an infection, a particular set of antibody-expressing B cells are selected and their antibody is refined to improve binding by a process called somatic mutation. This process provides the immune system with antibodies that are specifically engineered for optimal performance against the foreign invader. At the end of this process, a fully matured antibody response is maintained, providing a variety of different specificities and affinities, each recognizing different determinants on the target. Such a polyclonal response is generated by multiple clones of selected B cells. For therapeutic application, the multitude of individual antibodies that make up a polyclonal mixture can be examined individually and selected to find the most useful specific drug. This has been achieved using the mAb fusion technology developed by Kohler and Milstein, in which rodent antibodies are produced by somatic cell fusion. It is now possible to generate fully human mAb with identical specificities. These agents not only have the same precision for target specificity as provided by rodent reagents, but also interact far more effectively with natural protection system of the body and do not provoke anti-Ab response. The progress has significant potential for the development of the genuine diseases specific therapy (Winter and Milstein 1991; Glennie and van de Winkel 2003).

The first indication that mAb might have significant clinical therapeutic potential came in 1982 when a patient with follicular lymphoma was treated with a “tailor-made” mouse anti-idiotype (anti-Id) mAb and responded with a complete response (CR) (Miller, Maloney et al. 1982). Over the last 20 years, many B-cell specific mAbs have been tested to treat NHL. Rituximab, a human-mouse chimeric anti-CD20 mAb has been the most successful and was the first mAb to be approved by the United States Food and Drug Administration (US FDA) for treatment of cancer in 1997. Although the exact in vivo mechanisms of tumour killing remains to be understood, pre-clinical data have suggested that the action of Rituximab may include antibody dependent cellular cytotoxicity (ADCC), complement dependent cytotoxicity (CDC), and the direct induction of apoptosis through cell surface mediated signalling transduction (Cragg, French et al. 1999). Because of the rather modest single agent response rates, Rituximab has now being integrated into many treatment pathways for both indolent and aggressive NHL with impressive additional benefit (McLaughlin 2001; Press, Leonard et al. 2001; Avivi, Robinson et al. 2003; Coiffier 2004; Coiffier 2005).

The conjugation of radionuclide to mAb as part of radioimmunotherapy (RIT) enables the additional delivery of targeted radiotherapy and thus offers the possibility of enhancing the therapeutic potency of mAb, especially in lymphomas which remain radiosensitive even when refractory to chemotherapy. The recent US FDA approval of two radiolabelled anti-CD20 mAbs, <sup>90</sup>Y labelled ibritumomab tiuxetan (2B8) or Zevalin™ and <sup>131</sup>I labeled tositumomab (B1) or Bexxar™ for treating recurrent follicular lymphoma provides a new treatment approach and new hope for patients with NHL (Garber 2002; Pandit-Taskar, Hamlin et al. 2003; Friedberg and Fisher 2004).

## **1.4 The Principles of Radioimmunotherapy**

Radioimmunotherapy (RIT) generally refers to the therapeutic administration of radionuclides chemically conjugated to antibodies or antibody-derived constructs. The antibodies recognise and bind to antigens on tumour cells and usually serve as direct

carrier for the radionuclide which delivers systemically targeted radiation to areas of disease with relative sparing of normal tissue. Compared to unconjugated mAb therapy or conventional external beam radiation therapy (EBRT), RIT therefore holds potential advantages of enhanced therapeutic effect and targeted delivery of radiation. However, the nature of RIT determines that its efficacy depends on a number of factors, including properties of the targeted antigen (specificity, density, availability, shedding and heterogeneity of expression), the tumour (vascularity, blood flow and permeability), the mAb (specificity, immunoreactivity, stability and affinity) and the properties of chosen radionuclides (emission characteristics, half life and availability) (Knox and Meredith 2000).

#### **1.4.1 The Choose of Target Antigen**

Tumour specific antigens would be the ideal targets, but that degree of specificity is unusual and in practice tumour associated antigens, expressed abundantly on tumour cells as well as some normal tissues represent the majority of potential targets. As most NHL are of B-cell origin the pan-B-cell antigens such as Human Leukocyte Antigen DR (HLA-DR), CD19, CD20, CD22, CD37 and CD52 have been extensively evaluated as targets for RIT (Dyer, Hale et al. 1989; Goldenberg, Horowitz et al. 1991; Hekman, Honselaar et al. 1991; Kaminski, Fig et al. 1992; Press, Eary et al. 1993; Brown, Kaminski et al. 1997; DeNardo, DeNardo et al. 1998; Kaminski, Zelenetz et al. 2001; Press 2003). Among them, CD20 has many of the characteristics thought to be important for an ideal target (Table 1.3) (Grossbard, Press et al. 1992) which does not internalise or shed from the cell surface and initiates signal transduction that triggers apoptosis through a caspase dependent pathway (Shan, Ledbetter et al. 1998; Shan, Ledbetter et al. 2000). CD20 is highly expressed on the majority of B-cell lymphomas but not expressed on stem cells or plasma cells so that after treatment the B cell pool is replenished. Currently anti-CD20 directed approaches are dominating the clinical RIT

of NHL although other antigens such as the CD22 are still being actively investigated (Press and Rasey 2000; Goldenberg 2001).

**Table 1.3.**

<b>The characteristics of an ideal target antigen</b>
Tumour cell specific
Highly expressed on tumour cells
No tendency to mutation
Not secreted or shed
Not rapidly modulated on antibody binding
Critical for target cell survival
Not expressed on critical or non renewable host cells

#### **1.4.2 The Evolution of RIT**

Initially, radiolabelled antibody (Ab) were assessed in radioimmunodetection (RID) or radioimmunoimaging (RII) using gamma camera to localise and identify tumour specific binding. Early RIT trials dating back to the 1960's used  $^{131}\text{I}$  labelled polyclonal antibodies but, these antibodies, lacked homogeneity in specificity and affinity and resulted in tremendous in vivo variability (Milenic 2000). Accelerated by the availability of mAb technology, RIT attracted wide interest and led to extensive pre-clinical and clinical investigations in the 1980's however investigators have since met

with some despondency with realisation of some of the obstacles of using mAb in RIT: (1) The insufficient penetration of tumour tissue by mAb. (2) The low radiation doses delivered to tumours in patients via mAb were insufficient to have significant effects on tumour growth. (3) The prolonged retention of the radiolabelled mAb in the blood could lead to increased myelotoxicity. (4) The development of human anti-murine Ab (HAMA) to the administered murine origin mAb, that subsequently compromise repeated administration. These problems appeared to be related to the biological features of mAb molecules. Therefore most investigators have since focused on manipulating the mAb itself in an effort to improve its performance in radionuclide delivery. A variety of different approaches have been investigated including mAb fragments, single chain Fv (scFv), bispecific mAb and pre-targeting techniques (Knox and Meredith 2000; Milenic 2000; Yao, Zhang et al. 2002; Zhang, Yao et al. 2002; Zhang, Zhang et al. 2003; Sharkey and Goldenberg 2005; Sharkey, Karacay et al. 2005).

In order to deliver a therapeutic dose of radiation to all the tumour cells, the penetration of the radiolabelled mAb is crucial, especially for solid tumours. A variety of physical parameters are known to influence the penetration of protein molecules such as mAb into tumours. These include the infused protein dose of mAb, the circulating half-life of the mAb, the abundance of blood vessels perfusing tumour sites, the permeability of the tumour vessels, the interstitial fluid pressure and intratumoural pressure impeding mAb penetration of tumours, the binding avidity of mAb for tumour antigens and the specificity of Ab binding (Sharkey, Blumenthal et al. 1990). One of the easiest ways to increase the penetration seems to be using mAb fragments such as  $F(ab)_2$ , Fab or scFv constructs which are smaller than the intact mAb. Experimental data indicated that these fragments penetrate into tumours faster and have shorter circulating half-life which may benefit less radiation exposure to normal organs (Thomas, Chappell et al. 1989; Yokota, Milenic et al. 1992). However, clinical trials revealed that these fragments have high renal retention and the monovalent reagents (Fab and scFv) have lower avidities and much shorter tumour retention times and therefore, reduced radiation dose delivered to the tumour. Besides the above disadvantages, the difficulty of producing large enough

quantity of these fragments, and the inability of such fragments to recruit host immune effectors which require Fc segments also contribute to outweigh their penetration advantage. Although currently, there are still investigators using bioengineering techniques to improve the features of radiolabelled mAb fragments, intact mAb are preferred for clinical RIT studies (Press and Rasey 2000).

The HAMA reaction has been another big challenge in clinical RIT (DeNardo, Mirick et al. 2003). The development of a HAMA response is dependent on the integrity of the host immunity. For most cancer patients, greater than 80% of patients usually develop an immune response against a therapeutically administered murine or other species antibody even after a single injection. Such an immune response can occur with small protein doses of 1 mg of antibody fragments or smaller constructs, though with less frequency than found after administration of intact IgG (Khazaeli, Conry et al. 1994; Knox and Meredith 2000). Repeated administration of antibody in a patient with a HAMA response can result in a severe immune reaction and rapid blood clearance which may substantially reduce tumour uptake of radiolabelled mAb (Knox and Meredith 2000). NHL patients involved in most of the clinical RIT trials so far have been mainly chemotherapy refractory and relapsed. As previous treatments might have substantially damaged the host immune system, these patients are observed less prone to develop an immune response to the given antibody, occurring among 10-30% patients after  $^{131}\text{I}$ -Tositumomab or  $^{131}\text{I}$ -Lym-1 (DeNardo, Mirick et al. 2003; Zelenetz 2003). However, in a most recent report, Kaminski et al observed that in 76 stage III and stage IV previously untreated NHL patients, after a single dosimetric dose in the course of treatment with  $^{131}\text{I}$ -tositumomab therapy, 48 (63%) developed HAMA reaction. They also observed a reduced therapeutic effect in patients who developed HAMA reaction. In this study, among 23 patients in whom antibody levels were more than 5 times the lowest level of detection within the first seven weeks, the five-year rate of progression-free survival was 35 percent, as compared with 70 percent for the remaining 53 patients ( $p=0.003$ ). The authors did not however discuss if the potential mechanisms behind this compromised therapeutic effect in HAMA positive patients

was related to different biodistribution patterns of the infused therapeutic radiolabelled mAb (Kaminski, Tuck et al. 2005).

The use of recombination DNA technology to produce humanized or chimeric murine mAb has contributed effectively in overcoming HAMA problem. These mAbs are much less immunogenic and allow for repeated mAb administration. Rituximab is one of such chimeric mAb and a variety of others are under investigation (Avivi, Robinson et al. 2003). In a study to assess the safety and efficacy of Rituximab treatment, a multi-centre, phase II study of eight consecutive weekly infusions of  $375 \text{ mg/m}^2$  Rituximab in patients with low-grade or follicular B-cell NHL who had relapsed or had failed primary chemotherapy was conducted. Among the thirty-seven patients with a median age of 55 years who were treated, none of them developed human anti-chimeric antibody (HACA) (Piro, White et al. 1999; Looney, Anolik et al. 2004). Interestingly, in a recently conducted phase I/II dose-escalation trial of Rituximab in the treatment of systemic lupus erythematosus (SLE), although the amount of infused Rituximab was much less, six out of seventeen (35%) patients developed human anti chimeric antibodies (HACA) at a level  $> \text{ or } = 100 \text{ ng/ml}$ . In this study, Rituximab was administered as a single infusion of  $100 \text{ mg/m}^2$  (low dose), a single infusion of  $375 \text{ mg/m}^2$  (intermediate dose), or as 4 infusions (1 week apart) of  $375 \text{ mg/m}^2$  (high dose). These HACA titres were observed to be associated with African American ancestry, reduced B cell depletion, and lower levels of Rituximab at 2 months after initial infusion (Looney, Anolik et al. 2004).

The humanized or chimeric mAb have been found to have longer circulating half-lives which is thought to be secondary to their human Fc portion which is believed more compatible with human tissues. This prolonged circulating half-life may theoretically cause excessive radiation exposure to normal organs and this initially led to concerns that humanized mAb may be less favourable for RIT.

The first two radioimmunoconjugates to be clinically investigated and subsequently approved by the US FDA are namely,  $^{90}\text{Y}$  labelled ibritumomab tiuxetan (Zevalin<sup>TM</sup>)

and  $^{131}\text{I}$  labelled tositumomab (Bexxar<sup>TM</sup>). Both radiolabelled mAb are murine origin. It has been hypothesized that, the problem of long circulating half-life of humanized mAb might be mitigated by genetically engineering a chimeric antibody with a shorter circulating half-life (Press and Rasey 2000), however recent data suggests that radiolabelled chimeric mAb may not in fact has an increased myelotoxicity (Illidge 2004).

Recent preclinical work using syngeneic murine B-cell lymphoma models has demonstrated that RIT is not simply targeted radiation therapy and the mAb effector mechanisms played an important role in the success of RIT (Illidge, Cragg et al. 1999). Most recently, Sharkey et al. although could not provide direct evidence, also postulated that the possible interaction between mAb and host immune effectors might have contributed significantly to the otherwise inexplicable therapeutic responses of  $^{90}\text{Y}$  labelled humanized anti-CD22 IgG ( $^{90}\text{Y}$ -Epratuzumab) in NHL patients (Sharkey, Brenner et al. 2003). These findings will have important impact on the future selection of mAb for RIT.

Newer approaches include pre-targeting RIT. Here instead of labelling the vector mAb with radionuclides, the initial infused mAb is labelled with streptavidin and subsequently followed 1-2 days later by a clearing agent that binds to unbound mAb in the circulation before the therapeutic radionuclide labelled biotin is administrated. This radiolabelled biotin rapidly conjugates with the streptavidin ensuring rapid targeting of the radiation to the lymphoma cells and minimising exposure of non-antigen bearing cells to radiation. In animal models this technique has been shown to improve the ratio of tumour to normal tissue absorbed radioactivity by a factor of 9 enabling safer dose escalation and improved responses (Yao, Zhang et al. 2002; Zhang, Zhang et al. 2003). Limited numbers of patients have been treated by this pre-targeting approach thus far. Pilot clinical studies of this approach are now underway (Press, Corcoran et al. 2001; Pagel, Hedin et al. 2003). Most recently, Forero et al reported impressive phase I clinical study of pre-targeted RIT for B-cell NHL in 15 patients. In this study, the ratio of average tumour to whole body radiation dose reached 49. At the fixed low dose of

$^{90}\text{Y}$  administered (555MBq $^2$ ), 21% (3/14) patients achieved objective response and no RIT induced haematological toxicity was observed (Forero, Weiden et al. 2004).

### **1.4.3 The Selection of Radionuclide for RIT**

The optimal radionuclide delivers the maximal dose of ionizing radiation to tumour sites whilst minimizing the radiation dose to normal tissue and to medical personnel. The physical characteristics that are considered important for a radionuclide in RIT include half-life, type of radioactive emissions (alpha, beta or gamma) and ionization path length. Particle energy and mean path length in tissue are important determinants of therapeutic efficacy. The emission profile of radionuclide not only determines its suitability for therapy, but also the toxicological profile.

Animal studies have consistently indicated that the major dose-limiting organ for RIT is the bone marrow (Vriesendorp, Quadri et al. 1992). With the advent of bone marrow and peripheral blood stem cell transplantation, the upper limit of the amount of tolerable radiation dose is likely to increase and, in the mean time also the wider choice of radionuclides (Press and Rasey 2000).

The availability of radiolabelling techniques is another factor which limits the RIT application of radionuclides. The most frequently used radionuclides and their physical characteristics are listed in Table 1.4.

**Table 1.4. Physical Characteristics of Radionuclides Used in RIT**

<b>Radioisotope</b>	<b>Half-life</b>	<b>Emission</b>		<b>Path length</b>
Iodine-131	8.1 days	Beta	0.6 MeV*	0.8 mm
		Gamma (81%)	0.37 MeV	
Yttrium-90	2.5 days	Beta	2.3 MeV	5.3 mm
		Gamma	nil	
Rhenium-186	3.7 days	Beta	1.1 MeV	1.8 mm
		Gamma (9%)	0.14 MeV	
Iodine-125	60.1 days	Electron capture	7.45 MeV	0.001 mm
		Gamma	0.027 MeV	
Copper-67	2.5 days	Beta	0.4-0.6 MeV	0.6 mm
		Gamma	0.185 MeV	
Astatine-211	7 hours	Alpha	6.8 MeV	0.065 mm
		Electron capture	7.45 MeV	
Bismuth-213	1 hour	Alpha	7.8 MeV	0.07 mm
		Gamma	0.72 MeV	

\*Million Electron Voltage

In practice, the choice of the optimal isotope for RIT remains controversial, with proponents advocating the relative merits of iodine-131, yttrium-90, rhenium-186, copper-67, and alpha emitters such as astatine-211 (Press and Rasey 2000).

Comparative studies are difficult to conduct and scientifically sound randomized human trials have not been performed.

The vast majority of clinical trials so far have been conducted with either  $^{131}\text{I}$  or  $^{90}\text{Y}$  because of their favourable emission characteristics, availability, well documented radiochemistry that permit reliable and stable attachment to mAb.  $^{131}\text{I}$  has the advantage of a long history of successful use in the management of thyroid cancer and a well documented safety profile. It is readily available, inexpensive, easily conjugated and emits both beta particles with a path length of 0.8 mm and penetrating gamma emissions. The gamma emissions enable uncomplicated imaging using gamma camera for dosimetry purposes but result in a significant non targeted normal tissue radiation dose, as well as radiation protection issues for visitors and medical/nursing staff.

$^{90}\text{Y}$  offers a number of theoretical advantages over  $^{131}\text{I}$  although the radioisotopes have not been directly compared conjugated to the same mAb.  $^{90}\text{Y}$  is a pure beta emitter delivering higher energy radiation (2.3 MeV versus 0.6 MeV) at a longer path length (5.3 mm versus 0.8 mm). This increased path length would be expected to enhance the “crossfire effect” and could therefore potentially be advantageous in treating larger, poorly vascularized tumour nodules or tumours with heterogeneous antigen expression (DeNardo, O'Donnell et al. 2000). This longer path length will however increase the normal tissue dose when targeting microscopic disease for which the shorter path length of  $^{131}\text{I}$  may be preferable. The half-life of 64 hours matches the biological half life of murine monoclonal antibodies and the absence of penetrating gamma emissions enables delivery as an outpatient (Press and Rasey 2000). In addition, if a cell internalizes  $^{90}\text{Y}$ , it is likely to be retained within the cell (Sharkey, Behr et al. 1997). In contrast if  $^{131}\text{I}$  conjugates are internalized by a cell they will be rapidly dehalogenated and the small  $^{131}\text{I}$  products rapidly released into the blood stream, reducing desired tumour absorbed

radiation dose and increasing normal tissue exposure to radiation (Press, Shan et al. 1996).

The major disadvantages of  $^{90}\text{Y}$  relate to its greater expense, relatively limited availability and complicated chelation radiochemistry making radiolabelling more difficult. In addition as  $^{90}\text{Y}$  is a pure  $\beta$ -emitter, in the absence of gamma emissions, there is a need to use a surrogate isotope Indium-111 to obtain images for biodistribution and dosimetry studies.

Rhenium-186 and Copper-67 have physical and chemical properties that make them attractive alternatives however their current limited availability has meant that these radioisotopes have received limited clinical use (DeNardo, Kukis et al. 1999).

Astatine-211 is an alpha emitter producing a particle of very high energy but with a very short path length. The high Linear Energy Transfer (LET) radiation of alpha emitters may be lethal to cells with a single hit however the very short path length means that the isotope must be internalized to be effective and is likely to have little or no “cross fire” effect. The suitability of alpha emitters therefore appears limited to readily accessible tumours such as leukaemia cells in blood or bone marrow. The short half life of around 7 hours complicates administration meaning that such radioisotopes are likely to require generation on the same site as delivery in the clinic. Despite this logistical hurdle, early clinical data in the treatment of leukaemia appear extremely promising (McDevitt, Sgouros et al. 1998; Jurcic, Larson et al. 2002). Recent experimental RIT studies involving animal leukaemia models have also demonstrated the therapeutic potential of another alpha emitter, Bismuth-213 (Zhang, Yao et al. 2002; Zhang, Zhang et al. 2003).

Very recently, Oh et al reported impressive therapeutic effects using an Auger emitter, Iodine-125 labelled mAb targeting on a tumour blood vessel (endothelial cell) specific protein, anti-Annex A1 to treat lung tumour bearing rats (Oh, Li et al. 2004).

## **1.5. Clinical Progress of Radioimmunotherapy for NHL**

Although clinical RIT trials in NHL differ in terms of eligibility criteria, antibody and radioisotopes used, dose, number of treatments, doses of unlabelled mAb pre-infused or co-infused and the biodistribution or dosimetry estimations required for administration of a therapeutic dose of radiolabelled Ab, virtually all clinical studies performed to date have shown promising results. (Wilder, DeNardo et al. 1996; Knox and Meredith 2000; Press 2003; Davis, Kaminski et al. 2004; Kaminski, Tuck et al. 2005; Sharkey and Goldenberg 2005).

### **1.5.1 Non-Myeloablative RIT**

DeNardo et al pioneered RIT for NHL (DeNardo, DeNardo et al. 1990; DeNardo 2000). In their early studies, patients were given fractionated doses (30-60 mCi) of  $^{131}\text{I}$  labelled anti-HLA-DR mAb (Lym-1) at 2 to 6 week intervals (DeNardo, DeNardo et al. 1998). Thirty patients with relapsed NHL or chronic lymphocytic leukaemia were treated. Three (10%) achieved complete remission (CR) and 14 (47%) achieved partial remission (PR) for an overall response rate of 57%. A subsequent trial investigating the efficacy of escalating doses of iodine-131 labelled Lym-1 (40-100 mCi/m<sup>2</sup>) achieved an overall response rate of 52% in 21 treatment courses administered to 20 patient, with seven patients (33%) achieved CR, four patients (19%) achieved PR (DeNardo, DeNardo et al. 1998). Goldenberg et al. used iodine-131 labelled anti-CD22 Ab (LL2) to treat B-cell lymphomas. In one of their trials, 4 out of 17 patients achieved objective remission including 1 CR (Goldenberg, Horowitz et al. 1991). In another trial, yttrium-90 labelled LL2 were administered to seven patients with B-cell lymphomas, two of whom achieved PR (Juweid, Stadtmauer et al. 1999). A recent dose escalation trial reports 9 of 20 assessable patients showing objective responses with 2 complete responses (Hajjar, M. et al. 2001).

The majority of clinical trials of B-cell lymphomas and the most impressive clinical results to date have used radiolabelled anti-CD20 mAb. Kaminski and colleagues have conducted a series of trials at the University of Michigan using the iodine-131 labelled tositumomab, (Bexxar<sup>TM</sup>) for the treatment of relapsed follicular lymphoma (Kaminski, Zasadny et al. 1993; Kaminski, Zasadny et al. 1996; Kaminski, Zelenetz et al. 2001; Kaminski, Tuck et al. 2005). On the basis of these clinical trials, Bexxar<sup>TM</sup> was approved by the US FDA in June, 2003 (Friedberg and Fisher 2004).

The Bexxar<sup>TM</sup> therapeutic regimen is completed in 4 visits over 1-2 weeks as shown in Table 1.5. This regimen involves an initial biodistribution/dosimetry study followed by a therapeutic infusion given 7-14 days later.

**Table 1.5. Bexxar<sup>TM</sup> (<sup>131</sup>I-Tositumomab) Therapeutic Regimen**

<b>Dosimetric Step</b>			<b>Therapeutic Step</b>
<b>Day 0</b>	<b>Day 2, 3, or 4</b>	<b>Day 6 or 7</b>	<b>Day 7 to 14</b>
<b>Tositumomab</b> 450 mg (60 min iv infusion)	<b>Gamma Camera</b> <b>Count 2</b> (post-urination)	<b>Gamma Camera</b> <b>Count 3</b> (post-urination)	<b>Tositumomab</b> 450 mg (60 min iv infusion)
<b><sup>131</sup>I-Tositumomab</b> 35 mg mAb containing <sup>131</sup> I 185 MBq (20 min iv infusion)			<b><sup>131</sup>I-Tositumomab</b> 35 mg mAb containing <sup>131</sup> I activity to deliver 65-75 cGy total body dose (20 min iv infusion)
<b>Gamma Camera</b> <b>Count 1</b> (prior to urination)			Thyroid protection medication for 14 days

Each infusion of radiolabelled mAb is preceded by an infusion of 450 mg per patient of unlabelled “cold” tositumomab as a pre-dose. Whole body gamma imaging is performed three times over the week following the trace labelled infusion to calculate the whole body half-time and the dose required for the therapeutic infusion to deliver 65-75 cGy of whole body irradiation (usually 100-150 mCi) (Hohenstein, Augustine et al. 2003). In the study to evaluate the therapeutic efficacy of  $^{131}\text{I}$  labelled tositumomab, a single course of  $^{131}\text{I}$ -tositumomab has shown to provide far unreachable disease free survival over the last qualifying chemotherapy (LQC) received by extensively pretreated 60 patients with chemotherapy-refractory low-grade, or transformed low-grade NHL. In this study, the 60 patients acted as their own internal controls (Kaminski, Zelenetz et al. 2001).

Myelosuppression was found to be the dose-limiting toxicity. Since 1990 over 800 patients with “low grade” and transformed lymphoma have been treated with  $^{131}\text{I}$ -tositumomab. Long term follow up data was presented at American Society of Haematology Annual Meeting (ASH) 2002 on 250 of these patients indicating a response rate of 56% with 30% of patients achieving a complete response (CR). Perhaps the most impressive fact was that 70% of the patients who achieved a CR are alive and remain in CR at up to 7.8 years with a median follow up of almost 4 years (Kaminski 2002). An analysis of prognostic factors has confirmed that this remarkable durability of response cannot be accounted for by patient selection in the reported trials (Gregory 2002). Of the patients that achieved CR 89% had stage III/IV disease, 32% had no response to their last therapy, 45% had >4 prior therapies, 50% had bulky disease and 43% had bone marrow involvement.

Impressive response rates have also been seen in patients that were refractory to Rituximab. Horning and colleagues have treated 40 patients with low grade NHL, 72% of which had received four or more previous lines of therapy and 60 % of which had failed to respond to Rituximab. An overall response rate of 68% with a CR rate of 30% was noted and a median duration of response of 14.7 months reported. 9 of the 12 complete responders remained in CR at the time of presentation with a range of 12-26

months (Horning 2002). More recently an analysis including 230 patients treated with  $^{131}\text{I}$ -tositumomab was made. Independently assessed durable CR's were noted with similar frequency in patients with Rituximab-refractory disease (28%) and Rituximab naïve patients all of which had chemotherapy refractory disease (23%). With a median follow-up of 4.6 years, 75% of patients with durable CR continue in complete remission (Coleman M 2003).

Highly promising results have also been seen in the frontline treatment of previously untreated low-grade lymphomas using  $^{131}\text{I}$ -tositumomab. The most recent update included 76 patients with a median follow-up of 5.1 years. An encouraging overall response rate of 95% was seen with 75% achieving CR. The actuarial 5-year progression-free survival for all patients was 59%, with a median progression-free survival of 6.1 years. Haematological toxicity was moderate, with no patient requiring transfusion or haematopoietic growth factors (Kaminski 2002; Koral, Dewaraja et al. 2003; Kaminski, Tuck et al. 2005). In a recent multicentre, randomized study comparing treatment outcomes for tositumomab and  $^{131}\text{I}$  labelled tositumomab to an equivalent total dose of unlabelled tositumomab involving 78 patients with refractory/relapsed NHL (median follow-up 42.6 months), Davis et al reported that the responses in  $^{131}\text{I}$  labelled tositumomab versus unlabelled tositumomab groups: overall response 55% versus 19% ( $P = 0.002$ ); complete response 33% versus 8% ( $P = 0.012$ ); median duration of overall response not reached versus 28.1 months; median duration of complete response not reached in either arm; and median time to progression 6.3 versus 5.5 months ( $p = 0.031$ ), respectively. Although haematological toxicity was more severe and nonhaematological adverse events were more frequent after  $^{131}\text{I}$  labelled tositumomab than after tositumomab alone, there were no serious infectious or bleeding complications. The frequency of developing HAMA was similar in the two arms of 27% ( $^{131}\text{I}$  labelled tositumomab group) versus 19% (tositumomab alone group), respectively. This study demonstrated that although unlabelled tositumomab showed single agent activity, the conjugation of  $^{131}\text{I}$  to tositumomab significantly enhanced the therapeutic efficacy (Davis, Kaminski et al. 2004).

A parallel series of clinical trials has also been conducted by investigators using <sup>90</sup>Y labeled ibritumomab tiuxetan (Zevalin<sup>TM</sup>) which was the first radioimmunoconjugate to be granted US FDA approval in February, 2002 (Witzig, Gordon et al. 2002). The studies included in the FDA submission were a randomized controlled trial comparing <sup>90</sup>Y labeled ibritumomab tiuxetan with Rituximab in relapsed or refractory low-grade B-cell NHL (Witzig, Gordon et al. 2002). Seventy-three patients received two doses of Rituximab 250 mg/m<sup>2</sup> a week apart as pre-dosing followed by a single dose of <sup>90</sup>Y labeled ibritumomab tiuxetan 0.4 mCi/kg body weight. Seventy patients in the control arm received Rituximab 375 mg/m<sup>2</sup> weekly for 4 weeks. The overall response rate was 80% for the labelled antibody group versus 56% for the Rituximab alone group (P = 0.002). Complete responses were 30% and 16% in the <sup>90</sup>Y labeled ibritumomab tiuxetan and Rituximab groups respectively.

Myelosuppression was found to be the dose-limiting toxicity of RIT. An analysis of all patients treated in <sup>90</sup>Y labelled ibritumomab tiuxetan trials (n = 261) indicated that 28% will experience grade 4 neutropenia and 8% will experience grade 4 thrombocytopenia (Gordon, Witzig et al. 2002). <sup>90</sup>Y labelled ibritumomab tiuxetan also appeared able to deliver durable remissions and for those patients that achieved a CR, median duration of response approaching 2 years and ongoing responses of more than 4 years have been reported (L. I. Gordon 2003). These highly promising results demonstrated for the first time that RIT can lead to superior overall and complete response rates to those seen with “naked” mAb. Clinical responses have also been observed for <sup>90</sup>Y labelled ibritumomab tiuxetan in transformed follicular and relapsed diffuse large B cell lymphoma (DLBC). A phase I/II study reported a response rate of 58% with a 33% CR rate in a group of patients that had relapsed following 2 previous chemotherapy regimens that included CHOP (Gordon 2002).

The integration of <sup>90</sup>Y labelled ibritumomab tiuxetan (Zevalin<sup>TM</sup>) and <sup>131</sup>I labelled tositumomab (Bexxar<sup>TM</sup>) into routine clinical practice may ultimately depend on the cost and convenience of each therapy instead of the small differences in clinical efficacy. The characteristics of these two radioimmunoconjugates are summarized in

Table 1.6.  $^{90}\text{Y}$  is a more expensive radioisotope. However the radiation protection issues may make the extra expense of  $^{90}\text{Y}$  worthwhile, as the necessity for 5-6 days in-patient stay for patients receiving  $^{131}\text{I}$  labelled tositumomab may influence clinicians on health economic grounds. In addition the removal of the dosimetric dose will simplify the delivering of  $^{90}\text{Y}$  labelled ibritumomab tiuxetan as recent studies have failed to demonstrate a consistent correlation between the estimated bone marrow dose and toxicity but have shown that  $^{90}\text{Y}$  labelled ibritumomab tiuxetan can be safely prescribed according to body weight and platelet count (Wagner, Wiseman et al. 2002; Wiseman, Leigh et al. 2002).

**Table 1.6. Characteristics of  $^{131}\text{I}$  tositumomab (Bexxar<sup>TM</sup>) and  $^{90}\text{Y}$  ibritumomab tiuxetan (Zevalin<sup>TM</sup>)**

	$^{131}\text{I}$ tositumomab	$^{90}\text{Y}$ ibritumomab tiuxetan
<b>US Trade name</b>	Bexxar	Zevalin
<b>Monclonal antibody</b>	Tositumomab ( anti-B1) – murine	Ibritumomab ( 2B8) - murine
<b>Chelation</b>	Simple	More complex
<b>Isotope</b>	$^{131}\text{I}$	$^{90}\text{Y}$
<b>Isotope emissions</b>	$\gamma$ and $\beta$	$\beta$ only
<b>Beta energy</b>	0.606 MeV	2.293 MeV
<b>Beta particle path length</b>	0.8 mm	5.3 mm
<b>Isotope half life</b>	8 days	2.6 days
<b>Gamma energy,</b>	0.364 MeV	None
<b>Radiation protection measures</b>	4-6 day inpatient stay in shielded room	Outpatient
<b>Isotope excretion</b>	Renal (variable)	Limited
<b>Normal tissue uptake</b>	Thyroid ( blocked with potassium iodate)	Bone
<b>Pre-dose (unlabelled antibody)</b>	Tositumomab (450 mg/patient)	Rituximab ( $250 \text{ mg/m}^2$ ) x 2
<b>Dose</b>	65-75 cGy whole body dose Dosimetric dose obligatory	11.1-14.8MBq/kg depending on patient platelet count Dosimetric dose not required Dose reduction for thrombocytopenia.

## 1.5.2 Myeloablative RIT

Unlike most of the other investigators, the Seattle group has investigated the high-dose “myeloablative” RIT for patients with relapsed lymphomas supported by autologous stem-cell transplantation (ASCT) (Press, Eary et al. 1993; Press, Leonard et al. 2001). The use of ASCT has allowed dose escalation to at least three fold the dose delivered in the non-myeloablative approach, although the established approach of delivering 75 cGy to the whole body with  $^{131}\text{I}$  labelled tositumomab (anti-B1) has proven to be extremely well tolerated with predictable grade IV thrombocytopenia or neutropenia occurring in less than 10%, and is rarely manifested clinically (Kaminski, Zasadny et al. 1993; Zelenetz 2003).

Press and colleagues in Seattle, using  $^{131}\text{I}$ -anti-B1, have pioneered the myeloablative approach and have arguably achieved the best results thus far reported in clinical RIT, albeit in a highly selected group of patients. In a group of multiply relapsed patients with low grade lymphoma a durable CR rate of 73% was reported (Liu, Eary et al. 1998) and outcomes have been shown to be superior to conventional high dose chemotherapy and stem cell transplantation in a non randomized cohort analysis (Gopal, Gooley et al. 2003). Following this success the same group have reported a CR rate of 91% and a progression free survival of 61% at 3 years in poor prognosis mantle cell lymphoma using high dose RIT with Cyclophosphamide and Etoposide chemotherapy followed by ASCT (Gopal, Rajendran et al. 2002). More recently, Behr et al in Germany reported their initial myeloablative RIT study using high-dose (261-495 MBq)  $^{131}\text{I}$  labelled Rituximab treating 7 mantle cell NHL patients. In this study, 6 patients achieved CR and one PR (Behr, Griesinger et al. 2002). Nevertheless, the much higher dose of administered radioimmunoconjugate does impose bigger safety problems, and currently there are very few centres in the world that have the necessary facilities to reproduce this type of approach. This makes the more widespread establishment of this approach seem unlikely at the current time, however the data is sufficiently compelling to demand further investigation.

Although the high CR rates and prolonged remissions are encouraging, more than half of patients eventually relapse with single-agent RIT, even when given at maximal doses with stem-cell support. In an attempt to further increase the percentage of patients with durable remission, RIT is currently being investigated as a component of high dose therapy and both  $^{131}\text{I}$ -tositumomab and  $^{90}\text{Y}$  labelled ibritumomab tiuxetan have been added to high dose chemotherapy with BEAM (BCNU, Etoposide, Ara-C and Melphalan). The early results have confirmed the feasibility of this approach and studies are ongoing (Fung H 2003).

### **1.5.3 Non-Haematological Toxicities of RIT**

The short-term non-haematological adverse events are generally mild, typically fatigue, nausea, fever, vomiting, pruritus and rash which usually respond well to anti-histamines. Hypothyroidism appears one of the most notable long-term adverse effects after  $^{131}\text{I}$  labelled mAb treatment which can however be easily managed with thyroid hormone replacement. Most recently, Zelenetz reviewed the multicentre RIT trials using  $^{131}\text{I}$ -tositumomab in NHL patients and reported that elevated thyroid stimulating hormone (TSH) was observed in 5 out of 59 patients in the phase I study (Zelenetz 2003). However, Liu et al. observed elevated TSH in 59% of patients treated in Seattle with myeloablative dose of  $^{131}\text{I}$ -tositumomab (Liu, Eary et al. 1998). HAMA reactions appear to be substantially lower in previously treated NHL patients compared to the rates experienced in solid tumour RIT (Knox and Meredith 2000). DeNardo et al analyzed 617 samples from 112 subjects including 85 patients with B-cell malignancies. They found that 77% of B-cell malignancy patients developed no response or a weak response after multiple doses of mouse Lym-1 antibody (DeNardo, Mirick et al. 2003). In a separate study, Zelenetz observed similar results with approximately 10% of  $^{131}\text{I}$ -tositumomab treated patients developed positive HAMA reaction. However, in a most recent study involving previously untreated patients, Kaminski et al reported 48 out of 76 (63%) patients developed detectable HAMA after a single course of treatment with  $^{131}\text{I}$  labelled tositumomab (Kaminski, Tuck et al. 2005).

RIT treatment related malignancies have been found to be rare (Zelenetz 2003; Kaminski, Tuck et al. 2005). In a very recent study, 1071 RIT treated patients were assessed of treatment-related myelodysplastic syndromes (MDS) and acute myeloid leukaemia (AML). Among them, 995 patients with low grade and transformed low grade NHL had been treated with a median of 3 previous therapies (range, 1 to 13 therapies) prior to RIT. 76 patients received RIT as their initial therapy for follicular NHL. For the previously treated patients, the median follow-up from the diagnosis of NHL and RIT was 6 years and 2 years, respectively; for the patients who received RIT as their initial therapy, the corresponding median follow-up times were 5.6 years and 4.6 years, respectively. Of the 995 previously treated patients, 35 (3.5%) cases of treatment-related MDS/AML were reported and 13 cases were confirmed to have developed MDS/AML following RIT. This incidence was found to be consistent with that expected on the basis of patients' prior chemotherapy for NHL. With a median follow-up approaching 5 years, no case of treatment-related MDS/AML has been reported in the 76 patients receiving  $^{131}\text{I}$  labelled tositumomab as their initial therapy (Bennett, Kaminski et al. 2005).

## **1.6. Ongoing Issues in Radioimmunotherapy**

Although RIT has emerged an effective treatment for NHL, the underlying mechanisms of action as well as the interaction of irradiation and mAb in RIT are still poorly understood (Zelenetz 1999; Illidge and Johnson 2000; Press and Rasey 2000). To further optimize the RIT approach, several critical issues remain to be answered. These issues include: (1) whether a radiation dose response exists; (2) the requirement and the usefulness of dosimetry for predicting tumour responses and normal tissue toxicity; (3) how best to use RIT in the treatment of NHL.

### 1.6.1 Dosimetry and Radiation Dose Response in RIT

The estimation of the radiation absorbed dose has been an essential part of evaluating risks and benefits associated with conventional radiotherapy and it is vital in treatment planning, predicting radiation effects, correcting biological effects with dose and maintaining complete patient records. One of the fundamental potential advantages of RIT is the ability to deliver higher targeted radiation dose to the tumour than to normal tissue and thus enhance the specific tumour killing. The fact that radioisotopes emit ionising radiation not only enables them to be used in therapy but also to be quantified using radiation dosimetry. However, probably due to the relative complexity of the radiation dose estimation for RIT, the clinical importance of dosimetry in RIT of NHL currently remains controversial. Whilst some investigators regard dosimetry an essential component of RIT practice, others do not think it necessary (Koral, Kaminski et al. 2003; Britton 2004; Postema 2004; Goldenberg and Sharkey 2005).

Technically, the amount of radioisotope is measured in Becquerel, Bq, i.e. the number of decays per second. The absorbed dose, i.e. energy deposited per unit mass, caused by radiation, is measured in Gray (Gy), i.e. Joule per kg. An organ containing activity is designated a source organ and the organ that are irradiated is called a target organ. As for internal dosimetry, the calculation of the absorbed dose can be viewed as the conversion of activity into energy and then into absorbed energy per unit mass. The basic equation is:  $D = AS$  where  $D$  is the absorbed dose.  $A$  is the cumulated activity – the time integral of the radionuclide activity in a source organ. The unit of cumulated activity is Becquerel-seconds.  $S$  is the mean absorbed dose to a target organ per unit cumulated activity in the source organ. The unit for  $S$  is Gray per Becquerel-second. For certain tissue irradiated by certain radioisotope, the  $S$  value is constant. Therefore, based on phantom calculations, the Medical Internal Radiation Dose (MIRD) committee of the Society of Nuclear Medicine provide tabulated  $S$  values for nearly all the radioisotopes. Sampling the tissue at serial time points enables an estimation of the value of  $A$ , cumulated activity and therefore, the absorbed dose,  $D$ . In the cases of

animal experiments, the ease of sampling or dissecting provides the opportunity of obtaining sufficient data for accurate organ dosimetry. However, in most of the clinical RIT settings, frequent sampling or biopsy is not always practical and the limited input data makes the calculation of absorbed dose much less accurate. The inhomogeneous dose distribution within tumour or a certain organ also makes determination of the dose estimation more challenging (Fisher 1994; Behr, Sharkey et al. 1997; Fisher 2000).

Gamma camera, taking advantage of imaging emitted gamma radiation from  $\gamma$  emitting radioisotopes, contributes significantly to the patient dosimetry assessment. The distribution of a radioactivity in the body or in individual source organ can be roughly determined by sequential imaging using planar scintillation cameras or tomographic single photon emission computed tomography (SPECT). Conjugate imaging data with patient body weight, organ volumetrics, blood sampling, urine sampling, marrow biopsy, the patient dosimetry can be estimated (Goldenberg, Horowitz et al. 1991; Juweid, Stadtmauer et al. 1999; Fisher 2000). The MIRD committee developed a dedicated computer based program MIRDOSE to fulfil this task and this program is widely used in clinical RIT trials.

With solid tumours, better response rate with higher RIT doses have been observed (Knox and Meredith 2000). However, in the RIT for NHL, although much more effective, most of the clinical dosimetry studies have thus far failed to show a consistent dose-response relationship (Knox and Meredith 2000). More recently, the Michigan group who have extensively investigated  $^{131}\text{I}$ -tositumomab, have concluded from their results that there is radiation dose-response in RIT for this radioimmunoconjugate at least (Koral, Kaminski et al. 2003; Wahl 2003). However their conclusions are not shared by other investigators in the field (Postema 2004; Goldenberg and Sharkey 2005). Postema argued that none of the RIT dosing methods use tumour dosimetry to determine the dose administered to patients because the myelotoxicity of radiolabelled mAb will limit the increments of radioactivity dose, but not the tumour absorbed dose (Postema 2004). More recently, Goldenberg et al addressed that because RIT has two

potentially therapeutic arms, namely radiation and mAb mechanisms, poor radiation targeting dose not exclude good therapeutic response (Goldenberg and Sharkey 2005).

Another issue is whether the dosimetry study can reliably predict the normal tissue toxicity and especially haematological toxicity which is the initial dose limiting toxicity. In a recent analysis combining data from 4 clinical trials, Wiseman et al concluded that dosimetry of <sup>111</sup>In- ibritumomab tiuxetan failed to contribute to the prediction of myelotoxicity in subsequently treated patients with <sup>90</sup>Y- ibritumomab tiuxetan (Wiseman, Leigh et al. 2002; Wiseman, Kornmehl et al. 2003). In the “administration guidelines for RIT of NHL with <sup>90</sup>Y- ibritumomab tiuxetan (Zavelin<sup>TM</sup>)” Wagner et al indicated that dosimetry is not necessary in NHL patients who met the criteria for pre-treatment platelet count and percentage of marrow involvement with lymphoma (<25% as determined by bone marrow biopsy) (Wagner, Wiseman et al. 2002; Wiseman, Leigh et al. 2002). However, Wahl et al. who have also extensively investigated the RIT of NHL using <sup>131</sup>I-tositumomab (Bexxar<sup>TM</sup>) and found that whole-body dosimetry to be a reliable method to determine the patient-specific maximally tolerated therapeutic radiation dose and potentially increase tumour dose whilst minimising organ and bone marrow toxicity. By performing patient-specific dosimetry studies they have achieved significant rates of response and durable clinical remissions with relatively modest haematological toxicity (Koral, Kaminski et al. 2003; Wahl 2003). For previously untreated patients who received <sup>131</sup>I labelled tositumomab as initial therapy the haematological toxicity was mild and characterised by the fact that no patient received blood-product transfusion or haematopoietic growth factors related to treatment (Connors 2005; Kaminski, Tuck et al. 2005).

Notably, the <sup>90</sup>Y- ibritumomab tiuxetan (Zevalin<sup>TM</sup>) RIT protocol used by Wiseman et al and the <sup>131</sup>I-tositumomab (Bexxar<sup>TM</sup>) protocol used mainly by the Michigan group are slightly different in terms of dosimetry assessment: Zevalin<sup>TM</sup> contains <sup>90</sup>Y which requires <sup>111</sup>In as a surrogate for dosimetry study while Bexxar<sup>TM</sup> carrying <sup>131</sup>I which can fulfil the dosimetry purpose on its own; The amount of mAb protein carried by

therapeutic dose of mAb in the Zevalin<sup>TM</sup> protocol is only 3.2 mg versus 35 mg for the Bexxar<sup>TM</sup> regimen.

### **1.6.2 Pre-dosing in RIT**

Theoretically several factors may limit lymphoma targeting of radiolabelled pan-B-cell mAb in RIT such as: (1) complex formation of administered antibody with free circulating target antigen; (2) cross-reactivity with antigen-positive circulating lymphoma cells, normal B-cells in the blood or spleen, or non-lymphoid tissues; (3) non-antigenic binding of antibody, such as, Fc binding. In order to improve the biodistribution of radiolabelled mAb in RIT, it has become the adapted practice in clinical RIT with anti-CD20 radioimmunoconjugates to give a pre-dose of unlabelled mAb prior to the therapeutic dose with the intention of blocking circulating and accessible cross-reactive non-tumour binding sites (Wagner, Wiseman et al. 2002; Wahl 2003). For both <sup>90</sup>Y ibritumomab tiuxetan (Zevalin<sup>TM</sup>) and <sup>131</sup>I tositumomab studies, the trace-amount radioactivity labelled mAb for dosimetry study and the therapeutic dose are administered following the administration of a large amount of unlabelled mAb (250 mg/m<sup>2</sup> Rituximab in <sup>90</sup>Y ibritumomab tiuxetan protocol and 450 mg tositumomab per patient in <sup>131</sup>I tositumomab study).

However, the studies upon which this practice is based involve small patient numbers (Kaminski, Zasadny et al. 1993) and the choice of a dose of 250 mg/m<sup>2</sup> Rituximab prior to <sup>90</sup>Y ibritumomab tiuxetan was based on data from only 6 patients, 3 patients who received 125 mg/m<sup>2</sup> and 3 patients who received 250 mg/m<sup>2</sup>. This dose was chosen not because better biodistribution was seen with this dose than with the lower doses of Rituximab but because it was assumed that the single agent efficacy of this larger dose of Rituximab would contribute to the overall efficacy of the treatment (Witzig, White et al. 1999).

Furthermore, the most frequently cited preclinical experiments supporting the concept of pre-dose have methodological shortcomings (Buchsbaum, Wahl et al. 1992): Aiming to minimise the negative impact of those factors on the targeting of radiolabelled mAb, Buchsbaum et al performed pre-dose RIT dosimetry experiments using human lymphoma tumour xenograft mouse models. The authors concluded that pre-dose could significantly improve the targeting performance of the radiolabelled mAb. In this frequently cited publication Buchsbaum et al reported that the administration of 100 µg unlabelled anti-CD20 mAb anti-B1 (tositumomab) resulted in a 44% greater tumour uptake of the subsequently injected  $^{131}\text{I}$  labelled 0.3 µg tositumomab. However, in this study, they only reported the biodistribution data of 4 days after the administration of the radiolabelled mAb and not the earlier post-injection time points such as 24 hours, 48 hours, 72 hours, etc., which dominate more in the estimation of organ/tumour dosimetry (Buchsbaum, Wahl et al. 1992). The other major reservations in extrapolating these findings to the clinical situation are: (1) Lack of normal tissue cross-reactivity, ie, the anti-B1 mAb only reacts with the tumour xenograft cells and not the mouse host cells. (2) Different tumour distribution of xenograft model than syngeneic tumours.

It is understandable that, by blocking a certain amount of binding sites, the pre-dose prolongs the circulating half-life of the radiolabelled mAb and, could therefore increase the tumour retention of the labelled mAb at later time points. But the large dose of cold mAb used as pre-dose poses a theoretical risk of blocking tumour binding sites and may therefore decrease the tumour uptake of radiolabelled mAb perhaps in early time points. If this is the case, the radiation dose delivered to the tumour could be reduced especially for radionuclides with short physical half-lives.

Factors affecting clearance of the mAb include the size of the patients' tumours, presence of splenomegaly, lean body mass, and the amount of lymphomatous bone marrow involvement in the disease (Wahl 2003). However the amount of unlabelled mAb given as the pre-dose may have significant impact on the biodistribution of the subsequently administered radiolabelled therapeutic mAb. It has previously been reported that in standard Rituximab immunotherapy for NHL, after each infusion of 375

mg/m<sup>2</sup> Rituximab per week (which is comparable to the protein dose used as pre-dose in RIT, 250 mg/m<sup>2</sup> twice a week), the serum concentration of Rituximab increased and the circulating half-life of Rituximab was observed increased from 76.3 hours to 205.8 hours in average among 14 patients (Berinstein, Grillo-Lopez et al. 1998). By closely monitoring the serum Rituximab concentration in patients involved in fractionated RIT trail using a dedicated high affinity mAb with fine specificity for the idiotype of Rituximab, our group have recently also observed that the circulating half-lives of Rituximab significantly increase especially in patients with low burdens of tumour (Cragg, Bayne et al. 2004).

As shown in Table 1.7, for RIT therapy, the amount of mAb protein given as part of the radioimmunoconjugate is much smaller compared to the amount given as pre-dose in both <sup>90</sup>Y ibritumomab tiuxetan (Zevalin<sup>TM</sup>) and <sup>131</sup>I-tositumomab (Bexxar<sup>TM</sup>) regimens (3.2 mg versus 250 mg/m<sup>2</sup> per patient for <sup>90</sup>Y ibritumomab tiuxetan study, 35 mg versus 450 mg per patient for <sup>131</sup>I-tositumomab study) (Wagner, Wiseman et al. 2002; Wiseman, Kornmehl et al. 2003; Witzig, White et al. 2003; Wahl 2005). In both these two regimens, the pre-doses are given twice prior to the dosimetric study and the therapeutic infusion, respectively. The first pre-dose mAb given 7 days prior to RIT may still be at significantly high dose especially in low tumour burden cases to potentially block the desired tumour binding sites and could therefore decrease the radiation dose delivered to tumour. In addition, the pre-dose mAb may also block enough of the binding sites in the bone marrow to result in significantly altered biodistribution which could differ from the initial dosimetric data obtained after the first pre-dose and trace labelled “dosimetric” dose used for absorbed dose estimation. It is possible the second pre-dose may influence the myelotoxicity prediction based on the dosimetry study, especially for <sup>90</sup>Y ibritumomab tiuxetan because there is an even smaller dose of radiolabelled mAb (3.2 mg per patient) for therapy and the pre-dose is Rituximab, a chimeric mAb. Theoretically a chimeric or humanized mAb may have longer circulating half-life than a murine mAb, but there has not been clinical evidence to indicate if tositumomab, the murine mAb used for pre-dose in <sup>131</sup>I-tositumomab

regimen has shorter half-life than Rituximab used in  $^{90}\text{Y}$  ibritumomab tiuxetan studies (Press and Rasey 2000).

**Table 1.7. Pre-dose Schedules for Zevalin<sup>TM</sup> and Bexxar<sup>TM</sup> RIT Regimens**

		Dosimetric Step	Therapeutic Step
		Day 0	Days 0 - 7
<b>Bexxar<sup>TM</sup></b>	<b>Pre-dose:</b> <b>Tositumomab</b> 450 mg (60 min iv infusion)	<b>Serial <math>\gamma</math> – camera imaging/counting for dosimetric assessment</b>	<b>Pre-dose:</b> <b>Tositumomab</b> 450 mg (60 min iv infusion)
	<b>Dosimetric dose:</b> <b><math>^{131}\text{I}</math>-Tositumomab</b> 35 mg mAb containing $^{131}\text{I}$ 185 MBq (20 min iv infusion)		<b>Therapeutic dose:</b> <b><math>^{131}\text{I}</math>-Tositumomab</b> 35 mg mAb containing $^{131}\text{I}$ activity to deliver 65-75 cGy total body dose (20 min iv infusion)
<b>Zevalin<sup>TM</sup></b>	<b>Pre-dose:</b> <b>Rituximab</b> 250 mg/m <sup>2</sup> (60 min iv infusion)		<b>Pre-dose:</b> <b>Rituximab</b> 250 mg/m <sup>2</sup> (60 min iv infusion)
	<b>Dosimetric dose:</b> <b><math>^{111}\text{In}</math>-ibritumomab tiuxetan</b> 1.6 mg ibritumomab tiuxetan containing $^{111}\text{In}$ 185 MBq (10 min iv infusion)		<b>Therapeutic dose:</b> <b><math>^{90}\text{Y}</math>-ibritumomab tiuxetan</b> 3.2 mg ibritumomab tiuxetan containing $^{90}\text{Y}$ 14.8 MBq/kg or 11.1 MBq/kg for patients with platelet counts higher or lower than $150 \times 10^9/\text{L}$ (10 min iv infusion)

If taking the possible change of the tumour volume into account, during the one week interval between the dosimetry study and the therapeutic dose as recently indicated by Hindorf et al., the estimated absorbed dose would be much more variable and even less reliable (Hindorf, Linden et al. 2003). The same issue is also applicable to bone marrow dosimetry data. This may help to explain the fact that some investigators have found extremely good correction between the dosimetry study and subsequent therapy outcome, whereas others have not. Furthermore, an evidence based method for selecting the optimum dose and timing of the pre-dose may not only improve the efficacy of RIT but also reduce the cost and complexity of delivering this treatment if a subset of patients in whom the pre-dose can safely be omitted is identified.

Practically, the accurate estimation of bone marrow dosimetry has proven to be extremely difficult because of the irregular distribution of active bone marrow involvement of tumour cells and diminished healthy bone marrow in previously heavily treated patients (Fisher 2000). Whilst Wiseman et al argues that this complexity contributes to the lack of necessity of bone marrow dosimetry study, Wahl et al counter that their approach successfully integrates the bone marrow dosimetry data to enable patient-specific RIT and thus achieving significantly better therapy (Wiseman, Leigh et al. 2002; Wahl 2003; Wahl 2005). Notably, Wahl et al have mainly worked on <sup>131</sup>I labelled mAb and Wiseman et al worked on <sup>90</sup>Y labelled mAb which requires <sup>111</sup>In as a surrogate for dosimetric study. Further research seems particularly necessary to standardise the dosimetry methodology and studies in larger number of patients may be helpful in further clarifying this issue. Most recently Dewaraja et al reported that in comparison with their improved patient-specific, 3-dimensional methods for SPECT reconstruction and absorbed dose calculation, the currently widely used conventional clinical RIT dosimetry calculation protocol could have substantially underestimated the radiation doses delivered to tumours by RIT especially for smaller tumours (Dewaraja, Wilderman et al. 2005). In their report, they found that the mean tumour absorbed dose

estimate from the improved calculation protocol was 7% higher than that from conventional dosimetry.

Apart from the biological factors and dosimetry methodology factors mentioned above, the intrinsic physical property of Gamma camera/SPECT used in the clinical RIT dosimetry study could also jeopardise the accuracy of radiation dose estimation because its limited spatial resolution of around 0.8 cm makes it not possible for a Gamma camera image to accurately reflect the real distribution of infused mAb within a targeted tumour or normal organ which is actually at microscopic level.

Unlike the external beam radiation therapy (EBRT), RIT consists of targeted radiotherapy and mAb effector mechanisms. In the evaluation of RIT radiation dose response, however the antibody factor may help to explain the conflicting data regarding the correlation between tumour dosimetry and therapeutic results. The mAb effectors are difficult to measure and it is practically impossible to dissect the action of the two components in clinical RIT. As highlighted by Illidge et al., preclinical studies using well defined syngeneic animal models are required to investigate this further and clarify the relative contributions of mAb effector mechanisms and targeted radiation (Illidge, Cragg et al. 1999).

### **1.6.3 Radiation Dose-Rate-Effect in RIT of NHL**

An important determinant of the magnitude of damage inflicted by irradiation is the amount of ionizing radiation delivered per unit time or the “dose rate”. For a given total dose of radiation delivered, more tissue damage will occur if the radiation is given over a shorter period of time (high dose rate) than if it is delivered over a long interval (low dose rate). It is well known from external beam irradiation (EBRT) that higher dose rate may result in higher therapeutic efficacy but with more severe normal tissue damage. This is believed to be related to the biological capacity of the cells in repairing sublethal

damage taking place during the radiation delivery (Ling, Spiro et al. 1984; Amdur and Bedford 1994). This dose-rate effect is observed much more strikingly in some cell lines (eg. carcinoma cells, melanoma cancer cell lines) than in other cell types (eg. bone marrow cells, lymphoma cell lines). However this has not been investigated well with internal emitters (Knox, Levy et al. 1990; Behr, Memtsoudis et al. 1998; Behr, Blumenthal et al. 2000).

In contrast to EBRT which delivers radiation typically at a dose rate of 100 cGy/min to 200 cGy/min, the RIT usually delivers the radiation dose at an extremely low dose rate of between 0.1 cGy/min to 0.3 cGy/min. Therefore, it might be expected to be less effective than the same dose of irradiation given by conventional EBRT radiotherapy (Press and Rasey 2000). However on the other hand, several mitigating factors may attenuate the deleterious effect of low-dose-rate radiation on therapeutic efficacy: First, RIT delivers radiation continuously, whereas EBRT is usually given on a fractionated schedule in which brief periods of irradiation (1 to 2 minutes) are followed by long intervals (24 hours) before the next dose is administered. The fractionated approach allows cells to repair sub-lethal radiation damage before the next dose of irradiation is delivered. RIT does not permit radiation-free intervals, and thus repair of sub-lethal damage in tumour cells may be impaired by the continuous radiation exposure afforded by radiolabelled mAb.

Many cells, especially those have greatly reduced capacity to repair injury like lymphoma cells, become arrested at the G<sub>2</sub>/M interface of the cell cycle when exposed to low-dose-rate radiation. At low dose rates, many cell types progress through G<sub>1</sub>, S and early G<sub>2</sub> phase, but stop cycling during the late G<sub>2</sub> and M phase. Because the cells are much more sensitive to the lethal effects of irradiation during the G<sub>2</sub>/M phase, this G<sub>2</sub>/M block sensitizes the target cells to further irradiation and may cause inverse dose-rate effect (Press and Rasey 2000). Impressively, in comparative experiments using a subcutaneous murine lymphoma model (38C13), Knox et al. reported the significantly increased tumour-killing effect with decreased dose rate (Knox, Levy et al. 1990). However, in their experiments, the most effective treatment came from the

administration of  $^{131}\text{I}$  labelled anti-idiotype mAb in which the anti-idiotype mAb itself may have been intrinsically therapeutic. More recently, Knox et al reported that in clinical trials some responses have been observed when estimated tumour doses are considerably lower than doses usually required to achieve similar responses using conventional fractionated high-dose-rate EBRT (Knox and Meredith 2000).

On the contrast, Behr et al. using nude mice bearing human colon cancer observed different phenomena. In their experiments comparing the therapeutic effect of  $^{131}\text{I}$  labelled whole IgG,  $\text{F}(\text{ab}')_2$  and Fab fragments, they concluded that the radioimmunoconjugates which delivered higher dose-rate irradiation to the target achieved more efficient therapeutic effects (Behr, Memtsoudis et al. 1998; Behr, Blumenthal et al. 2000; Behr, Behe et al. 2002). These observations suggests that dose rate effects could be very important in the evaluation of RIT and further investigations are necessary to clarify if there exists a significant difference between different tumour types in terms of their responses to low dose-rate irradiation.

#### **1.6.4 The mAb Mediated Cytotoxicity in RIT**

The response of eukaryotic cells to ionising radiation includes cell cycle arrest, activation of DNA repair mechanisms and cell death by necrosis or apoptosis (Illidge 1998). Early RIT investigators regarded the mAb as only vectors of delivering radioisotopes to the targeted tumour.

Following the clinical progress of immunotherapy and RIT especially for NHL, more and more attention has been paid to the intrinsic therapeutic effect of the mAb in RIT. Works from our group have demonstrated that there is an additive effect of in vitro lymphoma cell killing when mAb treated cells were exposed to EBRT (Illidge, Cragg et al. 1999; Du, Honeychurch et al. 2004). In vitro work has demonstrated that the mAb could induce tumour killing through antibody dependent cellular cytotoxicity (ADCC),

complement dependent cytotoxicity (CDC) and by triggering intracellular apoptosis signalling transduction (Cragg, French et al. 1999; Du, Honeychurch et al. 2004; Teeling, French et al. 2004). Which factor plays the most important role in vivo remains largely unknown and probably varies from: (1) the mAb used, (2) tumour targeting, (3) host immune status, (4) tumour to tumour (Tutt, French et al. 1998; Cragg and Glennie 2003). There has been increasing evidence that ADCC may be of critical importance in determining clinical response (Denkers, Badger et al. 1985; Kaminski, Kitamura et al. 1986; Surfus, Hank et al. 1996). However, having compared a panel of anti-B-cell mAb in syngeneic animal models A31 and BCL<sub>1</sub>, Tutt et al suggested that results from in vitro assays do not correlate with activity in vivo and indicated that for B cell lymphomas, therapeutically successful mAbs appeared to be those directed at key receptor molecules, such as idiotype, CD19, and CD40 involved in trans-membrane signalling but not the mAb good at in vitro ADCC, such as anti-MHCII.

More recently, Cragg et al (Cragg and Glennie 2003) reported that three currently widely used anti-CD20 mAbs (Rituximab, 1F5 and anti-B1) act through distinctively different mechanisms in the therapy of two lymphoma xenograft models. While Rituximab and 1F5 redistribute CD20 into membrane rafts, are bound efficiently by the complement component C1q and deposit C3b resulting in CDC which forms the major therapeutic effect of these two mAbs. In contrast, complement depletion had no effect on the potent therapeutic activity of anti-B1 (tositumomab), a mAb that does not redistribute CD20 into membrane rafts, bind C1q or cause efficient CDC. F(ab')<sub>2</sub> fragments of anti-B1 (tositumomab) but not 1F5 were observed able to provide substantial immunotherapy, indicating that non-Fc dependent mechanisms are involved in the tositumomab action. In accordance with this, tositumomab was shown to induce much higher levels of apoptosis than Rituximab and 1F5, suggesting that, whilst complement is important for the action of Rituximab and 1F5, this is not the case for tositumomab, which more likely functions through its ability to induce downstream signal transduction that results in apoptosis. So far, clinical results concerning the action mechanisms of anti-CD20 mAbs has been controversial and there remains considerable uncertainty about their mechanisms of action, while some of the investigators addressed

the importance of CDC in clinical immunotherapy, others have found that it fail to predict the therapeutic response (Bannerji, Kitada et al. 2003; Chan, Hughes et al. 2003).

In summary, mAb is highly likely to contribute to the treatment effects of RIT through its intrinsic therapeutic mechanisms. Preclinical work has indicated that the intrinsic cytotoxicity of mAb could be as important as its ability to effectively deliver targeted radiotherapy in the RIT of lymphoma (Illidge, Cragg et al. 1999; Du, Honeychurch et al. 2004). Further investigation is however requested to elucidate the mechanisms of the interaction between the mAb and low dose rate irradiation. Such data may help to provide new insights into the mechanisms underlying successful RIT.

## **1.7 The Contribution of Experimental Radioimmunotherapy**

Experimental RIT has significantly contributed to the development of clinical RIT. Studies of experimental RIT have primarily used multicell spheroids (Langmuir, Atcher et al. 1990; Langmuir, Mendonca et al. 1992; Langmuir, Mendonca et al. 1992; Buchsbaum, Langmuir et al. 1993) and a variety of animals models((Knox 1995; Behr, Goldenberg et al. 1997). Findings from these preclinical studies have influenced the design of ongoing clinical studies and will continue to do so as the biology of RIT is better understood and additional knowledge is gained about ways to optimise the efficacy of RIT.

### **1.7.1 The Use of Animal Models in Radioimmunotherapy**

Multicell spheroids consist of aggregated tumour cells with a diameter of 1.0mm or more. In vitro spheroids contain an extracellular matrix. These spheroids can be useful in vitro mimicking three-dimensional models of micrometastases and microscopic

regions of tumours. Langmuir et al have reported the successful use of these spheroids on the comparison of therapeutic effects of different radionuclides and different moAbs (Langmuir, Mendonca et al. 1992; Langmuir, Mendonca et al. 1992). But multicell spheroids are of no use for the study of pharmacokinetics or the role of vascular effects or host effector mechanisms in RIT.

One of the unique properties of radiolabelled antibody therapy is the systemic radiation delivery with a selective tumour enhanced uptake. Only in vivo animal experiments and clinical studies are potentially able to demonstrate this selective uptake. The number of questions that can be answered from clinical studies involving patients is often limited by ethical and practical difficulties.

Therefore, animal modelling finds its greatest utility for RIT in terms of:

- (a) Initial radiolabelled antibody screening
- (b) Preliminary efficacy studies for target/non-target specificity and ways to improve low tumour uptake
- (c) Suitability of a radiolabel
- (d) Preliminary toxicity studies
- (e) Comparing the therapeutic efficacy of various radiolabels in combination with different antibodies or antibody fragments
- (f) Basic dosimetry evaluation

Animal models have been useful for studying radiolabelled mAb targeting of tumours *in vivo* and for the study of the biology and pharmacokinetics of RIT. A variety of animal models, radionuclides, and antibodies have been used in these studies (Buchsbaum, Langmuir et al. 1993; Knox 1995). The *in vivo* targeting of radiolabelled mAb and tumour response to the effects of irradiation have largely been focused on tumour xenograft RIT experiments (Buchsbaum, Brubaker et al. 1990; Buchsbaum, Langmuir et al. 1993; Kinuya, Yokoyama et al. 1998). The major advantage of this approach is that the human xenograft appears to preserve its intrinsic radiosensitivity in the nude

mice as well as the important determinants of tumour growth delay and the tumour control dose.

More recently, advances in experimental radioimmunotherapy have been characterised by the development of metastatic, rather than subcutaneous, tumor models in nude mice, which appear to reflect the clinical situation more accurately. Furthermore, the recent development of strategies to reduce the renal accretion of antibody fragments and peptides enables the use of such smaller molecules for therapy, especially those also labelled with radiometals and other forms of intracellularly retained radionuclides (Saga, Weinstein et al. 1994; Behr, Goldenberg et al. 1997; Saga, Sakahara et al. 1999; Sato, Saga et al. 1999).

Extrapolation from animal models to clinical studies in patients is primarily limited by the relatively small size and small volume of distribution in animals especially rodents. This would significantly affects the percentage of injected dose/gram tissue of radiolabelled antibody in tumour and the plasma half-life of radiolabelled antibodies. And, due to the lack of an intact immune system, nude mice are of limited use for the study of host immune responses.

Nevertheless, a syngeneic tumour model is likely to be of far more value in this regard than a human tumour mouse xenograft model. Differing from nude mice models in which the human tumour cells develop in murine hosts with severely compromised immune system, the syngeneic animal models mimic more aspects of the actual human cancer treatment situation better. Using these kinds of murine models, the targeting of radiolabelled mAb can be investigated with the presence of cross reaction with normal tissues and the cytotoxicity effects of mAb can be assessed with the presence of an intact host immune system especially in the RIT of lymphoma (Illidge, Cragg et al. 1999).

## 1.7.2 Approaches to Improve the Therapeutic Index of RIT

Wahl (Wahl 1994) has previously outlined the factors thought to be required to optimise RIT:

- (a) Increased targeting of radiolabelled mAb to tumour
- (b) Decreased uptake of radiolabelled mAb by normal tissue
- (c) Less normal tissue toxicity from the emitted radiation
- (d) Greater therapeutic effects of the radiation in tumour

A variety of approaches have been taken to increase the therapeutic efficacy and decrease the toxicity of RIT. Such approaches have included improvements in mAb, such as the development of chimeric or humanized mAb (Schlom, Siler et al. 1991), bifunctional antibodies (Le Doussal, Barbet et al. 1992; Sharkey, Karacay et al. 2003) and recombinant constructs/fragments (Schlom, Siler et al. 1991). Improvements in labelling and chelation chemistry have resulted in improved chelate stability (Safavy, Buchsbaum et al. 1993) and radioiodination with less tumour cell-mediated dehalogenation (Zalutsky, Noska et al. 1989). Studies using animal models have provided information that will allow for selection of radionuclides with desirable emission properties for specific clinical situation. In a human colon cancer xenograft model, Buchsbaum et al (Buchsbaum, Brubaker et al. 1990) compared the therapeutic effects of  $^{131}\text{I}$  labelled and  $^{90}\text{Y}$  labelled 17-1A mAb and concluded that  $^{131}\text{I}$  labelled 17-1A mAb was less toxic and more effective than  $^{90}\text{Y}$  labelled 17-1A mAb. However, in a recent study aiming to compare the therapeutic effectiveness of  $^{90}\text{Y}$  labelled mAb with  $^{131}\text{I}$  labelled mAb, Stein et al found that  $^{90}\text{Y}$  labelled mAb was superior to  $^{131}\text{I}$  labelled mAb (Stein, Chen et al. 1997). In this study, both radiolabels were evaluated when delivering to human tumour xenografts at their maximum tolerated doses (MTD).

Animal models have also been used to evaluate the RIT potential of Auger electron emitters (Behr, Sgouros et al. 1998; Behr, Behe et al. 2000) and  $\alpha$  emitters which have

the advantage of higher linear energy transfer (LET) such  $^{225}\text{Ac}$  (Borchardt, Yuan et al. 2003),  $^{213}\text{Bi}$  (Michel, Rosario et al. 2003) and  $^{211}\text{At}$  (Andersson, Elgqvist et al. 2003).

One of the greatest problems in RIT is the relatively low tumour uptake of radiolabelled mAb in human tumours and the relatively high background levels of radiolabelled mAb in normal tissues. Animal models have been extensively investigated for ways to improve delivery of radiolabelled mAb to tumour. Approaches that have been taken for increasing the localization of radiolabelled mAb in tumour include the use of unlabelled mAb to bind non-specific binding sites (Buchsbaum, Wahl et al. 1992), regional administration (Huber, Seidl et al. 2003; Janssen, Pels et al. 2003; Kinuya, Li et al. 2003), hyperthermia (Kinuya, Yokoyama et al. 2000; Saga, Sakahara et al. 2001), mAb fragments RIT (Behr, Blumenthal et al. 2000), drugs for increasing vascular permeability and blood flow (Hennigan, Begent et al. 1991), and pretargeting approaches in which the administration of a clearing reagent as part of pretargeting regimen has resulted in increased tumour/normal tissue ratios (Kraeber-Bodere, Sai-Maurel et al. 2002; Zhang, Yao et al. 2002; Kinuya, Li et al. 2003; Sharkey, McBride et al. 2003; Zhang, Zhang et al. 2003; Yao, Zhang et al. 2004). Animal models have also been extensively used to evaluate the therapeutic advantages of combination therapy approaches in which RIT has been combined with chemotherapy (Denardo, Richman et al. 1998; Behr, Memtsoudis et al. 1999; Kinuya, Yokoyama et al. 2000; Ng, Kramer et al. 2001) or conventional radiotherapy (Buchegger, Roth et al. 2000) or anti-vascular agents (Pedley, Hill et al. 2001).

### **1.7.3 Defining the Determinants of Successful RIT of Lymphoma**

Although impressive progress has been made especially in the application of RIT on NHL, the mechanisms of action are still poorly understood. Animal models provide unique opportunities to explore these important issues.

In the 38C13 murine B-cell lymphoma model described by Knox et al (Knox, Levy et al. 1990), the biological effect of  $^{131}\text{I}$  labelled mAb were compared with dose equivalent external beam irradiation. Continuous exponentially decreasing low dose rate (LDR)  $\gamma$ -irradiation and multiple fractions (MF) of X-irradiation were compared with dose equivalent  $^{131}\text{I}$  labelled mAb.

The relative therapeutic efficacy of RIT, and the relative contribution of (a) low dose rate; (b) whole body irradiation; and (c) dosimetry to the overall effect were determined. Groups of mice with or without B-cell lymphoma were treated with either (a)  $^{131}\text{I}$ -anti-idiotype mAb; (b)  $^{131}\text{I}$ -isotype-matched irrelevant control mAb; (c) 5-15 Gy 250 kV X-irradiation given as a single fraction; (d) 2.5-30 Gy 250 kV X-irradiation given in 10 fractions over two weeks; or by (d) continuous exponentially decreasing  $\gamma$ -irradiation via a  $^{137}\text{Cs}$  source, which simulated the effective  $t_{1/2}$  of the  $^{131}\text{I}$  labelled mAb.

In this study  $^{131}\text{I}$ -anti-idiotype mAb was found 3.25 times more effective than dose equivalent MF for tumour growth inhibition. This effect was postulated to be secondary to the combined effects of the low dose rate irradiation and specific uptake of  $^{131}\text{I}$ -anti-idiotype mAb by tumour. The data also demonstrated a significant increase in the tumour responses to low dose rate irradiation (<28.8 cGy/hour) as shown by the increased efficacy of continuous exponentially decreasing LDR irradiation compared with MF X-irradiation.  $^{131}\text{I}$ -anti-idiotype mAb was approximately twice as effective as LDR, on the basis of whole body dose equivalents, thought to be due to the concentration ratio of  $^{131}\text{I}$ -anti-idiotype mAb as the tumour/whole body ratio was approximately 1.7. Disappointingly, although there was a statistically significant difference ( $P=0.02$ ) between specific (anti-idiotype) and non-specific (irrelevant)  $^{131}\text{I}$ -mAb on tumour response, the relative efficacy was as little as 1.18. The authors suggested that this might be due to (a) the lack of sustained high concentrations of  $^{131}\text{I}$ -anti-idiotype mAb at the tumour site because of antigenic modulation and rapid dehalogenation (the effective  $t_{1/2}$  was 3.4 days for the non-specific  $^{131}\text{I}$ -mAb, and 2.5 days for specific  $^{131}\text{I}$ -mAb in tumour bearing animals); or (b) non-specific uptake of

non-specific antibody because of differences in vascular permeability between tumour and normal vasculature.

The authors concluded that the total effect of RIT on both tumour growth inhibition and toxicity is a function of the total dose, dose rate, and both specific and non-specific  $^{131}\text{I}$ -mAb distribution. However, the authors failed to adequately address the possible intrinsic tumour inhibitory effect of the anti-idiotype mAb at all. The potential effects of anti-idiotype therapy are now well documented in the literature for both B-cell lymphoma animal models (Tutt, French et al. 1998) and also in the clinic (Vuist, Levy et al. 1994).

Whilst the early RIT studies were focused solely on the ability to deliver tumourcidal doses of radiation by the radiolabelled mAb, the importance of the mAb tumour cytotoxicity effects have only recently been emphasised in RIT. In a comparison study using athymic nude mice bearing human Burkitt's lymphoma xenografts, Buchabaum et al (Buchsbaum, Wahl et al. 1992) compared the therapeutic effects of  $^{131}\text{I}$  labelled anti-B1 mAb (tositumomab),  $^{131}\text{I}$  labelled MB-1 mAb (anti-CD37) and their unlabelled forms. The  $^{131}\text{I}$  labelled MB-1 mAb demonstrated superior effects over the unlabelled mAb and same amount of  $^{131}\text{I}$  labelled control mAb. The unlabelled anti-B1 achieved similar therapeutic results to 300  $\mu\text{Ci}$   $^{131}\text{I}$  and 450  $\mu\text{Ci}$   $^{131}\text{I}$  labelled anti-B1 mAb.

The authors believed that this impressive tumour inhibitory effect of the unlabelled anti-B1 mAb should be explained by the in vitro cytotoxicity activity. The results of this study underscored the importance of mAb effector mechanisms in RIT. However, in this study, the radiolabelled mAb was given by intra-peritoneal (i.p) injection. Compare to intravenous infusions used in clinical settings, intraperitoneal injections could theoretically substantially delay the uptake of the injected mAb by the subcutaneously planted tumour xenografts especially in early time points and reduce the actually irradiation dose delivered to the tumour. Unfortunately, the authors did not perform the dosimetry analysis and only observed the tumour growth under different therapies.

More recently, our own group have explored this issue further on syngeneic murine lymphoma models using a panel of anti-mouse B-cell antibodies (Illidge, Cragg et al. 1999; Illidge, Honeychurch et al. 2000). By targeting highly expressed antigens on BCL<sub>1</sub> tumours as well as normal B-cells, the anti-major histocompatibility complex (MHC) class II mAb was found to be superior in delivering higher radiation dose to the tumour bearing organ. Although this antibody is not significant therapeutic when unlabelled, the <sup>131</sup>I labelled anti-MHCII mAb improved animal survival as a result of targeted irradiation alone. In contrast, for low tumour burdens, <sup>131</sup>I-anti-idiotype mAb, which has therapeutic activity as an unconjugated antibody, provided long term protection. These results demonstrated the relative contribution of mAb and of targeted irradiation to the therapeutic effects of RIT *in vivo*. With appropriate recognition of the limitations of animal experimental data, these findings have important implications for the selection of reagents in RIT of B-cell lymphoma (Illidge and Johnson 2000).

## **Optimisation of RIT for NHL**

Over the past 15 years, substantial progress has been made with RIT of lymphomas. The impressive results have attracted much attention and sparked expectation for the future role of RIT in the management of NHL. To explore the so far still poorly understood mechanisms lying behind the apparently successful RIT for NHL is therefore of imminent importance in order to fulfil more efficiently the potential advantages of RIT and to optimize the clinical application of this promising approach.

## **Aims of Thesis**

The aims of the thesis were:

1. To establish optimal radioiodination technique of mAb for preclinical and clinical RIT studies.
2. To further develop animal models of RIT and to explore the interaction of mAb with radiation in the clearance of tumour in vitro and in vivo.
3. To determine the relative contribution of mAb and targeted irradiation to tumour cell killing in RIT.
4. To explore whether radiation dose response exists in RIT of NHL.

## Chapter 2 Materials and Methods

### 2.1 Animals and Cell Lines

Mice were supplied by Harlan UK Limited (Blackthorn, UK), and maintained in local animal facilities. BCL<sub>1</sub> (Slavin and Strober 1978; Illidge, Cragg et al. 1999; Honeychurch, Glennie et al. 2003) and A31 (Cobb, Glennie et al. 1986; Honeychurch, Glennie et al. 2003) are B-cell lymphomas that arose spontaneously in mice and are maintained at our research facility by in vivo passage in BALB/c and CBA/H mice, respectively. Unlike most human lymphomas, which are disseminated, BCL<sub>1</sub> and A31 tumour cells develop predominantly in the spleen and at late stage the liver with a leukaemic spill in the terminal stages of the disease. Early studies had demonstrated that the spleen is the only host organ for the early development of BCL<sub>1</sub> tumour and BCL<sub>1</sub> cell did not grow in splenectomised recipients (Kotzin and Strober 1980). Enlarged spleens were taken at the terminal stage of disease, homogenised using BD Falcon cell strainer (BD Biosciences, Two Oak Park, Bedford, MA, USA) and lymphocytes isolated by centrifugation on Lymphoprep™ (Axis-Shield PoC, Oslo, Norway) at 2500 rpm for 20 minutes. Cell concentrations were determined using a Coulter Industrial D Cell Counter (Coulter Electronics, Bedfordshire). Single cell suspensions were passaged at 10<sup>6</sup> – 10<sup>7</sup> cells/mouse by intra-peritoneal (i.p) injection.

πBCL<sub>1</sub> is a transformed variant of the BCL<sub>1</sub> lymphoma established at our laboratory that can be maintained in culture as well as in vivo (Illidge, Honeychurch et al. 2000). In vitro πBCL<sub>1</sub> was maintained in RPMI medium (Life Technologies, Paisley, UK) supplemented with glutamine (2 mM), pyruvate (1 mM), penicillin and streptomycin (100 IU/mL), fungizone (2 µg/mL), 2-Mercaptoethanol (50 µM) (BDH, Poole, UK) and 15% FCS (Myoclon; Life Technologies) at 37°C in a 5% CO<sub>2</sub> humidified incubator. Medium was replaced every 2-3 days. Cells used for the assessment of intracellular

signalling transduction and immunoreactivity measurement were maintained in log phase growth for 24 hours prior to the experiments.

Human lymphoma cell lines, Daudi, EHRB and Raji were obtained from the European Collection of Cell Cultures (ECACC, Salisbury, United Kingdom). The cell lines were maintained also in RPMI medium (Life Technologies, Paisley, UK) supplemented with glutamine (2 mM), pyruvate (1 mM), penicillin and streptomycin (100 IU/mL), fungizone (2 µg/mL) and 10% FCS (Myoclon; Life Technologies).

## 2.2 Antibodies and Radioiodination

A list of rat anti-mouse mAbs used in this study and their sources is given in Table 2.1 (George, McBride et al. 1991; Torres, Law et al. 1992; Krop, de Fougerolles et al. 1996). The carrier free  $^{125}\text{I}$  and  $^{131}\text{I}$  radioisotopes were supplied from Amersham International, plc, UK. Different mAb radioiodine labelling methods such as Chloramine-T, Iodogen-Beads and N-bromosuccinimide (NBS) were compared for labelling efficiency and immunoreactivity of labelled mAb. Serial concentrations of anti-MHCII mAb (TI 2-3) ranging from 500 µg/ml to 5 mg/ml were labelled to 14.8 MBq  $^{125}\text{I}$  using Chloramine-T, Iodogen-Beads and NBS methods as previously reported (Lee and Griffiths 1984; Shani, Wolf et al. 1986; Mather and Ward 1987; Woltanski, Besch et al. 1990; Behr, Gotthardt et al. 2002). Briefly: For Chloramine-T method, 14.8 MBq  $^{125}\text{I}$  was added to two sets of 0.25 ml of two concentrations (500 µg/ml and 5 mg/ml) of TI2-3 mAb diluted with phosphate buffered saline (PBS). 100 µl freshly prepared chloramines-T solution (0.5 mg/ml in injection water) was added promptly into the mAb and was shaken for 10 seconds every 2 minutes for 10 minutes. For Iodogen-Beads method, 14.8 MBq  $^{125}\text{I}$  was added to same amounts of TI2-3 mAb followed by the prompt adding of 2 Iodogen-Beads (Pierce Chemicals Co, Rockford, IL, USA) and 10 seconds shaking every 2 minutes for 10 minutes. For NBS method, same amount of  $^{125}\text{I}$  was also added to the PBS diluted mAb followed by the addition of

50 µg of NBS (1.0 mg/ml in injection water) and 10 seconds shaking every 2 minutes for 10 minutes (Du 1995). Labelling efficiency was monitored by instant thin layer chromatography (ITLC, Gelman Sciences Inc., Ann Arbor, MI, USA, developing in 80% methanol) through counting the radioactivity of the ITLC strip sections using a  $\gamma$ -counter (Wallac 1282 Compugamma Gamma counter, PerkinElmer Life Sciences, Inc., MA, USA.). Labelling efficiency of chosen samples were also measured by high performance liquid chromatography (HPLC, Varian ProStar 320, Varian Analytical Instruments, Walnut Creek, CA, USA.) immediately after the labelling procedure (Mather and Ward 1987; Bhargava and Acharya 1989). After the labelling procedure, serial samples of radiolabelled mAb were taken and diluted in cell culture medium for the assessment of immunoreactivity as described below. The radioactive work was conducted in a designated isolated room designed for radioactive experiments and the labelling procedures were performed in a dedicated negative air flow hood.

**Table 2.1. Anti-mouse monoclonal antibodies used in this work**

Antibody Clone	Specificity	Isotype	Affinity (Ka; M <sup>-1</sup> )	Saturation level	Source (ref.)
<b>Mc10-6A5</b>	BCL <sub>1</sub> Id	Ratγ2a	1 x 10 <sup>9</sup>	3.5 x 10 <sup>5</sup>	(George, McBride et al. 1991)
<b>Mc39-16</b>	A31 Id	Ratγ2a	5 x 10 <sup>8</sup>	2.0 x 10 <sup>5</sup>	Tenovus
<b>1D3</b>	CD19	Ratγ2a	3 x 10 <sup>8</sup>	1.6 x 10 <sup>5</sup>	(Krop, de Fougerolles et al. 1996)
<b>NIMR6</b>	CD22	Ratγ1	1.2 x 10 <sup>8</sup>	1.5 x 10 <sup>5</sup>	(Torres, Law et al. 1992)
<b>YBW42.2.2</b>	CD45	Ratγ2a	2.4 x 10 <sup>8</sup>	5.8 x 10 <sup>5</sup>	Oxford**
<b>YW62.3.2</b>	CD45	Ratγ2b	2.8 x 10 <sup>8</sup>	6.3 x 10 <sup>5</sup>	Oxford**
<b>TI2-3</b>	MHCII	Ratγ1	5.3 x 10 <sup>8</sup>	7.8 x 10 <sup>5</sup>	(Illidge, Cragg et al. 1999)
<b>1A5E8</b>	CD38	Ratγ1	1.5 x 10 <sup>8</sup>	1.4 x 10 <sup>5</sup>	Parkhouse*

\* Generous gift from Michael E Parkhouse.

\*\* Generous gift from Dr. Stephen Cobbold in the University of Oxford.

Mouse anti-human CD20 antibody Tositumomab (anti-B1) was obtained from Coulter Pharmaceuticals (Miami, FL, USA). Chimeric anti-human CD20 antibody Rituximab (C2B8, Mabthera) was obtained from IDEC Pharmaceuticals (San Francisco, CA, USA) and Roche Registration Limited (Welwyn Garden City, UK).

## **2.3 Immunoreactivity of Radiolabelled mAb**

The immunoreactivity of radiolabelled antibodies was assessed according to the method described by Elliot et al (Elliott, Glennie et al. 1987). Briefly, log phase growth  $\pi$ BCL<sub>1</sub> tumour cells were serially diluted starting from the concentration of  $5 \times 10^7$ /ml. 0.25  $\mu$ g radiolabelled specific and non-specific mAbs were added to 500  $\mu$ l cells and incubated at 37°C for 2 hours. Endocytosis of bound antibody was prevented by the inclusion of NaN<sub>3</sub> (15 mM) and 2-deoxyglucose (50 mM). Following incubation, cells with bound antibody were rapidly separated from unbound antibody by centrifugation through a 1.1:1 (v/v) mixture of dibutyl phthalate:diethyl phthalate oils. The cell pellets with bound radiolabelled antibodies were counted on a  $\gamma$ -counter (Wallace 1282 Compugamma, PerkinElmer Life Sciences, Inc., MA, USA). The activity of 0.25  $\mu$ g radiolabelled mAb was also counted as the total count. The immunoreactivity was determined as the percentage of the radioactivity of the cell pellet (subtracted by non-specific binding) out of the total at maximal binding (mAb saturation level). For the chosen Iodogen-beads method which showed the highest labelled efficiency (95.5 - 98.5 %) and good post labelling immunoreactivity (65 – 75%), 185 MBq – 740 MBq <sup>131</sup>I were labelled (specific activity 37 - 185 MBq/mg) and the immunoreactivities of labelled mAb were assessed in comparison with the relatively lower activity of <sup>125</sup>I labelled products. For the assessment of immunoreactivity of <sup>131</sup>I labeled Rituximab (using Iodogen-Beads method, up to 3.0 GBq <sup>131</sup>I has been labelled with Rituximab with a higher than 95% labelling efficiency and specific activity of 600 MBq/mg), log phase growth human lymphoma cell line (Daudi cells) were used instead of murine  $\pi$ BCL<sub>1</sub> cells.

Similar to the immunoreactivity assay, as described by Tutt et al, the binding density of these mAb to  $\pi$ BCL<sub>1</sub> cells were assessed by the binding curve assay. Briefly, mAb were radiolabelled with trace amount of  $^{125}$ I and were serially diluted with culture medium before incubating with  $10^6$  cells in complete medium for 2 hours at 37°C in a 5% CO<sub>2</sub> incubator. Assuming the molecular weight of all the mAb is same ( $1.5 \times 10^5$ ), taking into account of the immunoreactivity of individual mAb, the cell binding curves of all the mAb were plotted as molecules of mAb per cell against the concentration of mAb.

## 2.4 Measurement of Surface Antigen by Immunofluorescence

Cultured cells or splenocytes at  $1 \times 10^6$ /ml were incubated at 4°C for 30 minutes with the fluorescein conjugated (direct) or unlabelled (indirect) antibody of choice (50  $\mu$ g/ml final concentration). Cells were then washed three times in PBS-BSA-azide (PBS, 1% Bovine Serum Albumin, 20 nM NaN<sub>3</sub>) and resuspended in PBS at approximately  $1 \times 10^6$ /ml. For indirect immunofluorescence, cells were further incubated for 30 minutes at 4°C with an fluorescein labelled secondary antibody directed to the first antibody and washed three more times in PBS-BSA-azide before resuspending to  $1 \times 10^6$ /ml and subsequent analysis with flow cytometer.

Analysis was performed on a FACScan flow cytometer (Becton Dickinson, Mountain View, CA, USA). Routinely, 10,000 events were collected per sample for analysis. Cell debris was excluded by adjustment of the forward scatter (FSC) threshold parameter. Samples were analysed using LYSIS II software (Becton Dickinson). Fluorescence intensities were assessed in comparison to negative control samples and usually expressed as histograms of fluorescence intensity versus cell number.

## **2.5 In Vitro Cytotoxicity Assessment of mAb: Complement Dependent Cytotoxicity (CDC) and Antibody Dependent Cellular Cytotoxicity (ADCC) Assays**

Complement dependent cytotoxicity (CDC) and antibody dependent cellular cytotoxicity (ADCC) are believed two of the most important mechanisms of mAb mediated tumour cytotoxicity. As previously reported by Tutt et al (Tutt, French et al. 1998), the ability of the mAb to kill BCL<sub>1</sub> and  $\pi$ BCL<sub>1</sub> cells in CDC and ADCC assays were determined and compared in this study.

For CDC assay, as described by George et al (George, McBride et al. 1991), target cells (harvested BCL<sub>1</sub> cells) were resuspended in DMEM to a cell density of  $3 \times 10^7$  cells/ml.  $^{51}\text{Cr}$  (185 MBq of Sodium  $^{51}\text{Cr}$ Chromate, supplied by Amersham International Plc., Bucks, UK) was added to 3 ml of cells which were then incubated at 37°C water bath for 30 minutes. 100  $\mu\text{l}$  of  $^{51}\text{Cr}$  labelled cells were aliquoted into plastic test tubes which were kept on ice before 100  $\mu\text{l}$  various concentrations of each mAb and control reagents were added. The tubes were then incubated on ice for 30 minutes. 300  $\mu\text{l}$  fresh rat serum (final dilution, 1/3 with supplemented DMEM) was then added as a source of complement, and the samples were transferred to 37°C water bath for 45 minutes. The samples were centrifuged at 1500 rpm for 5 minutes to sediment cells, and 200  $\mu\text{l}$  supernatant was removed from each sample for specific  $^{51}\text{Cr}$  release by counting the supernatant. All samples were run in triplicate and the maximum release was determined by measuring  $^{51}\text{Cr}$  release obtained after addition of 400  $\mu\text{l}$  1% Nonidet P-40 to same amount of cells. Specific  $^{51}\text{Cr}$  release was expressed as a percentage using the following equation:

$$\% \text{ specific release} = [( \text{sample release} - \text{background release}) / (\text{maximum release} - \text{background release})] \times 100.$$

In ADCC assay,  $^{51}\text{Cr}$ -labelled cells ( $5 \times 10^3$ ) at 50  $\mu\text{l}$  aliquots in supplemented DMEM were added to 96-well U-bottomed culture plates (Life Technologies, Paisley, U.K.) and

left on ice for 15 minutes. Human peripheral monocytes were used as effector cells and aliquots of 100  $\mu$ l of effector cells also in supplemented DMEM were added at an Effector:Target cell ratio of 50:1. The plates were centrifuged at 200 g for 5 minutes at room temperature, incubated for 6 hours at 37°C in a 5% CO<sub>2</sub> incubator, then centrifuged at 500 g for 5 minutes and harvest 100  $\mu$ l of the supernatant to calculate the specific <sup>51</sup>Cr release by comparing with the activity of same volume of 1% Nonidet P-40 treated cells using the standard formula: % specific release = [(sample release – background release)/(maximum release – background release)] x 100. All determinations were performed in triplicate.

## 2.6 Biodistribution Studies and Organ Dosimetry Estimation

Groups of BALB/c or CBA/H mice were injected via the tail vein with 10<sup>5</sup> BCL<sub>1</sub> or 10<sup>6</sup> A31 cells, respectively. The intravenous tumour inoculation of animals as well as the infusions of radiolabelled and unlabelled mAbs was performed by trained animal technicians at Tenovus Research Laboratory, Southampton. Ten days post tumour inoculation animals received 500  $\mu$ g of <sup>125</sup>I-labeled mAbs by intravenous injection. In the cases of late-stage tumour biodistribution studies, the <sup>125</sup>I-labeled mAbs were given 18 days post tumour inoculation. In order to investigate the impact of pre-dose on the dosimetry of subsequently administered radioisotope labelled mAb, 500  $\mu$ g unlabelled mAb was used as a pre-dose which was also given intravenously 2-3 hours prior to the injection of the identical <sup>125</sup>I-labeled mAb. To block thyroid uptake of radioactive iodine, mice were given Lugol's solution (5.0 ml Lugol's stock in 400 ml H<sub>2</sub>O; Lugol's stock: 10 g KI, 5 g elemental iodine in 100 ml water) in their drinking water 3 days prior to the administration of the <sup>125</sup>I-labeled mAb. Biodistribution of each radioactive mAb (anti-Id, anti-CD19, anti-MHCII) was compared with an isotype matched control antibody. Animals were sacrificed 1, 8, 24, 48 and 96 hours after receiving the radioactive mAb and the blood, spleen, liver, kidneys and lungs assessed.

The weight and radioactive counts of the dissected organs were measured, and the percentage of the injected dose/g of tissue (%ID/g) was calculated as described by Badger et al (Badger, Davis et al. 1991). Briefly, the radioactive counts of the particular tissue were measured by  $\gamma$ -counter (Wallace 1282 Compugamma, PerkinElmer Life Sciences, Inc. MA, USA.) which were divided by the weights of the tissue to calculate out the radioactivity/gram tissue. By comparing the radioactivity/gram tissue with the total injected dose (also measured by the same gamma counter), the injected dose per gram of tissue (%ID/g) was obtained. Through the assessment of the corresponding tissues at serial time points, the effective half-life and biodistribution of the labelled antibodies were determined. The absolute radioactivity of the total injected dose was also measured using a radioisotope dose calibrator (Atomlab 100 plus, Biodex Medical Systems, NY, USA.). Assuming total absorption of the non-penetrating radiation component with a homogeneous distribution, both the whole body and the organ doses were calculated by integrating the area under the retention curve (Loevinger 1988; Loevinger 1988).

## 2.7 RIT Experiments Using Murine B-cell Lymphoma Models

Age and sex-matched mice were inoculated by intravenous injection with  $10^6$  A31 or  $10^5$  BCL<sub>1</sub> lymphoma cells on day 0, and treated with RIT 10 days later. For RIT experiments, 500  $\mu$ g (anti-CD19, anti-CD38, anti-CD45, anti-MHCII, or anti-BCL<sub>1</sub> Id) or 100  $\mu$ g (anti-A31 Id)  $^{131}$ I-labeled mAb carrying 1.85 MBq – 37.0 MBq was injected via the tail vein intravenously per mouse. For therapies combining RIT with unlabeled mAb, mice were injected intravenously with unlabeled anti-BCL<sub>1</sub> or anti-A31 Id antibodies (doses as above), 2 to 3 hours prior to the injection of the  $^{131}$ I-labeled anti-MHCII or  $^{131}$ I-labeled anti-CD19 or  $^{131}$ I-labeled anti-CD45 mAb. Parallel groups of mice were treated with unlabeled antibodies alone or  $^{131}$ I labelled corresponding mAb

alone for comparison. For all RIT therapies mice were given Lugol's solution 3 days prior to the treatment (as described in biodistribution studies above).

Animal survival was monitored daily, and the results were analyzed using the  $\chi^2$  test of Peto (Peto 1974). Animal immunotherapy was approved by the local ethical committee and was performed under a UK Home Office project license.

## **2.8 Immunohistochemistry Localisation of Intravenously Administered mAb within the RIT Target Organ – the Spleen**

Parallel groups of  $^{125}\text{I}$ -labelled mAb treated and control animals were sacrificed and the obtained spleen biopsies were fixed overnight in -20°C cold acetone and embedded in glycol methacrylate (GMA) resin as described by Britten et al (Britten, Howarth et al. 1993). Briefly, the spleen was taken immediately after culling and was cut into small pieces of about 2 mm x 2 mm x 4 mm in size. The biopsy pieces were placed immediately into ice cold acetone containing 2 mM phenyl methyl sulphonyl fluoride (35 mg/100 ml) and 20 mM iodoacetamide (370 mg/100 ml). After fixation overnight at -20°C freezer, replace cold acetone with fresh room temperature acetone and leave at room temperature for 15 minutes. The acetone was replaced with methyl benzoate and left at room temperature for another 15 minutes before infiltrating with processing solution (5% methyl benzoate in glycol methacrylate) at 4°C for 6 hours and the processing solution was changed once every 2 hours. The biopsies were finally embedded with GMA embedding solution (10 ml glycol methacrylate, 70 mg benzoyl peroxide, 250  $\mu\text{l}$  N,N-dimethylaniline in PEG 400) in flat bottomed capsules at 4°C for 48 hours for complete polymerisation. Extremely thin 2 $\mu\text{m}$  sections of biopsies embedded with GMA resin were then cut using glass knives on a dedicated Leica 2065 microtome (Leica UK Ltd., Knowlhill, Milton Keynes, UK) for staining. The localisation of the intravenously administered mAb was revealed by staining the sections with biotinylated mouse anti-rat antibody as secondary antibody and subsequently applying the streptavidin biotin-peroxidase complexes and

diaminobenzidine tetrahydrochloride (DAB) substrate as described by Britten et al (Britten, Howarth et al. 1993).

Sequential sections of each biopsy sample were always cut and stained in comparison with control samples for which mAb used in the treatments were applied on slides in vitro prior to the adding of biotinylated mouse anti-rat antibody. All the slides were also counterstained with Mayer's haematoxylin for 2 minutes and mounted with crystal and DPX mountant before observing under light microscope. Images were acquired by a Nikon Coolpix 950 digital camera which was connected to a Nikon Eclipse E600 microscope (Nikon Corporation, Tokyo, Japan). The percentages of the positively stained areas by different mAb were observed and measured using the Zeiss KS400 imaging analysis package (Carl Zeiss Ltd, Welwyn Garden City, UK).

In order to observe the distribution of mAb in advanced stage tumours, groups of BCL<sub>1</sub> tumour cell inoculated mice with advanced stage tumour development (day 18 post inoculation by tail vein injection of 10<sup>5</sup> BCL<sub>1</sub> cells) were also sacrificed and biopsies were processed and stained as described above.

## 2.9 Haematological Toxicity of RIT

RIT toxicity experiments were carried out to evaluate the haematological impact of the <sup>131</sup>I-labeled anti-MHCII antibody. Groups of BALB/c mice (12 mice / group) were injected via the tail vein with 10<sup>5</sup> BCL<sub>1</sub> cells and given Lugol's solution, as before. Ten days post tumour inoculation animals received 500 µg of either 9.25 MBq or 18.5 MBq <sup>131</sup>I-labeled anti-MHCII mAb by intravenous injection 2 – 3 hours after unlabelled anti-BCL<sub>1</sub> Id. Parallel groups of untreated or non-tumour bearing mice were given the same therapy as controls. Animals were sacrificed on day 1, 7, 14, 21, 28 and 35 after

receiving the radioactive mAb. Blood samples were obtained from cardiac puncture and analysed using a Sysmex XE-2100 Blood Cell Analyzer (Sysmex, UK).

## 2.10 Phosphotyrosine Detection by Western Blot

Up-regulation of intracellular protein tyrosine phosphorylation was measured by Western Blot as described by Vuist et al (Vuist, Levy et al. 1994). Briefly, BCL<sub>1</sub> tumor cells were warmed for 15 minutes at 37°C and equal volumes of rat anti-mouse mAb solutions were added to a final concentration of 20 µg/mL and incubated for 2 minutes. Hyper-crosslinking of the primary mAb was performed by adding sheep anti-rat IgG or equal amount of control Ab to a final concentration of 50 µL/mL. The samples were incubated for a further 2 minutes, and washed once using 900 µL/sample of ice-cold phosphate-buffered saline (PBS) containing 1mM Na<sub>3</sub>VO<sub>4</sub>. In experiments where mAb were combined with EBRT, samples were irradiated with 5 Gy using a <sup>137</sup>Cs source (Gamma cell 1000, Kanata, Canada) directly after hypercrosslinking. Cell pellets were lysed on ice in 1 % Triton-X 100 buffer. The cell lysates were then centrifuged for 15 minutes at 16100 g, and 20 µL of the supernatant was mixed with 10 µL loading buffer, boiled for 5 minutes before being subjected to SDS-PAGE. Proteins in the gel were transferred to nitrocellulose and the blot was incubated overnight at 4°C in 5% bovine serum albumin (BSA). Phosphotyrosine was detected by incubating the blot with mAb 4G10 (Upstate Group, Inc. Milton Keynes, UK) and horseradish peroxidase (HRP) labeled goat anti-mouse antibody. Enhanced chemiluminescence (ECL) reagents were added as directed by the manufacturer (Pierce, Rockford USA) and the blot was exposed and acquired using real time image acquisition system, ChemiDoc XRS System (Bio-Rad Laboratories, Inc., CA, USA.).

## **2.11 Immunoprecipitation Analysis for Tyrosine Phosphorylation of Syk**

To detect Syk tyrosine phosphorylation, TX-100 lysates prepared as detailed above were first incubated with 4G10 (2 µg/sample) at 4°C overnight. Protein G-coated Sephrose beads (Amersham Biosciences, UK) pre-blocked with 5% (wt/vol) BSA were then added to the samples (15 µL/sample), and incubated for a further 60 minutes at 4°C. The resulting beads were then washed 4 times with cold lysis buffer and boiled in sample buffer. The precipitated proteins were separated by SDS-PAGE and immunoblotted as described above with the anti-Syk antibody C-20 (Santa Cruz Biotechnology, Inc. Santa Cruz, CA).

## Chapter 3 Developing Animal Models for RIT of Lymphoma

### 3.1 Introduction

Despite considerable advances in the field of clinical RIT in the treatment of Non-Hodgkin's Lymphoma (NHL), a number of important problems and uncertainties remain. These unresolved issues include:

- (a) The relative importance of the selection of the targeted antigen in delivering RIT dose *in vivo*;
- (b) The importance of dosimetry and the necessity for patient-specific pre-dosing;
- (c) The mechanisms of tumour cytotoxicity and the relative contributions of irradiation and mAb to tumour cell killing;
- (d) The importance of radiation dose-rate-effect in RIT
- (e) The existence of radiation dose response in RIT and whether high dose (myeloablative) has superior therapeutic response and overall survival over low dose (non-myeloablative) therapy.

An understanding of the mechanisms underlying the clinical responses is likely to be important in the further development and optimisation of this treatment approach. The ethical and practical difficulties of answering many of these important questions preclude the exposure of patients to repeated doses of uncertain therapies. In order to provide a link between the *in vitro* experiments and RIT, a fundamental aim of this chapter was to establish a well defined suitable model of RIT of B-cell lymphoma.

Most animal models to date have been mainly restricted to human lymphoma xenografts in immunodeficient mice. The significance of the results from these models is limited by the lack of interaction of the treatment mAb with normal mouse effector cells and by the unusual distribution of human tumours in immunodeficient animals. The

establishment of syngeneic B-cell lymphoma animal models is likely to be helpful in testing a variety of RIT treatment approaches in B-cell lymphoma. In this situation tumour develops in the presence of an intact immune system and the targeting mAb is able to cross-react with appropriate normal tissues in a manner analogous to the clinical situation and contrasting with the limitations of human xenograft models where there is no such host immunity or specific cross reaction of mAb with normal tissues.

Our group have previously reported the experimental RIT usage of two syngeneic B-cell lymphoma models, BCL<sub>1</sub> and nBCL<sub>1</sub> (Illidge, Cragg et al. 1999; Illidge, Honeychurch et al. 2000). In this chapter, (a) the radioiodination technique was further optimised prior to successfully performing further preclinical RIT studies and in clinical RIT trials; (b) the in vivo biodistribution characteristics of a panel of radioiodinated mAbs were extensively investigated in BCL<sub>1</sub> and A31 syngeneic lymphoma models with the presence of early stage tumour as well as in animals with advanced stage tumour; (c) based on the biodistribution data, the whole body as well as the individual organ dosimetry were estimated.

### **3.2 Materials and Methods**

By measuring the labelling efficiency and the post-labelling immunoreactivity, three commonly used radioiodination techniques, Chloramine-T, Iodogen-Beads and N-bromosuccinimide (NBS) methods were compared in labelling a rat-anti-mouse major histocompatibility complex class II (MHCI) mAb IgG 2a (TI2-3) as described in Chapter 2. Labelling efficiency was measured by instant thin layer chromatography (ITLC) and high performance liquid chromatography (HPLC) immediately after the labelling procedure (Mather and Ward 1987; Bhargava and Acharya 1989).

Immunoreactivity was assessed by cell binding activity as described by Elliott et al (Elliott, Glennie et al. 1987). The Iodogen-Beads method was the chosen optimal labelling method and subsequently all the mAbs used in the preclinical RIT experiments

were labelled using Iodogen-Beads. This labelling protocol was also used in the clinical RIT trial in which dosimetric and therapeutic doses of  $^{131}\text{I}$  in the range of 300 MBq to 3.0 GBq was successfully labelled with Rituximab.

For the biodistribution studies, groups of BALB/c or CBA/H mice were inoculated with  $10^5$  BCL<sub>1</sub> or  $10^6$  A31 tumour cells by intravenous injection, respectively. Ten days post tumour inoculation animals received 500  $\mu\text{g}$  of  $^{125}\text{I}$  labelled mAbs (anti-MHCII, anti-CD19, anti-Id and control mAb) by intravenous injection via the tail vein. In the cases of advanced-stage tumour biodistribution studies, the  $^{125}\text{I}$  labelled mAbs were given 18 days post tumour inoculation. To investigate the impact of pre-dose on the dosimetry of subsequently administered radiolabelled mAb, 500  $\mu\text{g}$  unlabelled mAb was used as a pre-dose which was given intravenously 2-3 hours prior to the injection of the corresponding  $^{125}\text{I}$  labelled mAb. Animals were sacrificed 1, 8, 24 and 96 hours after receiving the radioactive mAb and the blood, spleen, liver, kidneys and lungs assessed. To block thyroid and gastric uptake of radioactive iodine, mice were given Lugol's solution (5.0 ml Lugol's stock/400 ml H<sub>2</sub>O; Lugol's stock: 10 g KI, 5 g elemental iodine in 100 ml water) in their drinking water 3 days prior to the administration of the  $^{125}\text{I}$  labelled mAb.

The weight and radioactive counts of the dissected organs were measured and the percentage of the injected dose/gram of tissue (%ID/g) was calculated as described by Badger et al (Badger, Davis et al. 1991). Through the assessment of the corresponding tissues at serial time points, the effective half-life and biodistribution of the radiolabelled mAbs were determined. The absolute radioactivity of the total injected dose per animal was also measured using a radioisotope calibrator (Atomlab 100 plus, Biodex Medical Systems, NY). Assuming total absorption of the non-penetrating radiation component with a homogeneous distribution, both the whole body and the organ absorbed doses were calculated by integrating the area under the retention curve using the MIRD dose estimation formula  $D = AS$  as described by Loevinger et al (Loevinger 1988).

## 3.3 Results

### 3.3.1 The Establishment of Optimal Radio-iodine Labelling Technique

For RIT experiments, there is usually a requirement to label relatively large amount of radioactivity to a small amount of mAb. Therefore establishing an optimal labelling protocol, which comprises high labelling efficiency and satisfactory post-labelling immunoreactivity is a critical part of preclinical and clinical testing. My previous labelling experiments had demonstrated that higher labelling efficiency is more likely to be achieved with small labelling reaction volume and neutral pH value. For a reaction volume of no larger than 1.0 ml, stable radioiodination could be achieved through Chloramine-T, Iodogen-Beads or NBS methods largely depending on the pH value of the reaction fluid and the Iodogen methods (Iodogen-Beads or Iodogen-Vial) which has been shown to be the most adaptable to a wide pH range (Du 1995). The  $^{125}\text{I}$  and  $^{131}\text{I}$  used in this study, purchased from the Amersham International, plc., are carrier free, in the form of  $\text{Na}^+ \text{I}^-$ , dissolved in NaOH solution with a pH value around 10. The reduced form iodine (iodide ion,  $\text{I}^-$ ) is the most stable for halogens in aqueous, does not react with protein molecules, but can be oxidized to iodinium ( $\text{I}^+$ ), allowing electrophilic substitution for hydrogen at the most electronegative sites of various amino acid residues. In the electrophilic reactions, the most reactive are the aromatic amino acids such as tyrosine or histidine, but under some conditions, phenylalanine and tryptophan can also be labelled (Paganelli 1998). Many agents are available for oxidation of iodine, but Chloramine-T, Iodogen and more recently NBS are mainly employed for mAb labelling.

The comparison labelling experiments using Chloramine-T, Iodogen Beads and NBS methods were repeated three times and the labelling results of experiments are shown below in figure 3.1.

**Figure 3.1**

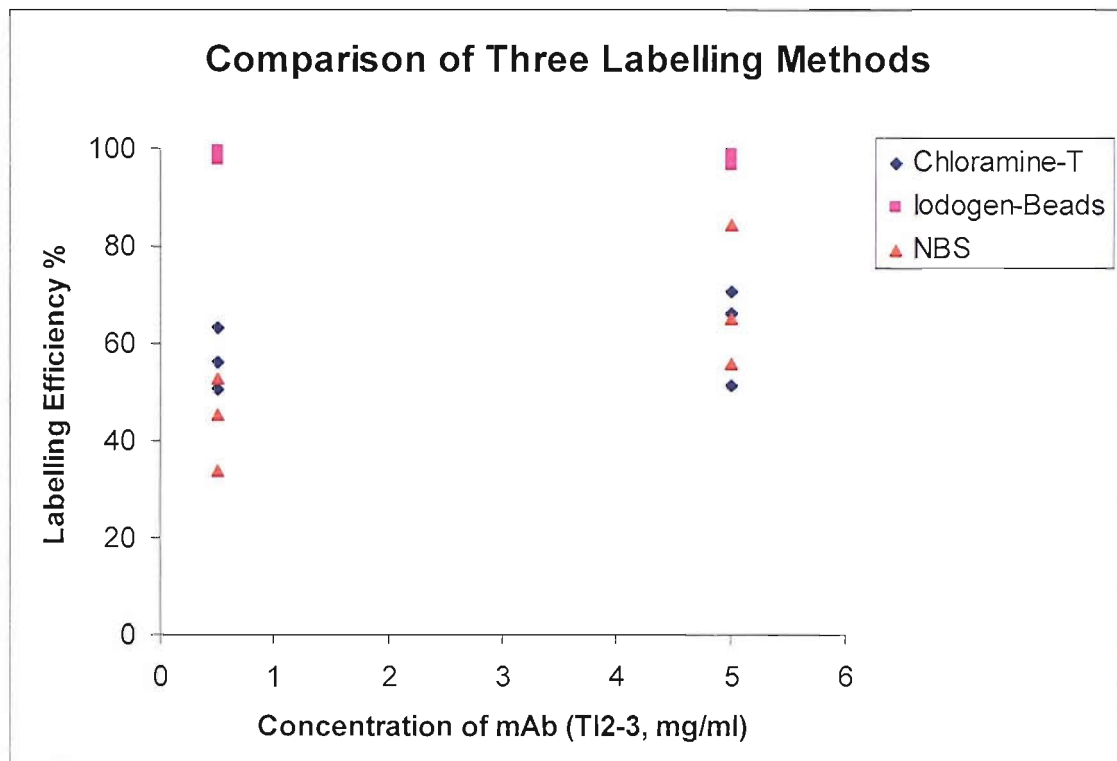


**Figure 3.1. Labelling efficiency of Chloramine-T, Iodogen-Beads and NBS iodination methods.** Different concentrations of anti-MHCII mAb (0.5 mg/mL & 5.0 mg/mL) were labelled by Chloramine-T, Iodogen-Beads and NBS methods respectively. This figure shows the labelling efficiencies of three comparison experiments. High labelling efficiencies of around 98% were achieved constantly using the Iodogen-Beads method at both high and low concentration mAb. The labelling efficiencies were measured by ITLC.

By comparing the three labelling methods, a convenient and highly effective Iodogen-Beads radioiodination protocol to label mAb with  $^{131}\text{I}$  (normally in the range of 2.0 MBq – 740 MBq) was successfully established. Briefly, carrier free  $^{131}\text{I}$  (or  $^{125}\text{I}$ ) was added into a certain volume of mAb in a bijou to make the final reaction volume less than 1.0 ml. 4 Iodogen-Beads were put into the mixed fluid promptly followed by an immediate 10 seconds shaking. The mixture was left for 10 minutes to fully react and every 2 minutes during this period, the bijou was given a 10-second shakings. The product was then taken out using pipette and diluted in PBS to the appropriate concentration for intravenous injection. Samples were taken for ITLC analysis, HPLC analysis and immunoreactivity assessment.

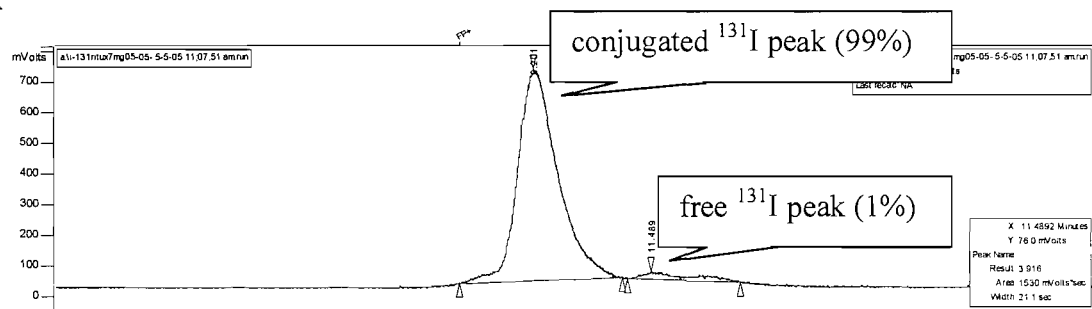
This protocol, using Iodogen-Beads enables us to achieve a consistently greater than 96% labelling efficiency and a greater than 60% post-labelling immunoreactivity when labelling TI2-3 or Rituximab. Such a high labelling efficiency makes it possible to omit the time consuming process of a post-labelling column purification step posing the additional radiation protection issues of potentially high finger doses. This labelling protocol has been successfully used in experimental RIT studies during the course of my work on more than 150 occasions whereby a panel of rat-anti-mouse mAbs have been labelled. This labelling protocol has subsequently been successfully used in the clinical RIT trial at Southampton General Hospital over 70 times in which the post labelling immunoreactivity of  $^{131}\text{I}$  labelled Rituximab has been consistently monitored with Daudi cell binding assessment. Greater than 95% labelling efficiency has been achieved when labelling up to 3.0GBq  $^{131}\text{I}$  to Rituximab. At such a dose level, a greater than 65% post labelling Rituximab immunoreactivity has been achieved consistently six times. The mean value of the immunoreactivity of the  $^{131}\text{I}$  labelled Rituximab in these 70 studies was 63.3% +/- 5.75% (mean +/- SD) and no significant immunoreactivity difference was found between different  $^{131}\text{I}$  doses.

Figure 3.2 Shows the HPLC profile of  $^{131}\text{I}$  labelled anti-CD20 mAb (Rituximab) in which 3.0 GBq  $^{131}\text{I}$  was labelled to 5 mg Rituximab (specific activity: 600 MBq/mg).

Figure 3.3 shows the post labelling Rituximab immunoreactivity at different  $^{131}\text{I}$  dose levels.

**Figure 3.2**

**A**



**B**

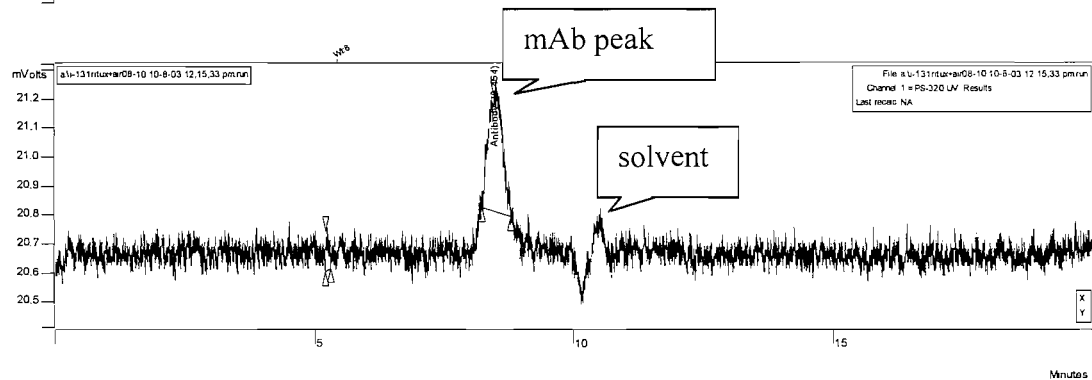


**Figure 3.2. HPLC analysis of  $^{131}\text{I}$  labelled Rituximab.** This figure shows the HPLC graph of  $^{131}\text{I}$  labelled Rituximab. In this experiment, 3.0 GBq  $^{131}\text{I}$  was labelled to 5mg Rituximab. Fig 2-2B (lower) is the graph of the UV channel showing that a clear IgG (mAb) peak appeared at around 8 minutes demonstrating the post labelling intact IgG mAb. Fig 2-2A (upper) is the corresponding graph of radioactivity channel showing that 99% of the radioactivity ( $^{131}\text{I}$ ) was conjugated to the IgG (mAb) achieving a 99% labelling efficiency.

Figure 3.3

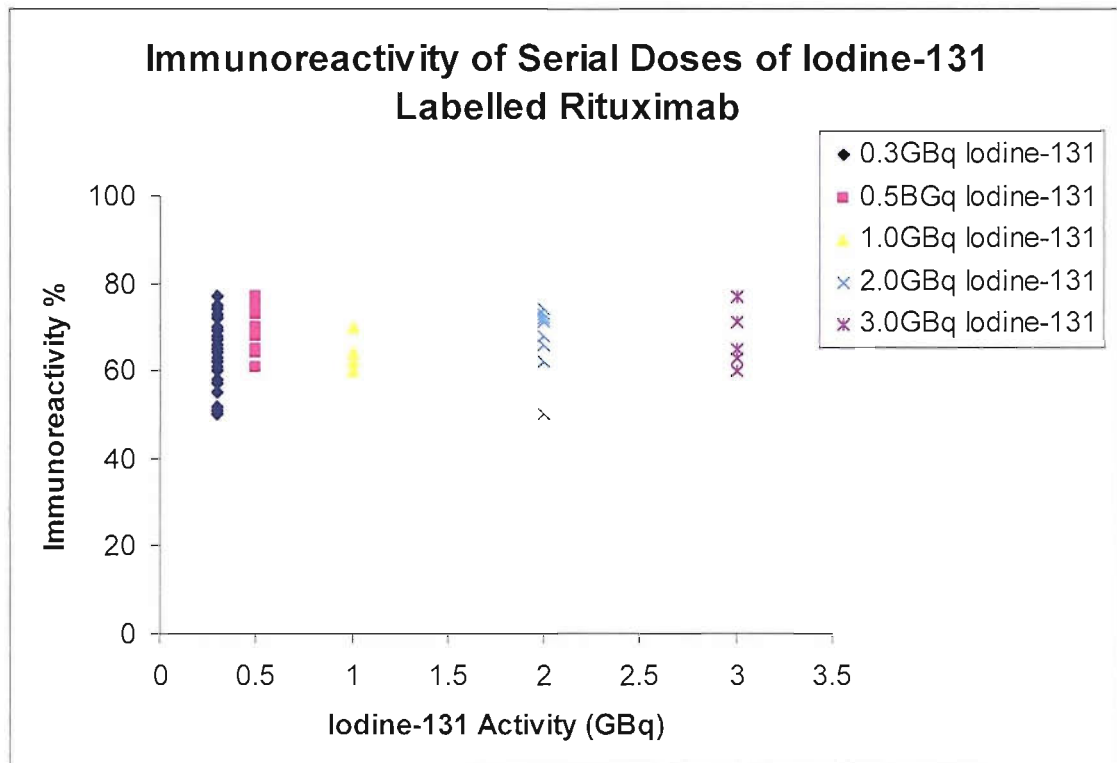


**Figure 3.3. Immunoreactivity of serial doses of  $^{131}\text{I}$  labelled Rituximab as measured by human lymphoma cell line Daudi cell binding activity.** Samples of different doses of  $^{131}\text{I}$  labelled Rituximab were taken immediately after the labelling process and the post labelling immunoreactivity of Rituximab was assessed by in vitro cell binding assay in the presence of serial numbers of Daudi cells which were diluted in culture medium. The labelling efficiency of  $^{131}\text{I}$  labelled Rituximab was no less than 95% as determined by ITLC and HPLC (data not shown). This figure shows that the  $^{131}\text{I}$  labelled Rituximab immunoreactivity (presented as Daudi cell binding percentage) was within the range of 50-78%. No significant immunoreactivity difference was found between different  $^{131}\text{I}$  doses, namely: 0.3 GBq (n=40), 0.5 GBq (n=8), 1.0 GBq (n=8), 2.0 GBq (n=8), and 3.0 GBq (n=6).

Immunoreactivity assays were also performed to evaluate the tumour cell binding capability of radiolabelled anti-mouse mAbs used in preclinical experimental RIT studies. All the radio-iodinated mAb used in this project have demonstrated a satisfactory immunoreactivity of within 50-75% and no significant difference was found when these mAbs were labelled with trace amount of  $^{125}\text{I}$  or therapeutic amount of  $^{131}\text{I}$  (up to 740 MBq). Figure 3.4 is the result of one of the three typical experiments showing the immunoreactivity of a panel of rat anti-mouse mAbs which were used in the preclinical RIT studies.

**Figure 3.4**

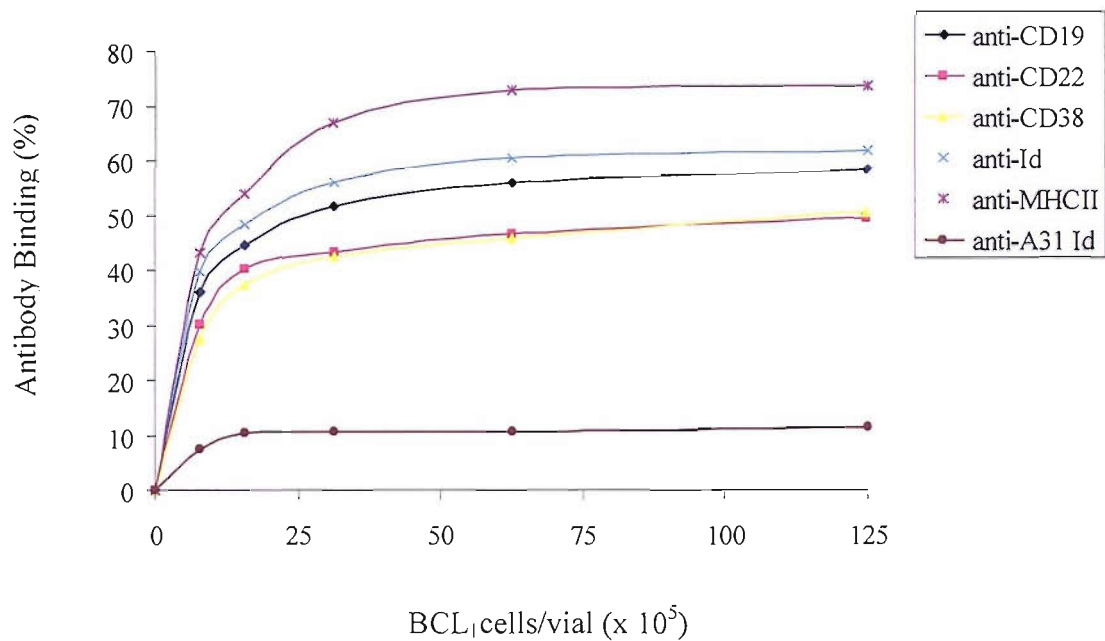


**Figure 3.4. Immunoreactivity assay of rat-anti-mouse mAb on BCL<sub>1</sub> cells.**

This figure shows one of three identical experiments (see Appendix 1 for raw data) demonstrating that the above 50% immunoreactivity of a panel of radioiodinated rat anti-mouse mAbs which were used in the preclinical RIT studies. In this study, the anti-A31 idiotype mAb (Mc39-16) was used as a negative control antibody.

The binding density of these mAbs to BCL<sub>1</sub> tumour cells was assessed by the cell binding curve assay as described by Tutt et al (Tutt, French et al. 1998). Cell binding curve describes the amount of radio-labelled mAb binds to each target cell. This is also an important factor which influences the radiation dose delivery capability of the mAb. In this experiment, fixed number of tumour cells ( $1 \times 10^6$ ) were incubated with serially diluted  $^{125}\text{I}$  or  $^{131}\text{I}$  labelled mAbs. Assuming the molecular weights of all the mAb are approximately the same ( $1.5 \times 10^5$ ), taking into account the immunoreactivity of individual mAb, the cell binding curves of all the mAbs were plotted as molecules of mAb per cell against the concentrations of mAb. Similar to the immunoreactivity study, no significant difference was found in the binding curve when mAbs were labelled with trace amount of  $^{125}\text{I}$  or higher doses of  $^{131}\text{I}$ . Figure 3.5 shows the result of one of three identical studies demonstrating that the amount of mAb binds to each tumour cell varies hugely whilst among these mAbs. The binding saturation level for anti-MHC class II mAb (TI2-3) was the highest at  $8 \times 10^5$  molecules per cell but it was only  $2 \times 10^5$  molecules per cell for the anti-CD19 mAb (1D3).

**Figure 3.5**

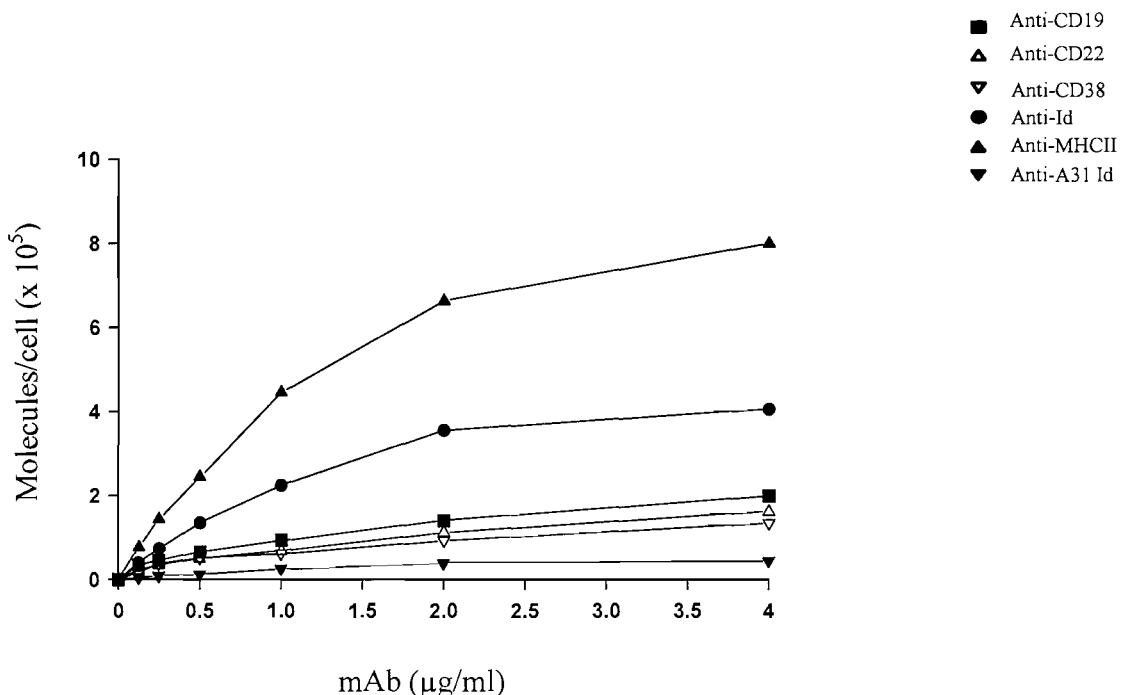


**Figure 3.5. Binding curves of radioiodinated rat-anti-mouse mAbs on BCL<sub>1</sub> cells.**

This figure shows one of three similar experiments performed (see Appendix 2 for raw data). The results are expressed as the number of molecules of mAb bound/cell. Among these mAbs, the anti-MHCII (TI2-3) demonstrated the highest mAb molecules/cell binding with peak value of nearly  $7.8 \times 10^5$  per cell, whilst the anti-Id (Mc106A5) came second at around  $3.8 \times 10^5$  per cell. In this study, the anti-A31 idiotype mAb was used as a negative control antibody.

### 3.3.2 Biodistribution and Organ Dosimetry of Radiolabelled mAb

Work from our group had previously showed that MHCII had a higher level of surface expression than CD19 or idiotype (Id) on BCL<sub>1</sub> cells. In addition it was demonstrated in vivo that the MHCII antigen complex unlike CD19 or Id did not modulate on binding mAb (Illidge, Cragg et al. 1999). It is therefore hypothesised that anti-MHCII would deliver more radiation to the tumour bearing organs and thus performed biodistribution experiments to confirm this hypothesis and to calculate the radiation dose delivered to both normal and tumour bearing organs. Figure 3.6 (A-D) demonstrated the biodistribution of a panel of B-cell specific mAbs given 10 days after tumour inoculation (BCL<sub>1</sub>, 1x10<sup>5</sup>, iv.). At specific time points (as shown in Figure 3.6), over the next 4 days, the animals were sacrificed and the major organs removed to determine the percentage of injected radioactive dose (ID) / gram of organ tissue (g). The ability of a single trace labelled (0.74 MBq) dose of 500 µg of <sup>125</sup>I labelled anti-MHCII to selectively target the major tumour-bearing organ (spleen) is clearly shown. In contrast, the B-cell specific mAb (anti-CD19 and anti-Id) were considerably poorer at delivering radiation to the spleen and provided similar targeting of radiation (%ID/g) to that seen with an irrelevant isotype matched (control) mAb.

**Figure 3.6**

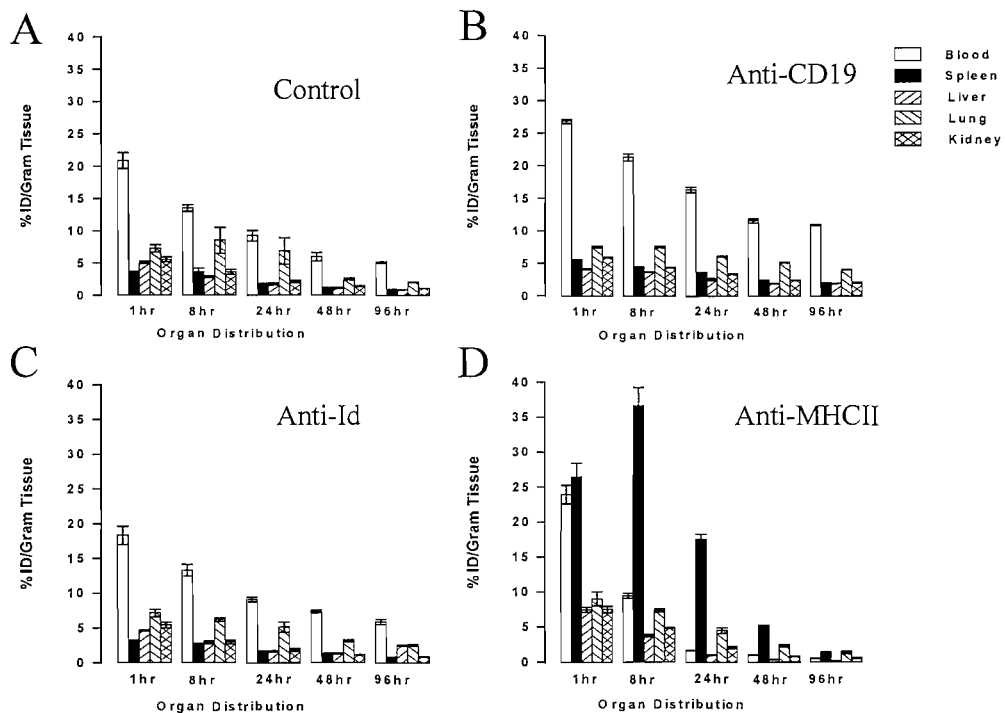


**Figure 3.6. Biodistribution of  $^{125}\text{I}$  labelled mAb in BCL<sub>1</sub> tumour inoculated mice.**

Age and sex-matched groups of mice (18 for each group) were inoculated with  $10^5$  BCL<sub>1</sub> cells intravenously and then treated with  $^{125}\text{I}$  labelled mAb (500  $\mu\text{g}$  per mouse) 10 days later. At the time intervals indicated, animals were killed and blood samples and various organs were removed for weighing and estimation of radioactive content. Results are expressed as the percentage of the injected dose of  $^{125}\text{I}$  mAb per gram of tissue recovered (% ID/g). Each bar shows the mean and range for 3 animals investigated and the results shown are representative of 1 of 2 identical experiments.

Assuming total absorption of the non-penetrating radiation component of  $^{131}\text{I}$  with homogeneous distributions within each individual organ or whole body, the approximate radiation doses delivered by these mAbs were calculated using the Medical Internal Radiation Dosimetry (MIRD) method for whole body, lung, liver, kidney and the tumour bearing organ – spleen were calculated in early (10 days after intravenous inoculation of  $10^5$  BCL<sub>1</sub> cells) tumour models and the doses are presented below in Table 3.1.

**Table 3.1**

Organs	Radiation Dosimetry				
	Weight (g)	Anti-MHC II	Anti-Id	Anti-CD19	Control
Whole body (22.45 $\pm$ 0.34)	2.90 $\pm$ 0.11	4.44 $\pm$ 0.23	7.25 $\pm$ 0.09	5.80 $\pm$ 0.17	
Spleen (0.15 $\pm$ 0.02)	18.00 $\pm$ 1.02	3.40 $\pm$ 0.21	5.14 $\pm$ 0.13	4.50 $\pm$ 0.20	
Liver (1.02 $\pm$ 0.21)	1.82 $\pm$ 0.17	5.14 $\pm$ 0.34	6.05 $\pm$ 0.44	3.04 $\pm$ 0.07	
Lung (0.15 $\pm$ 0.03)	4.54 $\pm$ 0.22	8.57 $\pm$ 0.25	10.15 $\pm$ 0.24	7.63 $\pm$ 0.36	
Kidney (0.45 $\pm$ 0.03)	3.80 $\pm$ 0.14	2.75 $\pm$ 0.12	7.60 $\pm$ 0.42	3.04 $\pm$ 0.15	

**Table 3.1. Internal radiation dosimetry of RIT treated mice.** Based on the biodistribution data, the absorbed radiation doses of whole body and individual organs of RIT treated mice were estimated according to the MIRD formula. This table shows the dosimetry results when BALB/c mice bearing early stage BCL<sub>1</sub> tumour (10 days after the inoculation of  $1 \times 10^5$  tumours given by intravenous injection) were treated with 18.5 MBq  $^{131}\text{I}$  labelled corresponding mAb. The absorbed radiation dose is measured as Gy (mean  $\pm$  range).

The same biodistribution studies were repeated in the A31 tumour model and found that the %ID/g of tissue studied for the anti-MHCII mAb were almost exactly the same as for the BCL<sub>1</sub> model (data not shown). The results confirmed the ability of anti-MHCII mAb to deliver larger doses of radiation per MBq of radiolabelled mAb infused to the spleen and less non-specific irradiation to the whole body. For an infusion of 18.5 MBq <sup>131</sup>I-anti-MHCII, the dose delivered to the spleen is estimated to be around 18 Gy in early stage tumour models, which is 3 – 6 times greater than that delivered by anti-CD19 (5.14 Gy), the irrelevant (4.5 Gy) and the anti-Id (3.4 Gy) mAb (Figure 3.6 A, B, C, D). This contrasts to the whole body dose, where anti-MHCII delivered around 2.9 Gy whereas the other mAbs delivered larger non-specific doses; anti-Id (4.4 Gy), anti-CD19 (7.25 Gy) and the irrelevant mAb (5.8 Gy).

### **3.3.3 Biodistribution and Organ Dosimetry of Radiolabelled mAb in Advanced Stage Tumour**

As shown below in figure 3.7, flow cytometry analysis demonstrated that on day 10 after  $1 \times 10^5$  of BCL<sub>1</sub> cells inoculation, BCL<sub>1</sub> tumour cells make up for about 3-5% of BALB/c mice splenocytes. In order to investigate whether BCL<sub>1</sub> specific mAb (anti-Id) could deliver more radiation to the target when the tumour was established, the biodistribution experiments were repeated in same strain of BALB/c mice with advanced stage disease. Figure 3.8 (lower panel) shows the biodistribution data obtained in animals with much advanced disease (day 18 after inoculation, when BCL<sub>1</sub> cells counted for about 95-98% of splenocytes as analysed by flow cytometry). In comparison with the biodistribution of early stage tumour as described in previous section (Figure 3.8 upper panel), this figure showed that the circulating half-lives of both anti-MHCII mAb and anti-Id are all substantially reduced presumably due to the availability of large amount of tumour cells and therefore large numbers of mAb binding sites. This figure demonstrates that, the rapid disappearance of radiolabelled anti-MHCII from the circulation in animals with advanced stage tumour (the blood presence of anti-MHCII at 1 hour post infusion was merely 4% ID/g, in stunning

contrast to 24% ID/g in early stage tumour) and the accumulation of radiolabelled anti-MHCII peaking in the spleen no later than 1 hour post-infusion. This is much faster than that seen in animals with early stage tumour in which the accumulation peak was seen at 8 hours post infusion of radiolabelled mAb. As a result, taking into account the larger tumour size, assuming the homogeneous distribution of radiolabelled mAb within each organ again using the MIRD dosimetry formula, the whole and organ dosimetry were determined as shown below in Table 3.2. The estimated actual radiation dose delivered to advanced stage tumour (spleen) decreased from 18 Gy to 9.12 Gy as shown below in Table 3.2.

**Figure 3.7**

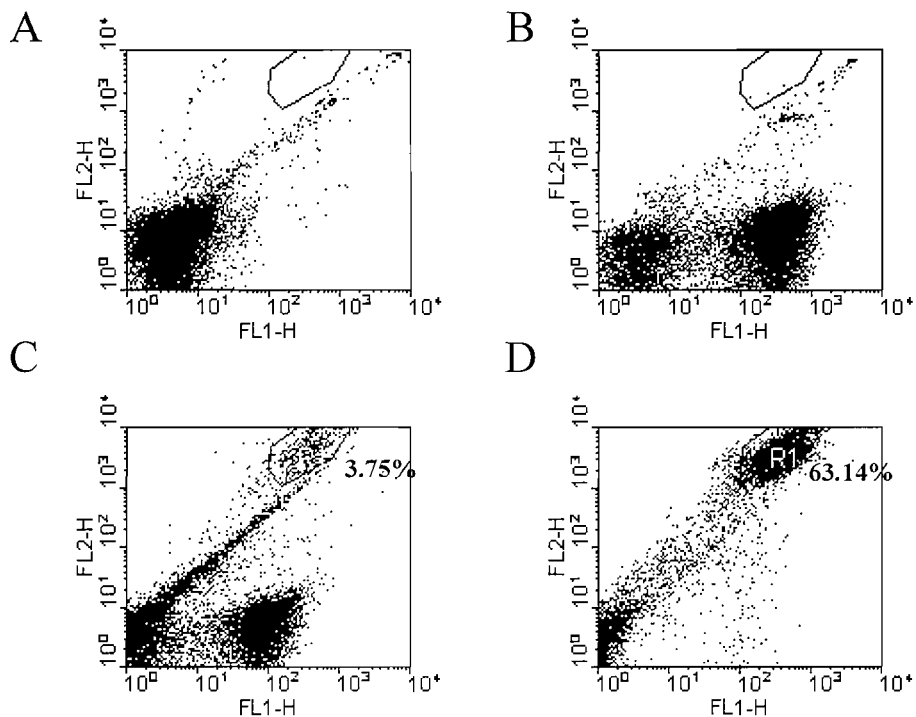


**Figure 3.7. The development of BCL<sub>1</sub> tumour in the spleen of BALB/c mice.** In this experiment, age and sex-matched groups of BALB/c mice (5 mice per group) were inoculated with  $10^5$  BCL<sub>1</sub> cells intravenously and were sacrificed at days 10 and 18 post-inoculation, respectively. The spleens were homogenised and splenocytes were isolated for two-colour cell surface antigen staining in comparison with control animals using fluorescein isothiocyanate (FITC) labelled rat anti-mouse MHCII mAb (TI2-3) (FL1) and phycoerythrin (PE) labelled rat anti-mouse BCL<sub>1</sub> idiotype mAb (Mc106A5) (FL2). For comparison, a FITC labelled irrelevant mAb was also used to stain control animal splenocytes (figure 3.7A). The flow cytometry profiles shown in this figure demonstrate the dynamic progression of BCL<sub>1</sub> tumour as expressed as percentage of BCL<sub>1</sub> tumour cells within the spleen. Figures 3.7A and 3.7B show the flow cytometry profiles of the splenocytes of control animals which were not inoculated by tumour cells. Figures 3.7C and 3.7D show the percentages of BCL<sub>1</sub> tumour cells at day 10 (3.75%) and day 18 (63.14%) post-inoculation.

**Figure 3.8**

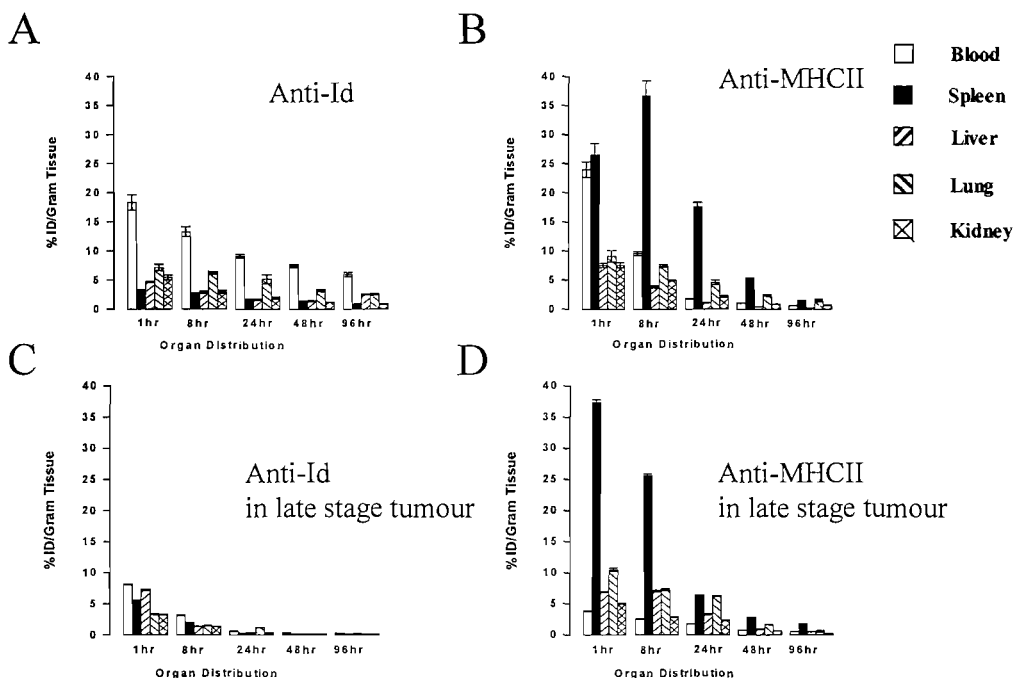


**Figure 3.8. Comparison biodistribution of  $^{125}\text{I}$  labelled mAb in early stage and advanced stage BCL<sub>1</sub> tumour models.** Further to the biodistribution experiments showed in figure 3.6, figure 3.8C and figure 3.8D show the biodistribution results of  $^{125}\text{I}$  labelled anti-Id and anti-MHCII mAb in advanced stage BCL<sub>1</sub> tumour models. In this experiment, age and sex-matched groups of mice were inoculated with  $10^5$  BCL<sub>1</sub> cells intravenously and then 18 days later treated with  $^{125}\text{I}$  labelled (500  $\mu\text{g}$  per mouse) anti-Id and anti-MHCII mAb respectively. At the time intervals indicated, animals were killed and blood samples and various organs were removed for weighing and estimation of radioactive content. Results are expressed at the percentage of the injected dose of  $^{125}\text{I}$  mAb per gram of tissue recovered (% ID/g). The biodistribution results of these two mAb in early stage BCL<sub>1</sub> tumour models are also shown in this figure (figure 3.8A and 3.8B) for comparison.

**Table 3.2.**

Organs	Radiation Dosimetry			
Weight (g) (advanced stage tumour)	Anti-Class II (advanced stage)	Anti-Class II (early stage)	Anti-Id (advanced stage)	Anti-Id (early stage)
Whole body (25.40+/-0.71)	1.74+/-0.31	2.90+/-0.11	0.27+/-0.04	4.44+/-0.23
Spleen (1.05+/-0.19)	9.12+/-0.35	18.00+/-1.02	0.73+/-0.11	3.40+/-0.21
Liver (1.11+/-0.24)	3.41+/-0.42	1.82+/-0.17	0.57+/-0.06	5.14+/-0.34
Lung (0.20+/-0.03)	4.86+/-0.51	4.54+/-0.22	0.49+/-0.02	8.57+/-0.25
Kidney (0.45+/-0.04)	2.43+/-0.16	3.80+/-0.14	0.49+/-0.04	2.75+/-0.12

**Table 3.2. Internal radiation dosimetry of advanced tumour in comparison with early stage tumour.** Based on the biodistribution data, the absorbed radiation doses of whole body and individual organs of RIT treated BALB/c mice were estimated according to the MRID formula. This table compared the dosimetry results of early stage tumour (10 days after the inoculation of  $1 \times 10^5$  BCL<sub>1</sub> tumours given by intravenous injection) with that of advanced stage tumour (18 days after the inoculation of  $1 \times 10^5$  BCL<sub>1</sub> tumours given by intravenous injection) were treated with 18.5 MBq <sup>131</sup>I labelled corresponding mAb. The absorbed radiation dose was measured as Gy (mean +/- range).

### **3.3.4 Impact of Pre-dose on the Biodistribution and Organ Dosimetry of Radiolabelled mAb**

As discussed in the Introduction, pre-dosing prior to the infusion of radio-labelled mAb with unlabelled mAb has been shown to be an effective solution to improve the biodistribution therefore mAb targeted radiation delivery. Pre-dosing has become a component of both of the two FDA approved clinical RIT treatments, namely <sup>90</sup>Y-ibritumomab tiuxetan (Zevalin<sup>TM</sup>) and <sup>131</sup>I Tositumomab (Bexxar<sup>TM</sup>) (Wagner, Wiseman et al. 2002; Witzig, Gordon et al. 2002; Kaminski, Tuck et al. 2005; Wahl 2005). In the next series of experiments the aim was to evaluate the influence of pre-dose on the biodistribution of subsequently injected radio-labelled mAb, pre-dose biodistribution experiments of anti-MHCII and anti-Id were performed respectively in both early stage and advanced stage BCL<sub>1</sub> inoculated same strain of BALB/c mice. Figure 3.9 showed the biodistribution of <sup>125</sup>I labelled anti-MHCII given 2-3 hours after the pre-dosing of 500 µg unlabelled same mAb in early stage tumour (Figure 3.9B) and in advanced stage tumour (Figure 3.9D) in comparison with the biodistribution figures without the addition of pre-dose (Figure 3.9A & 3.9C).

**Figure 3.9**

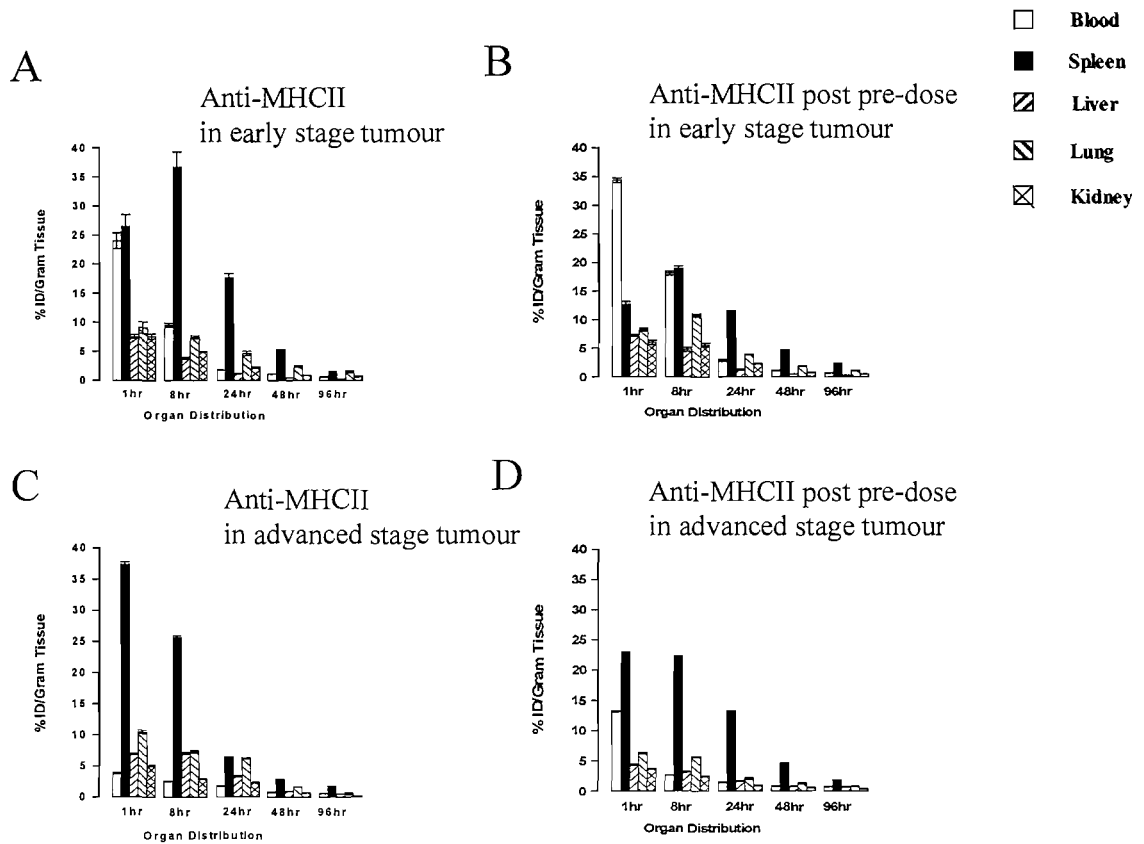


**Figure 3.9. Influence of pre-dose on biodistribution of radiolabelled anti-MHCII mAb in early stage and advanced stage BCL<sub>1</sub> tumour models.** In this experiment, early and advanced stage BCL<sub>1</sub> tumour inoculated mice were given 500 µg unlabelled anti-MHCII mAb by intravenous injection 2-3 hours prior to the administration of <sup>125</sup>I labelled anti-MHCII mAb as a pre-dose. The percentage of the injected dose of <sup>125</sup>I labelled mAb per gram of tissue were then determined as described before. Figure 3.9B shows the biodistribution of <sup>125</sup>I labelled anti-MHCII given 2-3 hours after the pre-dosing in early stage tumour and figure 3.9D shows the biodistribution of <sup>125</sup>I labelled anti-MHCII mAb after pre-dose in advanced stage tumour. For comparison, the biodistribution results of <sup>125</sup>I labelled anti-MHCII mAb without the addition of pre-dose in early and advanced stages of BCL<sub>1</sub> tumour models are also presented in this figure (Figure 3.9A & 3.9C).

The pre-dose of 500 µg anti-MHCII given intravenously 2-3 hours prior to the injection of the radio-labelled mAb as expected prolonged the circulating half-life of the subsequently administered  $^{125}\text{I}$  labelled anti-MHCII in animals bearing both early stage tumour and advanced stage tumour. The pre-dose substantially decreased the early uptake of the radiolabelled mAb at early time points with early stage tumour. The 1 hour time point splenic uptake of radiolabelled anti-MHCII decreased to 13% ID/g compared to 24% ID/g without pre-dosing and the peak uptake (still at 8 hour time point) decreased to 19% ID/g in comparison to 37% ID/g without pre-dosing. This resulted in a significant decrease of radiation dose delivered to the target organ (the spleen) from around 18 Gy to 11.50 Gy while the radiation activity to the whole body and other organs were all increased due to the prolonged circulating half-life of the radiolabelled mAb as shown in Table 3.3.

In the case of advanced stage tumour, the 1 hour spleen uptake also decreased, from around 38% ID/g to 23% ID/g and the 8 hour spleen uptake decreased slightly from 25% ID/g to 22% ID/g. However, an increased uptake of more than two-fold was seen at the 24 hour time point (14% ID/g compared to 6% ID/g without pre-dosing) and a slightly increased uptake was also seen at 48 time point (4% ID/g versus 2.5% ID/g). As a result, in advanced stage tumours the pre-dose improved the radiation delivery to the spleen from 9.12 Gy to 12.12 Gy. Notably, in the meantime, the animal whole body radiation exposure also increased from 1.74 Gy to 3.02 Gy which is due to the prolonged in vivo retention of radiolabelled mAb. Similar results were observed with anti-Id mAb but were less pronounced especially in the cases of advanced stage tumour probably due to the extremely fast internalisation of this mAb. Therefore we hypothesised that not enough dose of unlabelled mAb (500 µg, iv., same dose as used in the experiments with anti-MHCII mAb) was administered to fulfil the blockade purpose of pre-dosing. Figure 3.10 shows the impact of pre-dose on the biodistribution of  $^{125}\text{I}$  labelled anti-Id mAb in BALB/c mice bearing advanced stage BCL<sub>1</sub> tumour in comparison with that of anti-MHCII mAb.

**Table 3.3.**

Organs	Radiation Dosimetry			
	Anti-Class II (pre-dosing in early stage tumour)	Anti-Class II (early stage without pre- dosing)	Anti-MHCII (pre-dosing in advanced stage tumour)	Anti-MHCII (advanced stage without pre-dosing)
Whole body	5.40+/-0.25	2.90+/-0.11	3.02+/-0.14	1.74+/-0.31
Spleen	11.50+/-1.20	18.00+/-1.02	12.12+/-0.40	9.12+/-0.35
Liver	3.12+/-0.50	1.82+/-0.17	1.95+/-0.16	3.41+/-0.42
Lung	6.40+/-0.75	4.54+/-0.22	3.40+/-0.12	4.86+/-0.51
Kidney	5.30+/-0.40	3.80+/-0.14	1.70+/-0.09	2.43+/-0.16

**Table 3.3. Impact of pre-dose on the internal radiation dosimetry in comparison with those without pre-dose.** Based on the biodistribution data, the absorbed radiation doses of whole body and individual organs of RIT treated BALB/c mice were estimated according to the MRID formula. This table compared the dosimetry results with and without pre-dose in BALB/c mice bearing early stage tumour (10 days after the inoculation of  $1 \times 10^5$  BCL<sub>1</sub> tumours given by intravenous injection) and advanced stage tumour (18 days after the inoculation of  $1 \times 10^5$  BCL<sub>1</sub> tumours given by intravenous injection) when treated with 18.5 MBq <sup>131</sup>I labelled corresponding mAb. The absorbed radiation dose was measured as Gy (mean +/- range).

**Figure 3.10**

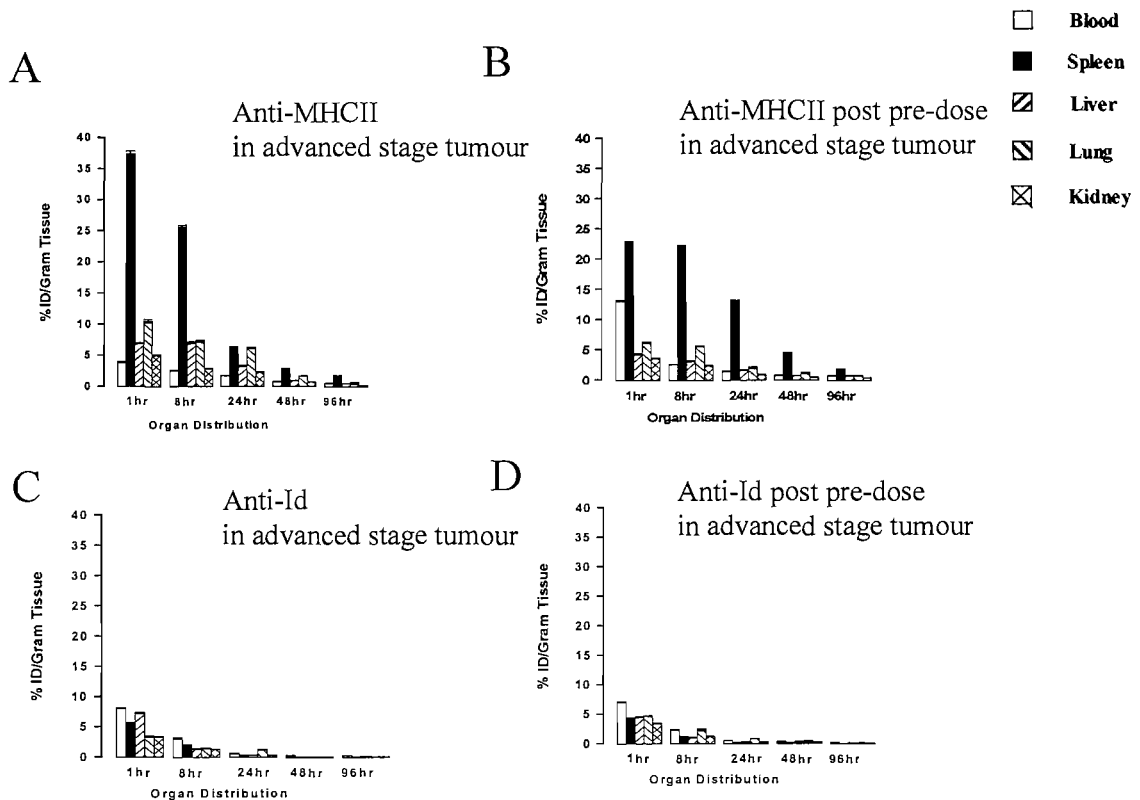


**Figure 3.10. Influence of pre-dose on biodistribution of radiolabelled anti-Id mAb in advanced stage BCL<sub>1</sub> tumour models.** In this experiment, BALC/c mice bearing advanced stage BCL<sub>1</sub> tumour were given 500  $\mu$ g unlabelled anti-Id mAb by intravenous injection 2-3 hours prior to the administration of  $^{125}\text{I}$  labelled anti-Id mAb as a pre-dose. The percentage of the injected dose of  $^{125}\text{I}$  labelled mAb per gram of tissue were then determined as described before. Figure 3.10D shows the biodistribution of  $^{125}\text{I}$  labelled anti-Id given 2-3 hours after the pre-dosing in advanced stage tumour and figure 3.10C shows the biodistribution of  $^{125}\text{I}$  labelled anti-Id mAb without the addition of pre-dose. For comparison, the biodistribution results of  $^{125}\text{I}$  labelled anti-MHCII mAb in advanced stages of BCL<sub>1</sub> tumour models are also presented in this figure (Figure 3.10A & 3.10B).

### 3.4 Discussion

In this chapter, an optimal Iodogen-Beads based radioiodination method was established. This labelling protocol has subsequently been successfully used in preclinical and clinical RIT studies. Using this radioiodination technique, the biodistribution and radiation dosimetry of a panel of radiolabelled mAbs were extensively investigated in syngeneic murine B-cell lymphoma models.

An optimal radiolabelling protocol to efficiently conjugate high activities of radioisotopes with mAb forms an important part of RIT. Although radiometals (such as yttrium-90, copper-67, samarium-153, lutetium-177) may possess some advantages over radioiodine in some settings (mainly with internalising antibodies), the majority of radioimmunotherapy studies has used and still use iodine-131 as therapeutic nuclide (Behr, Gotthardt et al. 2002; Press 2003). Whereas non-myeloablative, standard low-dose regimens require activities of up to 3.7-7.4 GBq, for high-dose regimens, up to 10 or 20 GBq are needed (Press and Rasey 2000; Press, Leonard et al. 2001). This requires an easy, simple, safe, efficient and reliable radioiodination system which produces high efficiency yield and minimises the radiation exposure of the labelling personnel (Behr, Gotthardt et al. 2002).

Many satisfactory techniques for labelling antibodies with iodine have been described and traditionally, different institutions tend to use different radiolabelling protocols mainly due to the degree of their familiarity to that particular method. Most of the traditional radioiodination techniques give labelling efficiency on the order of 70-80%, but effective modifications have continuously been made (Behr, Wormann et al. 1999; Behr, Gotthardt et al. 2002). Mather et al reported the extremely efficient radioiodination method using N-bromosuccinimide (NBS) as an oxidative reagent (Mather and Ward 1987). With this method, high labelling efficiency of above 90% was consistently achieved to label high activity of  $^{131}\text{I}$  with negligible damage to the immunoreactivity of mAb (Adam 1989; Du 1995). In this chapter, two widely used radioiodination techniques, Chloramine-T and Iodogen-Beads were tested in

comparison with NBS method in labelling a rat anti-mouse mAb (TI2-3). Iodogen-Beads method was found most effective and stable probably due to the relative high pH value of the reaction fluid (Du 1995). With this protocol, a higher than 95% labelling efficiency was consistently achieved and such a high labelling efficiency enabled us to omit the post labelling column purification step. This method was subsequently chosen for both preclinical RIT studies (in which a panel of rat anti-mouse mAbs including IgG1, IgG2 were successfully radioiodinated) and clinical RIT trials in which larger activity if  $^{131}\text{I}$  was labelled with Rituximab.

Apart from the high labelling efficiency, satisfactory post-labelling immunoreactivity is essential to the success of RIT. Immunoreactivity of the radiolabelled mAb determines the binding ability of the mAb to its target antigen and therefore the targeting performance of the radioimmunoconjugate. When the mAb was labelled with therapeutic amounts of radiounclides, the possible damage of its immunoreactivity has always been a big concern (Salako, O'Donnell et al. 1998; DeNardo, DeNardo et al. 2000; Schaffland, Buchegger et al. 2004). In this chapter, the immunoreactivity of  $^{131}\text{I}$  labelled Rituximab was monitored with human lymphoma cell line (Daudi) binding assay continuously for 70 times over 35 months. Over this period, the  $^{131}\text{I}$  radioactivity was 3.0 GBq (specific activity: 600 MBq/mg, n = 6), 2.0 GBq (specific activity: 400 MBq/mg, n = 8), 1.0 GBq (specific activity: 200 MBq/mg, n = 8), 500 MBq (specific activity: 100 MBq/mg, n = 8), and 300 MBq (specific activity: 60 MBq/mg, n = 40). The Rituximab post-labelling immunoreactivity has been very consistent (mean +/- SD: 63.3% +/- 5.75) and no significant difference was found between different radiation dose levels.

Recently, in a dedicated study, Schaffland et al investigated the relationship between immunoreactivity and specific activity of  $^{131}\text{I}$  labelled Rituximab (Schaffland, Buchegger et al. 2004). In their study, labelling was performed with Chloramine - T method. 370 MBq  $^{131}\text{I}$  and 185 MBq  $^{131}\text{I}$  were labelled to 2 mg and 5 mg Rituximab, respectively on just 6 occasions. Daudi cell binding assay was also used for immunoreactivity determination. In contrast to our results, they reported a significant

post-labelling immunoreactivity decrease in the high specific activity group (169.7 MBq/mg) compared with the low specific activity group (32.8 MBq/mg). The mean specific binding measured using  $10^7$  Daudi cells were  $42.0 \pm 13.0$  and  $57.1 \pm 8.3$ , respectively which were all lower than the immunoreactivity we observed. However, in a most recent publication aiming to evaluate the biodistribution and tissue kinetics of  $^{131}\text{I}$  labelled Rituximab between repeated injections of large amount of unlabelled Rituximab, the same group reported higher immunoreactivity of 740 MBq  $^{131}\text{I}$  labelled 2 mg Rituximab which was identical to the “high specific activity” group they reported previously and the labelling protocol was unchanged (Antonescu, Bischof Delaloye et al. 2005). In this most recent report, the Rituximab was labelled 12 times and the mean specific binding as measured on  $10^7$  cells was  $48.3 \pm 9.0\%$  which was higher than their previously reported value but still significant lower than our results. It is unclear whether such difference in immunoreactivity is due to the different labelling methods.

Achieving a high labelling efficiency and satisfactory immunoreactivity, the Iodogen-Beads iodination method was used to label a panel of rat anti-mouse mAbs to evaluate their radiation delivery capability. The anti-MHCII mAb (TI2-3) which targets the highly expressed and non-internalising MHCII antigen was found to be the most efficient mAb at targeted radioactivity delivery and anti-MHCII mAb delivered approximately 18 Gy to the tumour bearing organ spleen in early stage tumour and approximately 9.12 Gy to the spleen in advanced disease. Interestingly, despite the presence of a greatly increased tumour burden in animals with advanced stage tumour, there was not an increased accumulation of the radiolabelled tumour specific anti-Id in the splenic tumour. On the contrary, the radioactivity was expelled rapidly which resulted in a dramatic decrease of whole body radiation dose to 0.27 Gy and the spleen dose to 0.73 Gy. In contrast, the radiation doses delivered to early stage tumour animals was 4.44 Gy and 3.40 Gy, respectively. We believe that this was secondary to the fast endocytosis or internalization of anti-Id mAb once it binds to the tumour cell surface and the internalized mAb was quickly dehalogenated by intracellular enzymes and the free iodine being expelled swiftly through urine (Press, Farr et al. 1989; Press,

Appelbaum et al. 1995; Wahl 1998). The result of this experiment demonstrated that for the purpose of delivering radiation, non-internalizing mAb should be chosen.

Pre-dosing prior to the infusion of radio-labelled mAb with unlabelled mAb has been suggested to be an effective solution to improve the biodistribution therefore mAb targeted radiation delivery and pre-dosing is a component of both <sup>90</sup>Y-ibritumomab tiuxetan (Zevalin™) and <sup>131</sup>I Tositumomab (Bexxar™) RIT regimens (Wagner, Wiseman et al. 2002; Witzig, Gordon et al. 2002; Kaminski, Tuck et al. 2005; Wahl 2005).

In this chapter, aiming to evaluate the influence of pre-dose on the biodistribution of subsequently injected radio-labelled mAb, pre-dose biodistribution experiments of anti-MHCII and anti-Id were performed respectively in both early stage and advanced stage BCL<sub>1</sub> inoculated BALB/c mice.

In both early stage and advanced stage tumours, the pre-dose of 500 µg anti-MHCII prolonged the circulating half-life of the subsequently administered <sup>125</sup>I labelled anti-MHCII. The pre-dose also however substantially decreased the early uptake of the radio-labelled mAb at early time points especially with early stage tumour. This resulted in a significant decrease of radiation dose delivered to the target organ (the spleen) from around 18 Gy to 11.50 Gy while the radiation activity to the whole body and other organs were all increased.

In the case of advanced stage tumour, the splenic uptake of radiolabelled anti-MHCII mAb also decreased in early time points. However, an obviously increased uptake of more than two-fold was seen at the 24 hour time point and thereafter. As a result, in advanced stage tumours the pre-dose improved the radiation delivery to the spleen from 9.12 Gy to 12.12 Gy. Notably, in the meantime, the animal whole body radiation exposure also increased from 1.74 Gy to 3.02 Gy which is due to the prolonged in vivo retention of radiolabelled mAb.

The results of this experiment demonstrated that the impact of pre-dosing on dosimetry is determined by the quantity of the tumour present and the amount of mAb used for

pre-dosing. In the meantime, by prolonging the effective half-life of the radiolabelled mAb the pre-dosing would inevitably increase the non-specific whole body radiation exposure to the recipient. These results highlight the importance of patient specific pre-dosing to deliver an increased targeted radiation dose to the tumour and the importance of this approach in future clinical protocol design.

### 3.5 Conclusions

In this chapter, an optimal Iodogen-Beads based radioiodination method was established. Using this labelling method, a labelling efficiency of greater than 95% has been consistently achieved in over 150 radiolabelling procedures of rat anti-mouse mAbs used in the preclinical RIT studies. This labelling protocol has also been used in clinical RIT studies in which 300 MBq - 3.0 GBq  $^{131}\text{I}$  was successfully labelled to Rituximab over 70 times with specific activity ranging from 60 MBq/mg to 600 MBq/mg. Furthermore, continuous quality control assays have demonstrated satisfactory post labeling Rituximab immunoreactivity which is found slightly higher than those published by other groups.

The in vivo biodistribution characteristics of a panel of radioiodinated mAbs were extensively investigated mainly in BCL<sub>1</sub> lymphoma model and demonstrated that mAb targeting on highly expressed, non-internalising antigens was most effective in delivering radiation to the targeted tumour. The biodistribution studies have also demonstrated that the presence of antigen binding sites determined the circulating half-life of intravenously administered mAb. Therefore, in order to achieve increased targeted radiation delivery, the dose of pre-dosing should be ideally patient specific.

The extensive biodistribution and dosimetry data obtained in this chapter laid solid foundation for further studies to investigate the factors determining the successful clearance of tumour in RIT of B-cell lymphoma.

## **Chapter 4 Determinants of Successful Clearance of Tumour in RIT of B-cell Lymphoma**

### **4.1 Introduction**

Despite the clinical progress made with RIT outlined in the introduction, there remains considerable uncertainty regarding the optimal treatment approach in using RIT in NHL. One such issue is whether a radiation dose response exists and whether higher or lower doses of radioactivity should be used (Behr 2002; von Schilling 2002). Most groups including Kaminski and co-workers have elected to use a lower non-myeloablative dose (Kaminski, Zasadny et al. 1993; Kaminski, Tuck et al. 2005). In contrast, Press and colleagues have adopted a high dose myeloablative approach with peripheral blood stem cell transplantation support (Press, Eary et al. 1993; Press, Eary et al. 1995; Press 2003). Both approaches have resulted in impressive durable clinical responses and there is currently no randomised evidence to support the superiority of either approach (Press, Leonard et al. 2001). Using higher doses of radiation and stem cell transplantation does however create a number of radiation protection and logistical issues that make widespread use of this approach more difficult. A clear benefit of using higher doses of radiation would therefore have to be demonstrated before higher doses of radiation could enter routine clinical practice.

Furthermore, the mechanisms involved in clearance of tumour by RIT remains poorly understood and some mAbs, such as Lym-1 (binding to HLA-DR) have often been considered simply as vectors for delivering radiation to tumour or “systemic radiotherapy” (DeNardo, DeNardo et al. 1998). Recent preclinical and clinical data have however clarified that some mAbs are intrinsically therapeutically active and may operate by interacting with the host immune system or through a direct cytotoxic effect via cell surface signalling (Tutt, French et al. 1998; Illidge, Cragg et al. 1999; Glennie and Johnson 2000; Glennie and van de Winkel 2003). An understanding of the mechanisms underlying the clinical responses is likely to be important in the further

development and optimisation of this treatment approach. Dissecting the mechanism of action of RIT and attributing the relative importance of mAb, targeted radiation and non-specific whole body irradiation to the therapeutic efficacy is difficult or impossible in a clinical setting. Such fundamental issues are therefore ideally approached in syngeneic tumour models. In this situation tumour develops in the presence of an intact immune system and the targeting mAb is able to cross-react with appropriate normal tissues in a manner analogous to the clinical situation and contrasting with the limitations of human SCID xenograft models where there is no such host immunity or specific cross reaction of mAb with normal tissues.

Our group have previously reported the importance of antibody specificity in the successful eradication of tumor with RIT (Illidge, Cragg et al. 1999). The aim of this chapter was to demonstrate whether a radiation dose response exists for RIT in the presence of cell surface signaling in B-cell lymphomas *in vivo* and to characterise the relative contributions made by targeted irradiation and mAb effector mechanisms. To do this two different mAbs were used to fulfill different functions and work cooperatively to successfully eradicate lymphoma *in vivo*. In this situation, the characteristics of one mAb are exploited to target radiation effectively to the tumour whilst the second mAb provides intracellular signaling by ligating key cell surface receptor molecules.

## **4.2 Materials and Methods**

### **4.2.1 Animal Models**

Ten to twelve week-old female BALB/c and CBA/H mice were supplied by Harlan UK Limited (Blackthorn, Oxon, UK), and maintained in local facilities. In previous chapter (chapter 3) the biodistribution and dosimetry data of two syngeneic murine B-cell lymphoma models, BCL<sub>1</sub> and A31 had been obtained. Therefore, in this chapter these

two animal models were used to investigate the factors determining the therapeutic outcome of RIT of B-cell lymphoma. These two tumours develop primarily in the spleen of BALB/c and CBA/H mice, respectively.

#### **4.2.2 Antibodies and Radioiodination**

A panel of rat anti-mouse mAbs, namely anti-MHCII, anti-Id, anti-CD19, anti-CD22, anti-CD38 and isotype matched control mAbs were radioiodinated with Iodine-131 using Iodogen-Beads method as described previously. The labelling efficiency was monitored by instant thin layer chromatography (ITLC) and high performance liquid chromatography (HPLC). The specific activity was 37 to 185 MBq/mg (1.0-5.0 mCi/mg). The post-labelling immunoreactivity was assessed by BCL<sub>1</sub> cell binding assay as described by Elliott et al (Elliott, Glennie et al. 1987).

#### **4.2.3 Radioimmunotherapy**

Same as the settings of biodistribution studies (early stage tumour), age and sex-matched mice were inoculated by intravenous injection with 10<sup>6</sup> A31 or 10<sup>5</sup> BCL1 lymphoma cells on day 0 and therapies were given on day 10.

<sup>131</sup>I labelled 500 µg mAb per animal (anti-CD19, anti-CD22, anti-CD38, anti-MHCII, or anti-BCL<sub>1</sub> Id) or 100 µg (anti-A31 Id) carrying 1.85 MBq to 18.5 MBq radioactivity was given to parallel groups of animals by tail vein injection. For therapies combining RIT with unlabelled mAbs, mice were injected intravenously with unlabelled anti-BCL<sub>1</sub> Id, or anti-A31 Id, or anti-CD19, or anti-CD38 (doses as mentioned above) 2 to 3 hours prior to the injection of the <sup>131</sup>I labelled anti-MHCII. Parallel groups of mice were treated with unlabelled antibodies alone or <sup>131</sup>I-anti-MHCII alone for comparison. For all RIT therapies mice were given Lugol's solution as described previously in biodistribution studies. Animal survival was monitored daily, and the results were

analysed using the  $\chi^2$  test of Peto (Peto 1974). All the animal experiments were performed under a Home Office project license.

#### **4.2.4 Haematological Toxicity of RIT**

Due to practical difficulty to accurately obtain and weigh the mouse bone marrow, the haematological impact of RIT ( $^{131}\text{I}$ -anti-MHCII) was evaluated alternatively by measuring the peripheral blood count of treated mice. Comparable to the RIT settings, groups of BCL<sub>1</sub> tumour inoculated BALB/c mice (12 mice/group) received 500  $\mu\text{g}$  of either 9.25 MBq or 18.5 MBq  $^{131}\text{I}$ -labelled anti-MHCII mAb by intravenous injection 2 to 3 hours after the infusion of unlabelled anti-BCL<sub>1</sub> Id. Parallel groups of untreated or non-tumour-bearing mice were given the same therapy as controls. Animals were killed on days 1, 7, 14, 21, 28, and 35 after receiving the radioactive mAb. Blood samples were obtained from cardiac puncture and analysed using a Sysmex XE-2100 Blood Cell Analyzer (Sysmex, Milton Keynes, UK)

#### **4.2.5 Phosphotyrosine Detection by Western Blot**

Up-regulation of intracellular protein tyrosine phosphorylation was measured by Western Blot as described by Vuist et al (Vuist, Levy et al. 1994). In this experiment, BCL<sub>1</sub> tumor cells were incubated with rat anti-mouse mAbs and hyper-crosslinking of the primary mAb was performed by adding sheep anti-rat IgG. In experiments where mAb were combined with EBRT, samples were irradiated with 5 Gy using a  $^{137}\text{Cs}$  source (Gamma cell 1000, Kanata, Canada) directly after hypercrosslinking. Cell pellets were lysed and centrifuged for 15 minutes at 16100 g. 20  $\mu\text{L}$  of the supernatant was mixed with 10  $\mu\text{L}$  loading buffer, boiled for 5 minutes before being subjected to SDS-PAGE. Proteins in the gel were transferred to nitrocellulose and the blot was incubated overnight at 4°C in 5% bovine serum albumin (BSA). Phosphotyrosine was detected by incubating the blot with mAb 4G10 (Upstate Group, Inc. Milton Keynes, UK) and horseradish peroxidase (HRP) labeled goat anti-mouse antibody. Enhanced chemiluminescence (ECL) reagents were added as directed by the manufacturer (Pierce,

Rockford USA) and the blot was exposed and acquired using real time image acquisition system, ChemiDoc XRS System (Bio-Rad Laboratories, Inc., CA, USA.).

#### **4.2.6 Immunoprecipitation Analysis for Tyrosine Phosphorylation of Syk**

To detect Syk tyrosine phosphorylation, TX-100 lysates prepared as above were first incubated with 4G10 (2 µg/sample) at 4°C overnight. Protein G-coated Sephrose beads (Amersham Biosciences, UK) pre-blocked with 5% (wt/vol) BSA were then added to the samples (15 µL/sample), and incubated for a further 60 minutes at 4°C. The resulting beads were then washed 4 times with cold lysis buffer and boiled in sample buffer. The precipitated proteins were separated by SDS-PAGE and immunoblotted as described above with the anti-Syk antibody C-20 (Santa Cruz Biotechnology, Inc. Santa Cruz, CA).

### **4.3 Results**

#### **4.3.1 Radiation Dose Delivered by RIT Does Not Correlate with Survival**

In chapter 3, the in vivo biodistribution of a panel of pan-B-cell mAbs was assessed and the anti-MHCII mAb was shown to deliver larger doses of targeted radiation to the main tumour bearing organ, the spleen. In this experiment, the therapeutic effects of 9.25 MBq  $^{131}\text{I}$  labelled pan-B-cell mAbs were investigated to determine whether a relationship exists between the radiation dose delivered to tumour bearing organs and the therapeutic results observed. Under conditions similar to that seen during the biodistribution studies, mice received  $10^5$  BCL<sub>1</sub> cells intravenously and were treated 10

days later with unlabeled or 9.25 MBq  $^{131}\text{I}$ -labeled mAb. Unlabeled anti-MHCII mAb gave no protection over controls, both anti-Id and anti-CD19 produced a small therapeutic effect, increasing survival with anti-Id by around 8 days and with anti-CD19 by around 2-3 days (Figure 4.1). This therapeutic activity was however further enhanced by the conjugation of 9.25 MBq  $^{131}\text{I}$  to the anti-CD19 mAb. Interestingly, all three radioimmunoconjugates produced a similar level of therapeutic performance (Figure 4.1). The same amount of  $^{131}\text{I}$  radiolabelled control mAb provided only approximately 5 days improvement in survival over control animals (data not shown). Therefore, despite  $^{131}\text{I}$ -anti-CD19 and  $^{131}\text{I}$ -anti-Id delivering significantly less radiation dose to tumor, these radioimmunoconjugates provided a similar level of tumour protection to  $^{131}\text{I}$ -anti-MHCII. These data indicated that there did not appear to be a relationship between radiation dose delivered with single mAb and therapeutic response seen if the intrinsic therapeutic effect of individual mAb was not counted, strongly suggesting that there are two components in RIT namely targeted radiation and mAb mediated cell killing.

Currently, anti-CD20 mAb are dominating clinical RIT for lymphoma. However, there has been a longstanding controversy over whether a radiation dose response exists in RIT and debate over the necessity of radiation dosimetry for individual patients (Wagner, Wiseman et al. 2002; Koral, Kaminski et al. 2003; Britton 2004; Goldenberg and Sharkey 2005). It is well documented that most of the anti-CD20 mAb are intrinsically effective in tumour killing probably through the combination of ADCC, CDC and trans-membrane signalling induction (Avivi, Robinson et al. 2003; Bannerji, Kitada et al. 2003). However, it is practically impossible to differentiate mAb effector mechanisms and radiation dosimetry effects in clinical RIT and therefore it is difficult to find a calculation between tumour doses and therapeutic response. The data obtained from this experiment provided some support to the clinical phenomena where some investigators failed to observe any radiation dose response and suggest the future RIT treatment strategies might involve two mAbs, one mAb for mediating antibody dependent cell killing mechanisms and another mAb for targeted radiation.

**Figure 4.1**

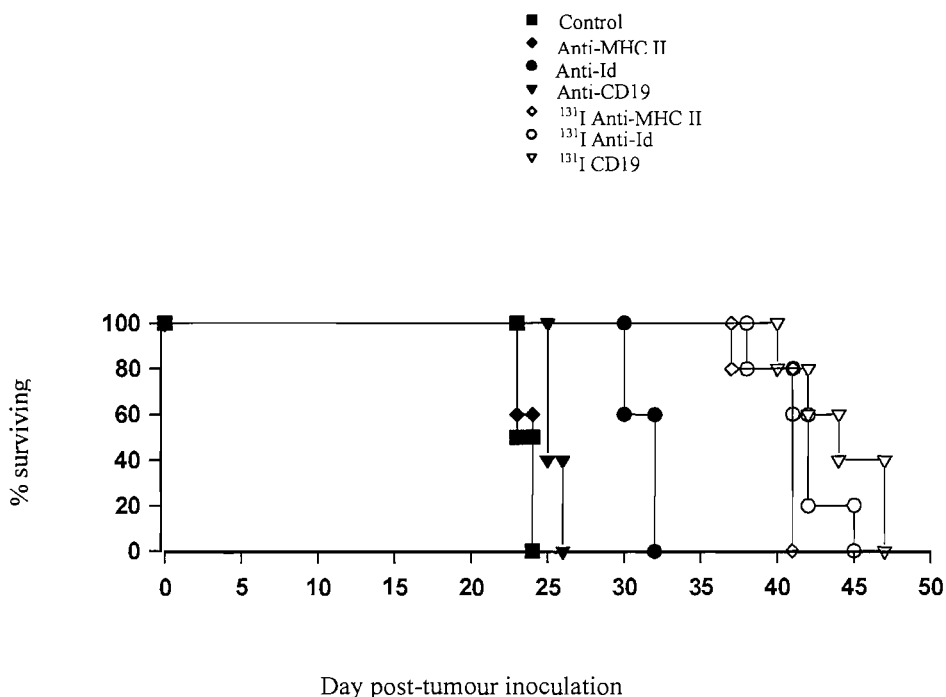
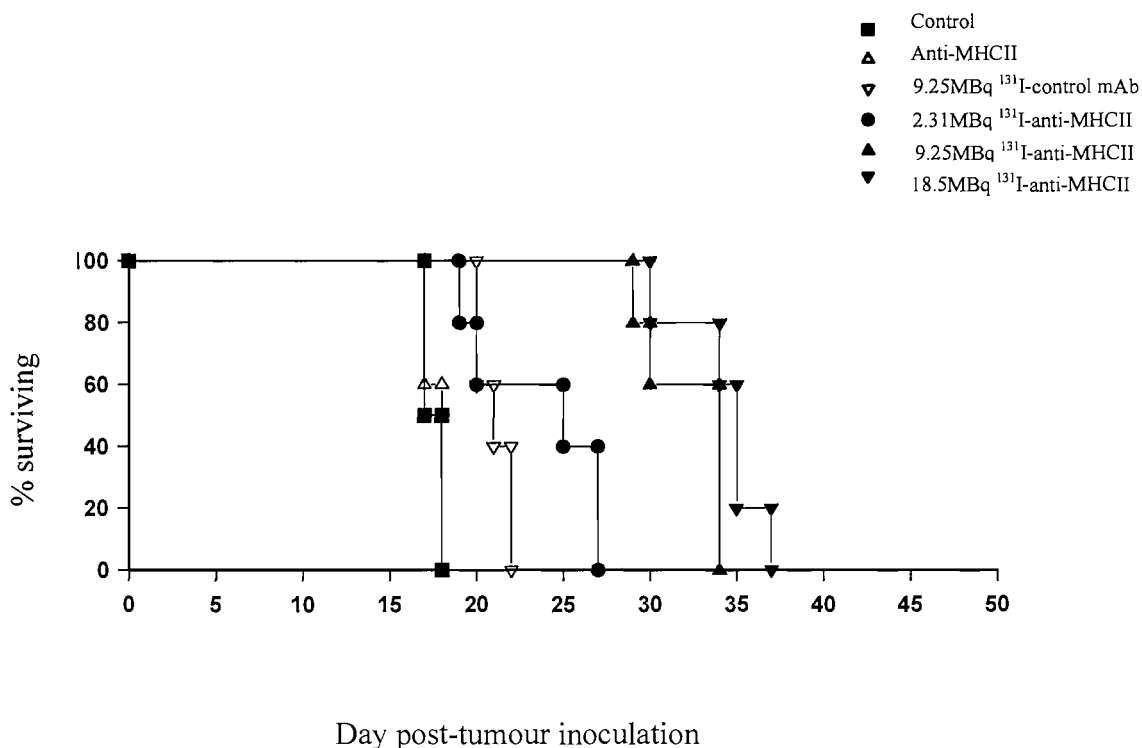


**Figure 4.1. RIT of BCL<sub>1</sub> lymphoma showed that radiation dose delivered by RIT does not correlate with animal survival.** In this experiment, BCL<sub>1</sub> cells ( $10^5$  per animal, intravenous inoculation) were given on day 0, and RIT treatments were administered also by intravenous injection 10 days later (500  $\mu\text{g}$  mAbs with or without 9.25 MBq  $^{131}\text{I}$  labelling). Unlabelled anti-MHCII showed no therapeutic effect ( $P>0.05$ ) whereas anti-Id and anti-CD19 showed modest improvements in survival of a few days ( $P<0.01$ ). A similar therapeutic affect was seen for all three radioimmunoconjugates (9.25 MBq  $^{131}\text{I}$  labelled anti-MHCII, anti-CD19, and anti-Id) ( $P>0.05$ ).

#### **4.3.2 RIT of BCL<sub>1</sub> Lymphoma with Serial Doses of <sup>131</sup>I-anti-MHCII**

Anti-MHCII mAb (TI2-3) has demonstrated to be the most efficient radiation delivery mAb. In this experiment, anti-MHCII was labelled with serial doses of <sup>131</sup>I trying to see whether there is a radiation dose response in RIT using such a mAb. Figure 4.2 shows a typical RIT experiment in BCL<sub>1</sub> the model. When the dose of <sup>131</sup>I labelled anti-MHCII was increased from 2.31 MBq to 9.25 MBq a dose response was seen with the highest dose providing an increase of around 15-20 days of survival. However, when the dose of <sup>131</sup>I was further escalated to 18.5 MBq, no further improvements were observed. Importantly, the unlabelled anti-MHCII mAb had no therapeutic effect and 9.25 MBq <sup>131</sup>I labelled control mAb provided only about 4-5 days of protection over untreated animals which were similar to those achieved by the lowest dose of 2.31 MBq <sup>131</sup>I labelled anti-MHCII mAb. This experiment confirms the effective tumour targeting of the <sup>131</sup>I anti-MHCII and argues against a non-specific whole body irradiation effect. This experiment also suggested that targeted radiation alone has limited therapeutic efficacy in this model.

**Figure 4.2**

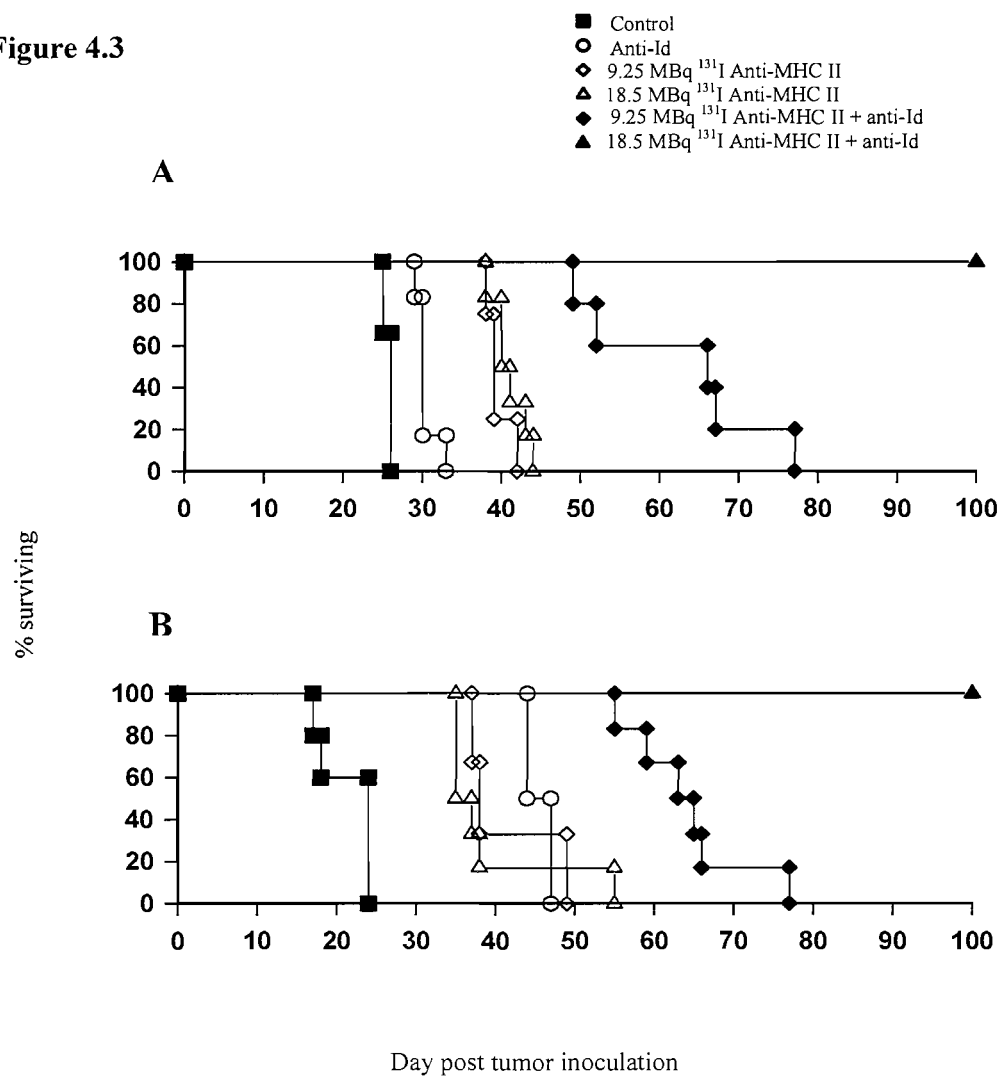


**Figure 4.2 RIT of BLC<sub>1</sub> lymphoma with serial doses of  $^{131}\text{I}$ -anti-MHCII.** In this experiment, groups of age and sex-matched BALB/c mice were inoculated by intravenous injection of  $10^5$  BCL<sub>1</sub> tumour cells and were treated 10 days later by intravenous injection of unlabelled anti-MHCII mAb, 9.25 MBq  $^{131}\text{I}$  labelled control mAb, 2.31 MBq, 9.25 MBq, and 18.5 MBq  $^{131}\text{I}$  labelled anti-MHCII mAb respectively. This experiment is representative of 1 of 3 similar experiments. When 9.25 MBq  $^{131}\text{I}$  labelled control mAb provided approximately only 5 days protection, a much smaller dose of 2.31 MBq  $^{131}\text{I}$  labelled anti-MHCII mAb achieved similar protection and 9.25 MBq  $^{131}\text{I}$  labelled anti-MHCII mAb gave about 15 to 20 days protection demonstrating the superiority of  $^{131}\text{I}$  labelled anti-MHCII mAb in RIT ( $P<0.01$ ). However, when the dose of  $^{131}\text{I}$  labelled anti-MHCII mAb increased from 9.25 MBq to 18.5 MBq, no further improvements were seen ( $P>0.05$ ).

### 4.3.3 A Radiation Dose Response Exists for RIT of Lymphoma in the Presence of anti-Id mAb

Having demonstrated that there are two potential components of RIT namely targeted radiation and mAb mediated cell killing, the combination of  $^{131}\text{I}$ -anti-MHCII with unlabelled anti-Id mAb was subsequently investigated. Anti-MHCII was shown to be the most effective mAb for delivering radiation to tumour and anti-Id had demonstrated single agent activity unlabelled. Parallel groups of BCL<sub>1</sub> and A31 inoculated animals were treated with two doses of  $^{131}\text{I}$  (9.25 MBq and 18.5 MBq) labelled anti-MHCII mAb with and without the addition of unlabelled anti-Id (500  $\mu\text{g}$ /animal, intravenous injection 2-3 hours prior to  $^{131}\text{I}$  labelled anti-MHCII) (Figure 4.3A and B).

These experiments led to two important observations. Firstly, there was not a radiation dose response with targeted radiation alone at the  $^{131}\text{I}$  dose level above 9.25 MBq, as similar levels of animal survival were seen with 9.25 MBq and 18.5 MBq of  $^{131}\text{I}$ -anti-MHCII mAb in both the A31 and BCL<sub>1</sub> models. The second most striking observation was the impressive therapeutic efficacy of combining  $^{131}\text{I}$  -anti-MHC II with unlabeled anti-Id mAb (Figure 4.3A and B). When 9.25 MBq  $^{131}\text{I}$ -anti-MHCII was given with unlabeled anti-Id, an increase of approximately 30 days survival was seen over that seen with either the  $^{131}\text{I}$ -anti-MHCII or anti-Id alone. Furthermore, in the presence of anti-Id mAb there was a clear radiation dose response with animal survival improving as the dose increased from 9.25 MBq to 18.5 MBq  $^{131}\text{I}$ -anti-MHCII. Whilst there were no long-term survivors seen with 9.25 MBq  $^{131}\text{I}$ -anti-MHC II plus anti-Id, when the dose of  $^{131}\text{I}$  was increased to 18.5 MBq, 100% of animals survived over 100 days with no sign of tumour development. This important observation was also reproduced using the A31 model and a similar dose response was again seen, with 18.5 MBq  $^{131}\text{I}$ -anti-MHCII plus anti-Id treatment consistently producing 100% long-term disease free survivors (Figure 4.3B). It is important to note that in these experiments, 18.5 MBq  $^{131}\text{I}$  labelled control mAb provided only around 5-7 days of protection over untreated animals (data not shown).

**Figure 4.3****Figure 4.3. Dose response of RIT in BCL<sub>1</sub> and A31 B-cell lymphoma models.**

Unlabelled anti-Id mAb was added to  $^{131}\text{I}$  labelled anti-MHCII mAb in the RIT treatment. (A) BALB/c mice were inoculated intravenously with  $10^5$  BCL<sub>1</sub> tumour cells and treated with 500  $\mu\text{g}$  anti-Id mAb per animal given 2 hours before on day 10. (B) CBA/H mice were inoculated with  $10^6$  A31 tumour cells and treated with 100  $\mu\text{g}$  anti-A31-Id mAb 8 days later. This experiment is representative of 1 of 3 similar experiments. In both animal models, 9.25 MBq and 18.5 MBq  $^{131}\text{I}$  labelled anti-MHCII provided similar levels of protection. In contrast, with the addition of anti-Id mAb, a clear dose response was seen in both BCL<sub>1</sub> and A31 models. In combination with anti-Id, 18.5 MBq  $^{131}\text{I}$  labelled anti-MHCII achieved 100% long-term protection which were significant improvements in survival over the 9.25 MBq RIT dose ( $P<0.01$ ).

#### **4.3.4 The Impact of Pre-dose on RIT with $^{131}\text{I}$ -anti-MHCII mAb**

The biodistribution studies had demonstrated that for BCL<sub>1</sub> lymphoma model bearing early stage tumour (10 days after intravenous inoculation of  $10^5$  tumour cells), 500  $\mu\text{g}$  unlabelled anti-MHCII given as a pre-dose could actually decrease the radiation dose delivered to the tumour by the subsequently administered 18.5 MBq  $^{131}\text{I}$  labelled anti-MHCII mAb from approximately 18 Gy to 11.5 Gy. In this experiment, the therapeutic impact of pre-dose was investigated in  $^{131}\text{I}$ -anti-MHCII RIT therapy. BALB/c mice were inoculated with  $1 \times 10^5$  BCL<sub>1</sub> cells by intravenous injection and therapies were given 10 days after inoculation. For the pre-dosing groups, animals received an additional intravenous injection of 500  $\mu\text{g}$  of unlabelled anti-MHCII 2-3 hours prior to the administration of radiolabelled same mAb (TI2-3). In the case of combination RIT with unlabelled anti-Id mAb, the pre-dose anti-MHCII mAb was given together with the unlabelled anti-Id.

Pre-dosing was shown to reduce the therapeutic efficacy of same amount of  $^{131}\text{I}$  labelled anti-MHCII especially in the presence of anti-Id, as a result of decreased radiation dose delivery in these animals bearing early stage tumour (Figure 4.4). In the groups of 18.5 MBq  $^{131}\text{I}$  labelled anti-MHCII plus unlabelled anti-Id, while all the animals treated without pre-dose became long term survivors, all the animals in the pre-dose group were culled due to advanced tumour at around the same time as the animals treated with half dose  $^{131}\text{I}$  (9.25 MBq  $^{131}\text{I}$ -antiMHCII + anti-Id).

**Figure 4.4**

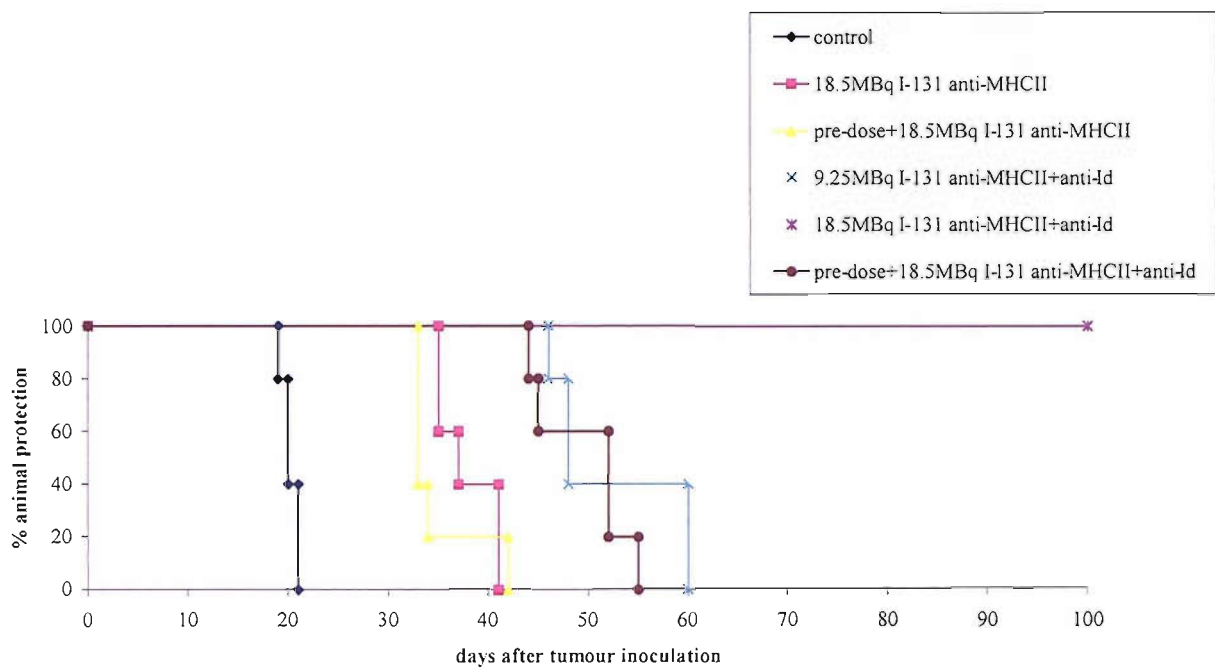


**Figure 4.4. The impact of pre-dose on RIT with  $^{131}\text{I}$ -anti-MHCII mAb in BCL<sub>1</sub> lymphoma model.** BALB/c mice were inoculated with  $10^5$  BCL<sub>1</sub> cells by intravenous injection on day 0 and treated 10 days later with 9.25 MBq or 18.5 MBq  $^{131}\text{I}$  labelled anti-MHCII plus anti-Id with or without the addition of a pre-dose of 500  $\mu\text{g}$  unlabelled anti-MHCII mAb which was intravenously injected 2 to 3 hours prior to the RIT. This figure shows that the pre-dose significantly decreased the therapeutic efficacy of combination RIT (18.5 MBq  $^{131}\text{I}$  labelled anti-MHCII plus anti-Id) ( $P<0.01$ ).

#### **4.3.5 Anti-CD19 Improves Survival in Combination with $^{131}\text{I}$ -anti-MHCII RIT**

Previous experiments have confirmed that apart from anti-Id, other mAb such as anti-CD19 also has therapeutic activity. Therefore, the effects of anti-CD19 mAb as well as two other B-cell specific mAbs, anti-CD22 and anti-CD38 were investigated in combination with  $^{131}\text{I}$ -anti-MHCII to see whether the long-term clearance of tumour achieved with anti-Id plus  $^{131}\text{I}$ -anti-MHCII could be reproduced. Figure 4.5 showed that when anti-CD19 mAb (1D3) was substituted for anti-Id and used in combination with 18.5 MBq  $^{131}\text{I}$ -anti-MHCII in the BCL<sub>1</sub> model, impressive tumour protection was also seen of around 35 days over that with control (untreated) animals and 15 days more than  $^{131}\text{I}$ -anti-MHCII alone ( $p<0.01$ ). Another B-cell specific mAb, anti-CD22 (NIMR6), to a lesser extent, also gave 5-6 days further protection ( $p<0.01$ ). However, despite the CD38 antigen being expressed on B-cells at similar levels to CD19 (Table 2.1) the enhancement in therapy with  $^{131}\text{I}$  labelled anti-MHCII which was seen with anti-CD19 mAb was not observed with the anti-CD38 mAb (1A5E8), where the level of animal protection observed was similar to that achieved with  $^{131}\text{I}$ -anti-MHCII alone. As usual, 18.5 MBq  $^{131}\text{I}$  labelled control mAb provided only around 5-7 days of protection over control animals (Figure 4.5).

**Figure 4.5**

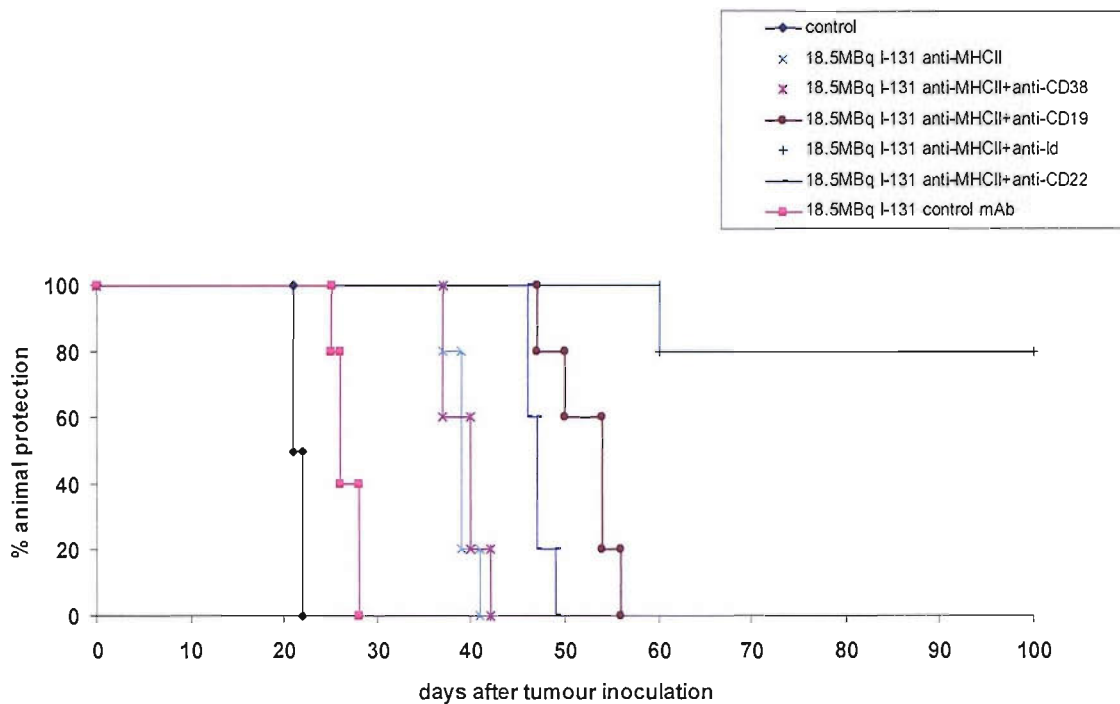


**Figure 4.5. Anti-CD19 improved survival in combination with  $^{131}\text{I}$  labelled anti-MHCII mAb in the BCL<sub>1</sub> lymphoma model.** BALB/c mice were inoculated with  $10^5$  cells by intravenous injection on day 0 and treated 10 days later with 18.5 MBq  $^{131}\text{I}$  labelled anti-MHCII plus anti-Id, anti-CD38, or anti-CD19 mAb (500  $\mu\text{g}$  of each mAb given intravenously 2-3 hours prior to the administration of radiolabelled anti-MHCII mAb). The above experiment is representative of 3 identical experiments and shows that when the anti-Id or anti-CD19 was added to 18.5 MBq  $^{131}\text{I}$  labelled anti-MHCII, significant survival improvements over 18.5 MBq  $^{131}\text{I}$  labelled anti-MHCII alone were achieved ( $P<0.01$ ). No improvement was observed following the addition of anti-CD38 mAb.

#### **4.3.6 Anti-Id and Anti-CD19 mAb Induce Direct Cell Surface Mediated Signalling**

The mechanisms behind the clearance of tumour *in vivo* and a potential link between the ability of some mAbs to induce cell surface signalling to therapeutic performance were then investigated. The signal transduction was initially assessed by measuring the up-regulation of cellular protein tyrosine phosphorylation (PTP) using western blot analysis. After stimulating BCL<sub>1</sub> tumour cells with a panel of B-cell binding mAb in the presence or absence of a second hyper-crosslinking polyclonal Ab (sheep anti-rat polyclonal antibody) it was clear that mAb directed to the IgM heavy chain or Id regions of the BCR clearly induced profound up-regulation of PTP on proteins of approximately 72 kDa (Figure 4.6A). Anti-CD19 mAb and to a lesser extent anti-CD22 (NIMR6) mAb (Compared to that of anti-Id, the phosphorlation intensities induced by anti-CD19 and anti-CD22 were approximately 57% and 19%, respectively.) the proteins of same molecular weight but only after hyper-crosslinking which was in accordance with previously reported by Torres et al (Torres, Law et al. 1992). In contrast, no demonstrable increase in PTP was seen for anti-MHCII, anti-CD38 (1A5E8) or an isotype matched control irrelevant mAb in the presence or absence of hyper-crosslinking antibody.

As in the previous RIT experiments, it had been observed that significantly improved therapeutic effects existed when these signalling mAb were used in addition to the targeted irradiation (delivered by <sup>131</sup>I labelled anti-MHCII). The cell surface signalling experiment described above was repeated with the addition of 5 Gy external beam radiotherapy (EBRT) delivered using a <sup>137</sup>Cs irradiator (Gamma cell 1000, Kanata, Canada). The addition of 5 Gy irradiation appeared to significantly increase the amount of PTP seen on the western blot over and above that seen with hypercrosslinking mAb alone (Figure 4.6B). Using the Quantity One software provided with the image acquisition system (ChemiDoc XRS System, Bio-Rad Laboratories, Inc., CA, USA.), a 1.82 fold increase of grey scale was observed over the band of 72 kDa molecular weight under the treatment of anti-Id.

Syk is known to be one of the key initiators of the complex signalling cascades triggered following BCR ligation and has a molecular weight of 72 kDa (Kurosaki, Johnson et al. 1995). I therefore hypothesised that the protein seen on the western blot analysis might be phosphorylated Syk. Immunoprecipitation experiments were performed using a Syk-specific antibody. The tyrosine phosphorylated proteins immunoprecipitated by the anti-Syk antibody were identical to the approximately 72 kDa proteins detected by direct immunoblotting using a phosphotyrosine-specific antibody. Therefore, phosphorylation of Syk appears to correlate with therapeutic responsiveness (Figure 4.6C). Interestingly, comparison immunoprecipitation experiments using an anti-Lyn mAb (sc-15, Santa Cruz Biotechnology, Inc., Santa Cruz, CA, USA.) did not demonstrate any observable difference between different treatments (data not shown).

**Figure 4.6**

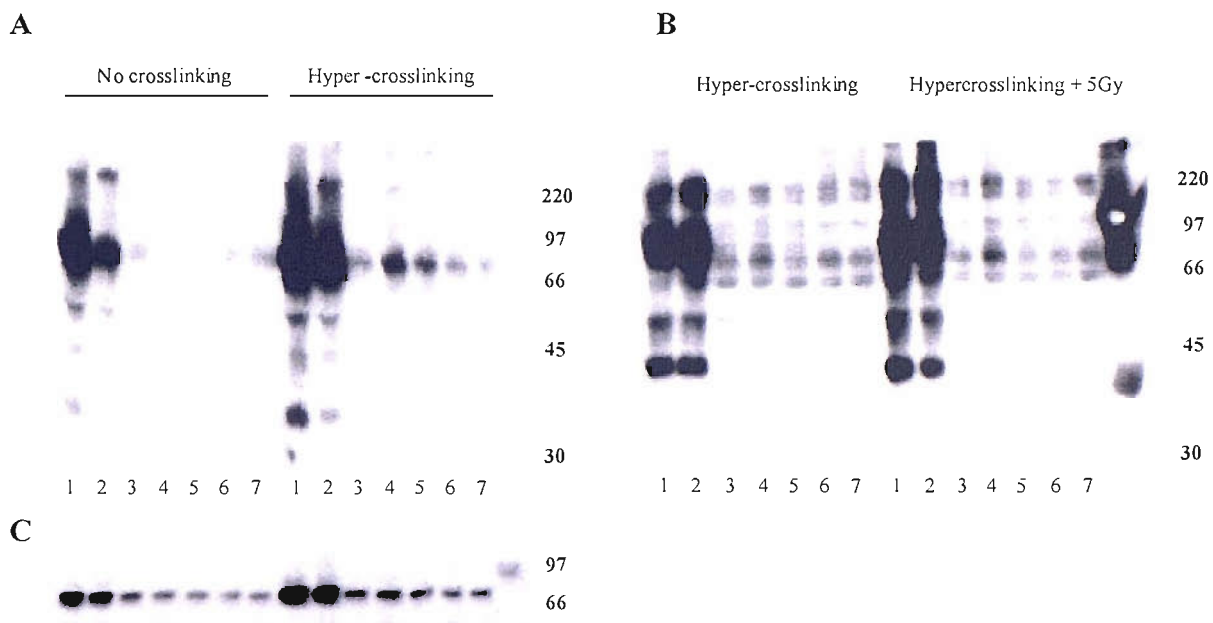


**Figure 4.6. Measurement of intracellular signalling.** (A) Western blot analysis of protein tyrosine phosphorylation was performed using fresh BCL<sub>1</sub> cells as described in materials and methods. 1 = anti- $\mu$  (IgM heavy chain); 2 = anti-Id; 3 = anti-MHCII; 4 = anti-CD19; 5 = anti-CD22; 6 = anti-CD38; 7 = Control. Anti- $\mu$  and anti-Id as single mAb demonstrate intracellular signalling through the surface Ig receptor (BCR) as measured by the induction of cellular protein tyrosine phosphorylation. Hyper-crosslinking of primary mAb with sheep anti-Rat IgG demonstrates signal transduction, to a lesser extent, in anti-CD19 and anti-CD22 as well as via the BCR. (B) Addition of radiation enhances the level of signalling observed through these molecules. (C) Immunoprecipitation of phosphorylated proteins using 4G10, followed by immunoblotting with anti-Syk mAb, revealed that the ~70 kDa phosphorylated protein is likely to be Syk.

#### **4.3.7 Haematological Toxicity of Therapeutic RIT Using $^{131}\text{I}$ -anti-MHCII mAb**

In clinical RIT trials, myelotoxicity has been found to be the dose-limiting toxicity. Unfortunately it is practically impossible to accurately measure the weight and the radioactivity of mouse bone marrow secondary to the small size of the bone marrow. Therefore, it was not possible to calculate directly the bone marrow dosimetry as was performed for the blood, spleen, liver, lung and kidney. Instead, peripheral blood count was measured as a surrogate measure of bone marrow toxicity.

Figure 4.7 shows that the toxicity of  $^{131}\text{I}$ -anti-MHCII treatment was mild, dose dependent, and reversible. The haemoglobin level was not significantly affected (figure 4.7A), while there was a dose dependent decrease in the platelet and white cell counts as the dose of  $^{131}\text{I}$  was increased from 9.25 MBq to 18.5 MBq (Figure 4.7B & Figure 4.7C). For 18.5 MBq  $^{131}\text{I}$  anti-MHCII plus anti-Id mAb, there was a substantial fall in the platelet count from around  $500 \times 10^9/\text{L}$  to  $200 \times 10^9/\text{L}$  which recovered to pretreatment level by 21 days after the therapy. A dose dependent decrease in the lymphocyte count could be seen as early as one day post RIT remaining suppressed for 14 days, with initial recovery being seen by day 21. In contrast, neutrophils appeared more resistant to the effects of  $^{131}\text{I}$  labelled anti-MHCII with the total numbers unaffected (Figure 4.8D).

**Figure 4.7**

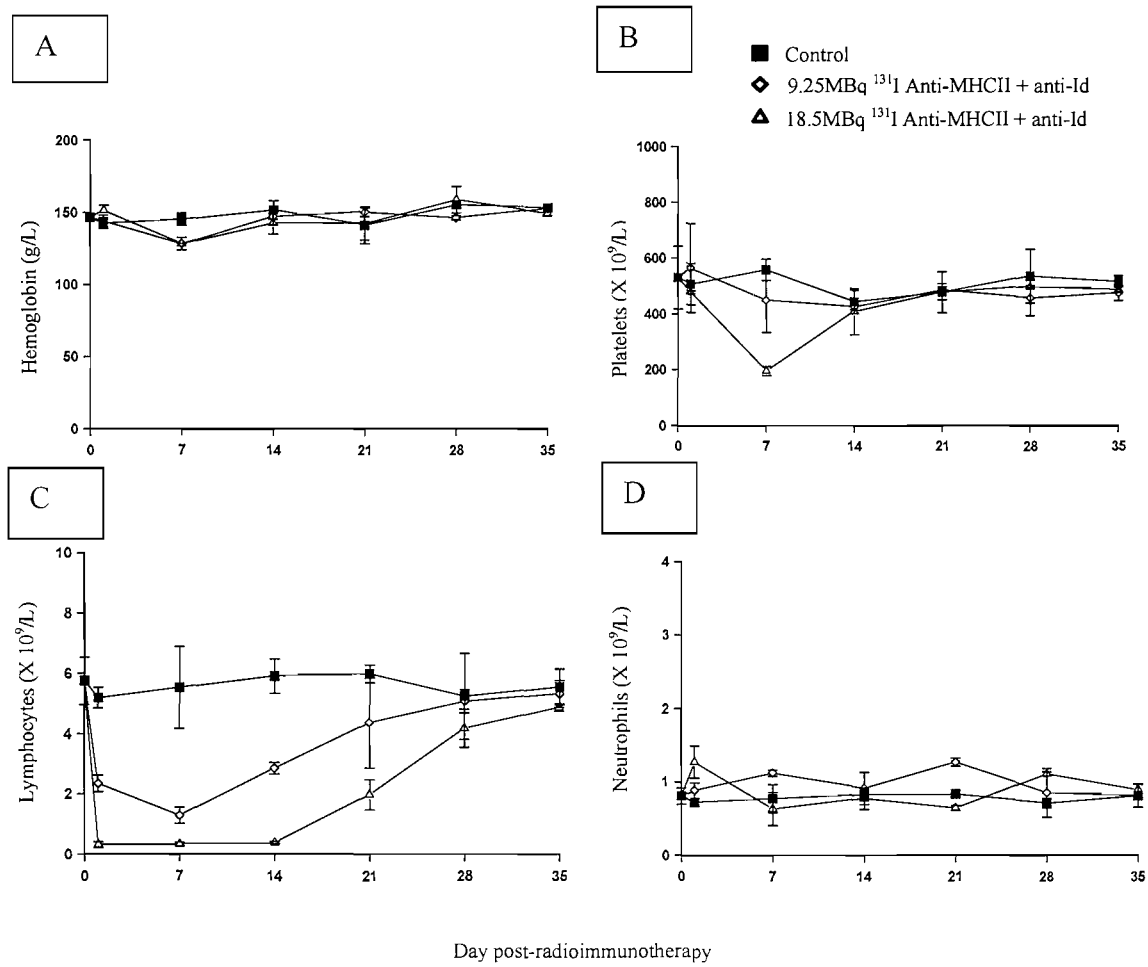


**Figure 4.7. Haematological toxicity of RIT with  $^{131}\text{I}$  labelled anti-MHCII mAb.** The haematological toxicity of higher doses of  $^{131}\text{I}$  labelled anti-MHCII mAb revealed a dose-dependent effect on the platelet (B) and white cell (C) counts, whereas the haemoglobin level (A) and neutrophil count (D) were not significantly affected. In this experiment, groups of BALB/c mice (12 mice per group) were injected via the tail vein with  $10^5 \text{ BCL}_1$  cells. Ten days after tumour inoculation animals received 500  $\mu\text{g}$  of 9.25 MBq or 18.5 MBq  $^{131}\text{I}$  labelled anti-MHCII mAb by intravenous injection 2 to 3 hours after the injection of unlabelled anti- $\text{BCL}_1$  Id. In comparison, parallel groups of non-tumour- bearing BALB/c mice were given the same mAb therapy, and a group of untreated mice were set up as controls. Animals from respective groups were killed on days 1, 7, 14, 21, 28 and 35 after treatment and blood counts were measured as described in "Materials and Methods". Each point represents the mean value of 2 mice and the error bars represent the range seen.

## 4.4 Discussion

In this chapter some of the mechanisms operating in RIT of B-cell lymphoma have been investigated in two syngeneic models and the contributions of “targeted” irradiation and the intrinsic mAb effector mechanisms to the long-term clearance of tumour have been explored *in vivo* in these two syngeneic murine models. It has been shown that the successful clearance of tumour in RIT can be provided by using two different mAb working in combination, whereby one mAb is more effective at targeting the radiation to tumour and the second mAb initiates intracellular signalling. Finally it has been shown that a radiation dose response exists for RIT of B-cell lymphoma in the presence of a signalling mAb.

Work from our group had previously shown the importance of mAb specificity to the therapeutic outcome of RIT in the BCL<sub>1</sub> tumour model (Illidge, Cragg et al. 1999). In the current study that initial work has been substantially expanded and using MIRD dose calculations, the radiation dose delivered to the target organs as well as whole body by a panel of B-cell antigen targeting mAb has been determined *in vivo*. Although the anti-MHCII mAb and anti-Id mAb bound to BCL<sub>1</sub> tumour at similar levels, the anti-MHCII mAb delivered approximately 3-6 times more irradiation to the spleen which is the target organ. This observation appears to be explained by the fact that anti-MHCII mAb has a longer half-life and remains on the surface of tumour cells *in vivo*, whilst the anti-Id mAb is cleared rapidly (Illidge, Cragg et al. 1999). The rapid clearance of anti-Id mAb and poor delivery of radiation to tumour by anti-Id, we believe, is due to rapid endocytosis and dehalogenation of <sup>131</sup>I, in keeping with previously published work on anti- $\mu$  mAb (Press, Farr et al. 1989; Vervoordeldonk, Merle et al. 1994).

The requirement for individual patient dosimetry and its role in predicting response to RIT has been a controversial issue in clinical RIT (Illidge and Bayne 2001; DeNardo, Siantar et al. 2002; Sgouros, Squeri et al. 2003). Currently, different investigators still hold contradictory opinions, probably due to the lack of convincing experimental data.

While Britton and Wahl et al. recently addressed the importance of patient specific dosimetry in RIT of lymphoma, others like Postema and Goldenberg et al. remain unconvinced that dosimetry makes a significant contribution (Wagner, Wiseman et al. 2002; Wahl 2003; Britton 2004; Postema 2004; Goldenberg and Sharkey 2005; Kaminski, Tuck et al. 2005).

This study indicated that there was a poor correlation between the radiation dose delivered by RIT and the therapeutic outcome when there was additional tumour cell killing via the therapeutic effect of mAb. Even accurate radiation dosimetry appeared inadequate at predicting the tumour response. Thus it was found in this study that a similar level of performance for the three different radioimmunoconjugates  $^{131}\text{I}$  labelled anti-CD19, anti-Id and anti-MHCII mAb in these B-cell lymphoma models, despite widely different radiation dose delivery to tumour bearing organs. This may be explained by the fact that the tumour cell killing induced by the mAb was not quantified by such radiation dosimetry. Therefore for the radiolabelled anti-CD19 and anti-Id mAb there appears to be two components to the therapy, namely mAb effector mechanisms and targeted radiotherapy. Only the targeted radiation was measured by the radiation dosimetry. This has a limited usefulness in predicting therapeutic response for radioimmunoconjugates where the mAb has supplement activity.

Although the lymphoma models used in this study have different growth patterns from human lymphomas, the mAb used in this work all target antigens where equivalents have been tested in clinical trials (Meeker, Lowder et al. 1985; DeNardo, DeNardo et al. 1998; Juweid, Stadtmauer et al. 1999; Longo, Duffey et al. 2000; Ma, McDevitt et al. 2002; Dechant, Bruenke et al. 2003). Indeed, the  $^{131}\text{I}$ -Lym 1 which is similar to the anti-MHCII mAb used in this chapter has been extensively investigated in clinical trials (DeNardo, DeNardo et al. 1988; DeNardo, DeNardo et al. 1998). These results demonstrated an important principle that RIT is more than simply targeted radiation. Furthermore, these results may help to clarify why clinical RIT tumour dosimetry using radiolabelled anti-CD20 mAb in B-cell lymphoma frequently failed to correlate with the

clinical responses seen, as the tumour dosimetry is unable to quantify the anti-CD20 mAb effector mechanisms.

From these experiments, it appears that larger doses of targeted  $^{131}\text{I}$  are best delivered by a mAb directed against a highly expressed target antigen that fails to modulate upon binding, such as the MHCII complex. However, it is clear from this study that radiation alone is inadequate in producing long-term clearance of tumour. For RIT or “systemic radiotherapy”, no improvement in survival was seen as the radiation dose was increased above 9.25 MBq  $^{131}\text{I}$  anti-MHCII. However, when  $^{131}\text{I}$  labeled anti-MHCII mAb was combined with a signalling mAb, significant improvements in the therapy were seen, resulting in long-term survivors in the anti-Id plus  $^{131}\text{I}$  labeled anti-MHCII mAb groups. Interestingly, under these circumstances in the presence of anti-Id mAb, it was found that a radiation dose response existed for targeted radiation. The dose response was reproducible in two different B-cell lymphoma models, underlying the potential importance of this observation. The relevance of this observation to the clinical situation has been demonstrated by Cragg et al (Cragg and Glennie 2003; Cragg, Morgan et al. 2003) who have shown that the direct signalling capacity plays a critical role in the tumour killing effect of the anti-CD20 mAb, tositumomab (unlike Rituximab or 1F5), which is conjugated to  $^{131}\text{I}$  to form one of the FDA approved radioimmunoconjugate for the treatment of B cell lymphoma, the Bexxar<sup>TM</sup>. The Michigan group who have extensively investigated the clinical RIT application of this radioimmunoconjuagte reported that they observed clear radiation dose response (Wahl 2003; Zelenetz 2003; Kaminski, Tuck et al. 2005; Wahl 2005). This group’s work with Bexxar<sup>TM</sup> confirm that dosimetry study is critical to effective delivery of clinical RIT for NHL.

This study suggests that the substantial increases in therapeutic effect seen with the addition of anti-Id and anti-CD19 to targeted radiotherapy occurred because these mAb initiated intracellular signal transduction. Previous work from our group had shown that the anti-Id and anti-CD19 performed relatively poorly in complement dependent

cytotoxicity (CDC) and antibody dependent cellular cytotoxicity (ADCC) assays but these mAb were the most therapeutically active (Tutt, French et al. 1998). In contrast, the anti-MHCII mAb was the most potent in the CDC and ADCC assays, but provided no protection in vivo. These data argue that Fc-dependent effector mechanisms as measured in these assays cannot themselves explain the therapeutic activity of mAb. However, other in vitro assays revealed that mAb directed to the BCR complex were particularly active at inducing growth arrest of tumour cell-lines, presumably through intracellular signalling (Tutt, French et al. 1998). These results now provide direct evidence that anti-Id and anti-CD19 mAb, but not other mAb specificities (CD38, MHCII), initiated intracellular signalling shown by up-regulation of protein tyrosine phosphorylation.

It is well documented that signals transmitted by the BCR control the fate of normal and neoplastic B cells and that mAb directed to this receptor can induce apoptotic cell death (Cragg, Zhang et al. 1999; Donjerkovic and Scott 2000). Furthermore it is well established that signals from the BCR can be modulated by co-receptors such as CD19 (Niilo and Clark 2002) and that anti-CD19 mAb are capable of transmitting growth inhibitory/apoptotic signals, when sufficiently cross-linked (Chaouchi, Vazquez et al. 1995). Presumably therefore, the signals induced by these two mAb are similar and are generated through a shared pathway. The Western blot analysis and subsequent immunoprecipitation suggests that the protein tyrosine kinase Syk is involved in this signal transduction. Phosphorylation of Syk is one of the key steps in the complex signalling cascades activated following BCR ligation and is an important trigger for intracellular calcium flux (Kurosaki, Johnson et al. 1995). This is again in keeping with our data, where there was a good correlation between the degree of calcium mobilization (Du, Honeychurch et al. 2004) observed and the extent of Syk phosphorylation. Moreover, the strength of intracellular signal obtained appears to be proportional to the amount of BCR cross-linking (Marches, Racila et al. 1995). We observed that anti- $\mu$  and anti-Id mAb signalling was potentiated after hyper-crosslinking and that potent signalling through CD19 was only observed after such treatment. Evidence suggests that the function of hyper-crosslinking in vivo is likely to be fulfilled

by Fc-receptor bearing cells, such as macrophages and NK cells, which are able to bind and aggregate the Fc domains of mAb (Shan and Press 1995). Thus, this data supports the notion that the therapeutic efficacy of anti-Id and anti-CD19 mAb is related to the signalling activity of these reagents and that the response seen is proportional to the strength of intracellular signal delivered. These results appear entirely compatible with the clinical results published by the Stanford group using anti-Id mAb in the treatment of follicular lymphoma, where the clinical response appeared to correlate with the degree of signal transduction (Vuist, Levy et al. 1994).

This study does not exclude the possibility that other host immune effector mechanisms, such as T-cells, may act as an important component of clinical RIT. However, in our models, the long-term clearance of tumour by radiation and anti-Id does not appear to involve a T-cell response. Indeed, the number of CD4+ and CD8+ T-cells was actually lower in mice treated with RIT and anti-Id than in untreated controls (data not shown). From previous studies, we know that the tumour itself can stimulate an increase in CD4+ and CD8+ cells (Honeychurch, Glennie et al. 2003). This decrease may therefore reflect a reduction in the amount of tumour (and therefore antigen) present due to the potent cytotoxic activity of the combination therapy, as well as the direct immunosuppressive effect of the RIT itself.

## 4.5 Conclusions

The data from this chapter have demonstrated that the biodistribution of a single radiolabelled mAb does not predict tumour response when a significant biological contribution is derived from a signalling mAb. Furthermore, it has been shown that successful eradication of lymphoma in RIT consists of targeted irradiation and mAb signalling. Long-term clearance of tumour *in vivo* can be achieved by combining a therapeutically active signalling mAb that is itself poor at delivering radiation with a mAb that is a more effective vector for targeting radiation to tumour. Importantly, this tumour eradication is achieved with minimal and reversible haematological toxicity.

These results have confirmed that RIT is much more than targeted radiation and provide a scientific rationale to support the use of selecting combinations of mAbs in RIT rather than using a single mAb. These results also suggested that a radiation dose response might exist for RIT in B-cell lymphoma, when the targeted radiation is augmented by the presence of a signalling mAb. In this study both anti-Id and anti-CD19 mAb initiated cell surface signalling and this appeared to dramatically enhance the clearance of tumor when combined with targeted radiation delivered by  $^{131}\text{I}$ -anti-MHCII. It has been demonstrated for the first time *in vivo* that this combination approach is effective in RIT and we believe that these provocative data indicate that this type of approach could be readily translated to the clinic.

These results provide new insights into the mechanisms of action of RIT and should influence the design of further clinical studies integrating combinations of mAb to successfully treat lymphoma.

## **Chapter 5 The Microscopic Intratumoural Distribution of $^{131}\text{I}$ Labelled mAb is Critical to Successful RIT of B-cell Lymphoma**

### **5.1 Introduction**

RIT is theoretically a good approach for cancer treatment, because radiolabelled mAb that binds to the antigen on the cancer cells can specifically irradiate tumour cells with minimal irradiation damage to normal tissue (Illidge and Johnson 2000; Press 2003). Unlike external beam radiotherapy, the radiation delivered by radioisotopes is of relatively short path length. This path length is dependent upon the radioisotope and for the most commonly used radioisotopes ( $^{131}\text{I}$ ,  $^{90}\text{Y}$ ) used in clinical RIT this is between 50 – 200 tumour cell diameters. With a maximum beta energy of 0.6 MeV (average 0.2 MeV),  $^{131}\text{I}$  is only a medium range beta emitter, with a mean range of between 200  $\mu\text{m}$  and 1 mm. The maximum range of 1.5 mm in soft tissue can lead to dose inhomogeneity and lack of useful crossfire radiation in tumour deposits larger than around 2.5 – 5.0 mm (Langmuir, Mendonca et al. 1992).  $^{90}\text{Y}$  is a pure beta emitter with a mean beta energy of 0.93 MeV that gives a maximum penetration of approximately 11 mm in tissue and a mean range of about 3.5 mm.

Effective clearance of tumour by RIT is thought to be critically dependent upon delivering a sufficiently high tumour or surrounding tissue uptake which enable every tumour cell to be given a lethal dose of irradiation (Kassis and Adelstein 2005). However, based on current experimental data, it is believed that the tumour penetration of radiolabelled mAb is poor and the intratumoural distribution of intravenously administered mAb is extremely heterogeneous which lead to the very variable radiation deposition and insufficient radiation delivery to certain parts of the tumour (Del Vecchio, Reynolds et al. 1989; Thomas, Chappell et al. 1989; Sharkey, Blumenthal et al. 1990; Press and Rasey 2000; Jhanwar and Divgi 2005). The heterogeneous intratumoural distribution pattern of radiolabelled mAb is therefore regarded one of the major limitations of RIT. (Yang, Brown et al. 1992; Kinuya, Yokoyama et al. 1998;

Zhang, Yao et al. 1998; Steffens, Boerman et al. 1999; Behr, Blumenthal et al. 2000; Kinuya, Yokoyama et al. 2000; Smith-Jones, Vallabhajosula et al. 2003). Although these data are mainly derived from autoradiography studies on solid tumours, some common themes are believed to apply to lymphomas as well (Hui, Fisher et al. 1992; Brown, Kaminski et al. 1997). Contradictory to this widely accepted “heterogeneity hypothesis”, the conventional dosimetry estimation method, Medical Internal Radiation Dose (MIRD) formulation requires to assume the homogeneous distribution of radioisotope within a target organ or tumour (Fisher 1994). MIRD methodology is used as standard dosimetry method both in clinical practice and animal biodistribution studies. As a result, in clinical RIT practice, it is believed that some areas of the tumour of poorer perfusion receive less radiation dose than that which is calculated from the MIRD and this is believed to be an important factor for RIT failure (Fisher 1994).

A number of clinical trials have been performed in patients with haematological malignancies using a variety of antibodies, delivery schedules, radioisotopes and doses of radioactivity. To date the target antigens that have been used include CD20 (Kaminski, Zasadny et al. 1993; Press, Eary et al. 1993; Press 2003; Davis, Kaminski et al. 2004; Kaminski, Tuck et al. 2005), MHC II allele; HLA-DR10 (DeNardo, Lewis et al. 1994; DeNardo, DeNardo et al. 1998), immunoglobulin idiotype (Parker, Vassos et al. 1990; White, Halpern et al. 1996), CD22 (Goldenberg, Horowitz et al. 1991; Goldenberg and Sharkey 2005), CD37 (Kaminski, Fig et al. 1992; Press, Eary et al. 1993) and CD45 (Matthews, Appelbaum et al. 1999).

CD45 is the most broadly expressed of the known haematopoietic antigens. It is expressed on virtually all leukocytes, including myeloid and lymphoid precursors in bone marrow and mature lymphocytes in lymph nodes (Matthews, Appelbaum et al. 1999). Clinical studies have demonstrated that more than 90% of acute myeloid leukaemia samples and most acute lymphoblastic leukaemia samples express this antigen and, the antigen does not internalise after antibody binding (van der Jagt, Badger et al. 1992; Matthews, Appelbaum et al. 1999). These biological characteristics suggested that radiolabelled mAbs targeting on CD45 could deliver high dose of

radiation to the haematopoietic tissues and, CD45 was one of the first targets to emerge as a target for RIT in haematological malignancies. Both  $^{131}\text{I}$  and  $^{90}\text{Y}$  labelled anti-CD45 mAbs have been investigated to treat B-cell lymphoma (Matthews, Appelbaum et al. 1997; Matthews, Appelbaum et al. 1999), acute leukaemia and myelodysplasia syndrome (Matthews, Appelbaum et al. 1999; Ruffner and Matthews 2000; Nemecek and Matthews 2003; Nemecek, Hamlin et al. 2005).

In clinical RIT practice, the dosimetry assessment is based upon the MIRD formula which assumes the homogenous distribution of radiolabelled mAb within a target organ or tumour (Fisher 1994). There has been few detailed analysis of the microscopic tumour heterogeneity seen with RIT and none to our knowledge in syngeneic animal models of lymphoma. We therefore chose to investigate the marked differences seen in therapeutic outcome observed between two radioimmunoconjugates that on MIRD calculations delivered similar dose of radioactivity to tumour, namely  $^{131}\text{I}$  labelled anti-MHCII and  $^{131}\text{I}$  labelled anti-CD45. We hypothesised that the poorer performance of  $^{131}\text{I}$  labelled anti-CD45 mAb might be explained by the different patterns of intratumoural distribution of radiolabelled mAbs at cellular level.

The initial aims of this chapter were (a) to observe the biodistribution of radiolabelled anti-CD45 mAb in syngeneic B-cell lymphoma models and to investigate the effects of pre-dose on the biodistribution; (b) to further test the radiation dose effect in RIT in B-cell lymphoma by comparing the therapeutic effects of  $^{131}\text{I}$  labelled anti-CD45 mAb with that of other radiolabelled mAbs in particular  $^{131}\text{I}$ -anti-MHCII mAb; (c) to investigate the relationship between RIT therapeutic efficacy and microscopic tumour dosimetry using  $^{131}\text{I}$  labelled anti-CD45 mAb and  $^{131}\text{I}$ -anti-MHCII mAb in the BCL<sub>1</sub> tumour model.

## 5.2 Materials and Methods

Two rat anti-mouse CD45 mAbs (YW62.3.2, IgG 2b and YBM42.3.2, IgG 2a) were kindly provided by Dr. Stephen Cobbold from the University of Oxford. The in vitro cell binding activity of this two mAbs and their in vitro cytotoxicity (ADCC & CDC) activity were assessed in comparison with other mAbs using BCL<sub>1</sub> tumour cells as described in chapter 2. The mAbs were radioiodinated using Iodogen-Beads method and the labelling efficiency, post labelling immunoreactivity were determined as described in chapter 2.

BALB/c mice were supplied by Harlan UK Limited (Blackthorn, United Kingdom), and maintained in local animal facilities. The biodistribution characteristics and the in vivo radiation dosimetry of radiolabelled anti-CD45 mAbs were assessed in comparison with other mAbs in BCL<sub>1</sub> tumour inoculated BALB/c mice and in A31 tumour inoculated CBA/H mice respectively in the situations identical to that described in chapter 3.

RIT studies using <sup>131</sup>I labelled anti-CD45 mAb (IgG 2b, YW62.3.2) were performed in comparison with same doses of <sup>131</sup>I labelled other mAbs (anti-CD19, anti-MHCII, anti-Id, and isotype matched control mAb) in BCL<sub>1</sub> inoculated BALB/c mice (treatments were given ten days after the intravenous inoculation with 10<sup>5</sup> tumour cells) as described in chapter 4.

The splenic intratumoural distribution of radioiodinated mAbs was assessed by immunohistochemistry. Parallel groups of <sup>125</sup>I-labelled mAb treated and control animals were sacrificed and the obtained spleen biopsies were fixed overnight in -20°C cold acetone and embedded in glycol methacrylate (GMA) resin as described by Britten et al (Britten, Howarth et al. 1993). Extremely thin 2 µm sequential sections of biopsies embedded with GMA resin were then cut using glass knives on a dedicated resin microtome for staining. The localisation of the intravenously administered mAb was

revealed by staining the sections with biotinylated mouse anti-rat antibody as secondary antibody and subsequently applying the streptavidin biotin-peroxidase complexes and diaminobenzidine tetrahydrochloride (DAB) substrate as described by Britten et al (Britten, Howarth et al. 1993). Sequential sections of each biopsy sample were always cut and stained in comparison with control samples for which mAb used in the treatments were applied on slides in vitro prior to the adding of biotinylated mouse anti-rat antibody. All the slides were also counterstained with Mayer's haematoxylin. Images were acquired by a Nikon Coolpix 950 digital camera which was connected to a Nikon Eclipse E600 microscope (Nikon Corporation, Tokyo, Japan). The percentages of the positively stained areas by different mAb were observed and measured using the Zeiss KS400 imaging analysis package (Carl Zeiss Ltd, Welwyn Garden City, United Kingdom).

In order to observe the intratumoural distribution of these mAbs in advanced stage BCL<sub>1</sub> tumours, groups of tumour cell inoculated mice bearing advanced stage tumour (day 18 post inoculation by tail vein injection of 10<sup>5</sup> BCL<sub>1</sub> cells) were also sacrificed and biopsies were processed and stained as described above.

## 5.3 Results

### 5.3.1 Binding of Radioiodinated Anti-CD45 mAb to the Surface of BCL<sub>1</sub> Cells

In this study, two rat anti-mouse pan-leukocyte antigen CD45 mAbs, YBM42.2.2 (rat anti-mouse IgG 2a) and YW62.3.2 (rat anti-mouse IgG 2b) were analyzed in comparison with a panel of rat anti-mouse mAbs. Similar to the results reported in chapter 3 where the immunoreactivity and cell binding characteristics of radiolabelled rat anti-mouse mAb (anti-BCL<sub>1</sub> Id, anti-CD19, anti-CD22, anti-CD38, anti-MHCII) were assessed. The results showed that the two anti-CD45 mAbs bind to BCL<sub>1</sub> cells at

high density of around  $6 \times 10^5$  molecules per cell and also have good post-labelling immunoreactivity of around 55% as shown below in figure 5.1 and figure 5.2.

**Figure 5.1**

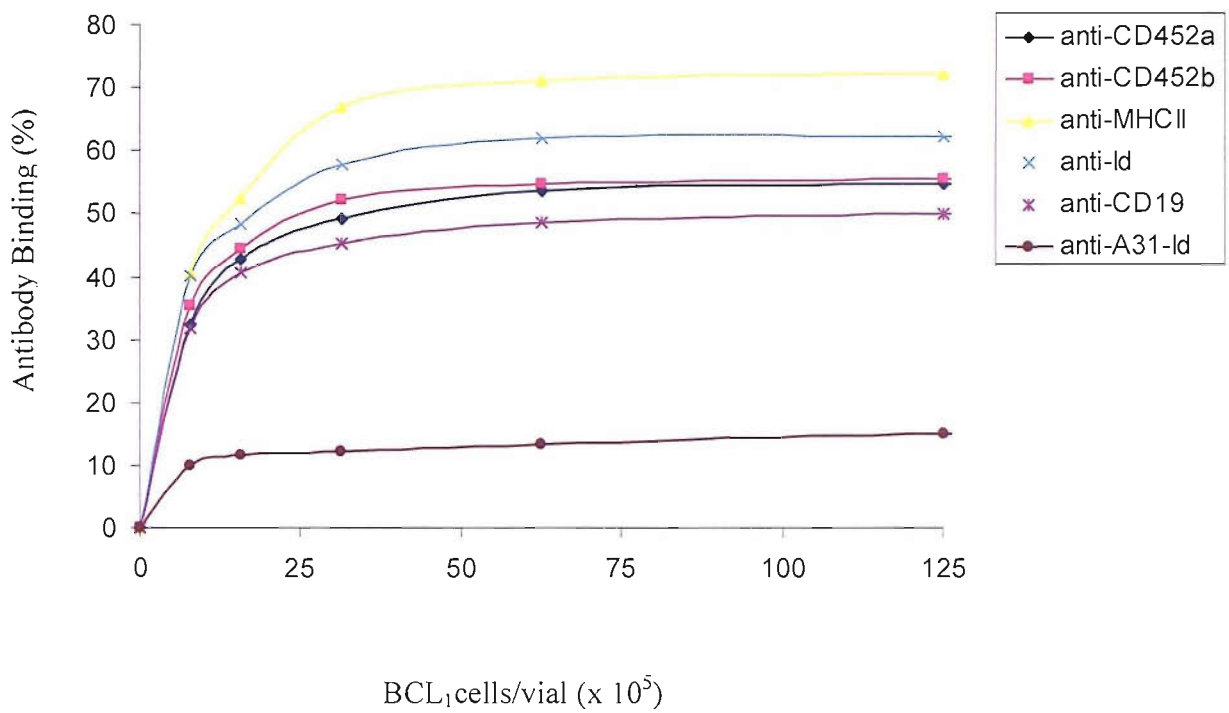


**Figure 5.1. Immunoreactivity assay of rat-anti-mouse mAb on BCL<sub>1</sub> cells.** This figure shows one of three identical experiments (see Appendix 3 for raw data) demonstrating the above 50% immunoreactivity of a panel of radioiodinated rat anti-mouse mAbs (including two anti-CD45 mAbs which show similar immunoreactivity of around 55%) which were used in this study.

**Figure 5.2**

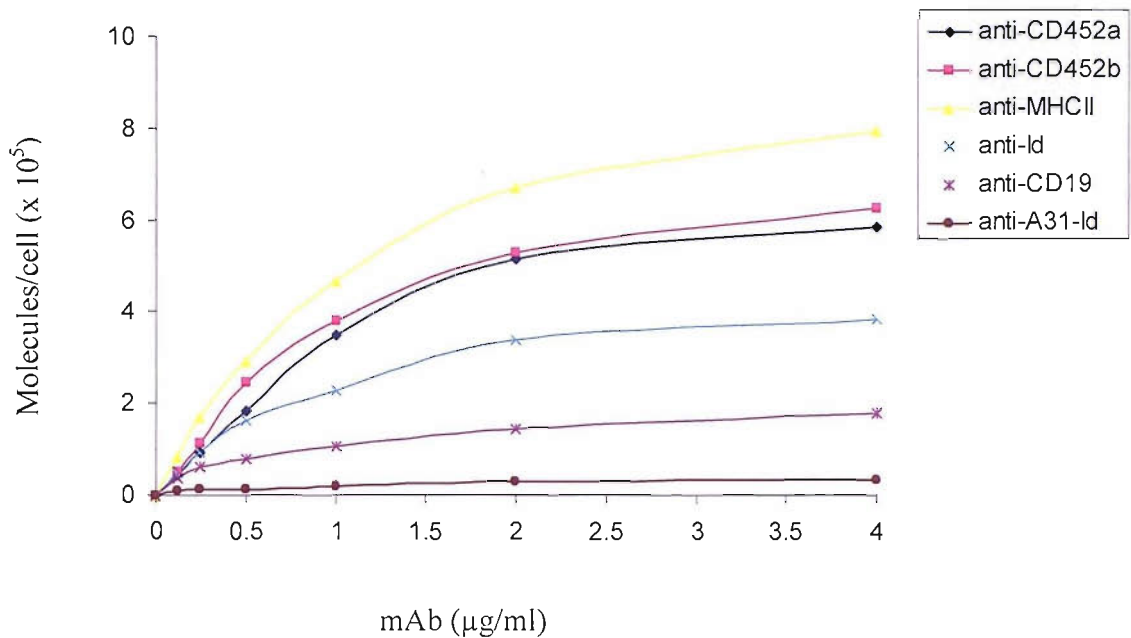


**Figure 5.2 Binding curve of rat-anti-mouse mAb on BCL<sub>1</sub> cells.** This figure shows one of three similar experiments performed (see Appendix 4 for raw data). The results are expressed as the number of molecules of mAb bound/cell. Among these mAbs, while the anti-MHCII (TI2-3) still has the highest mAb molecules/cell binding with peak value of nearly  $7.8 \times 10^5$  per cell, the two anti-CD45 mAb also demonstrated high molecules/cell binding with peak values close to  $6 \times 10^5$ . Notably, the anti-CD45 2b (YW62.3.2) shows slightly higher molecules/cell than the other anti-CD45 mAb (YBM42.2.2).

### **5.3.2 Complement and Antibody Dependent Cellular Cytotoxicity of BCL<sub>1</sub> Cells**

The in vitro cellular cytotoxicity of these rat anti-mouse mAbs was then compared using the CDC and ADCC assays. The results are shown in figure 5.3 and figure 5.4. In these assays, a hamster anti-mouse MHCII mAb (N22) was added as a positive control. This mAb has previously been shown to produce high level of CDC. Figure 5.3 shows that both of the two anti-MHCII mAb produced highest cell lysis of more than 55% in CDC assay. Likewise, anti-Id mAb also produced very marked cell lysis of slightly above 50%. Neither of the two anti-CD45 mAbs showed high cell lysis in CDC. The anti-CD45 2b (YW62.3.2) showed moderate cell killing of around 20% lysis while another (YBM42.2.2) performed similarly to anti-CD19, anti-CD22 mAb and anti-CD38 mAb achieved only around 10% BCL<sub>1</sub> cell lysis.

**Figure 5.3**

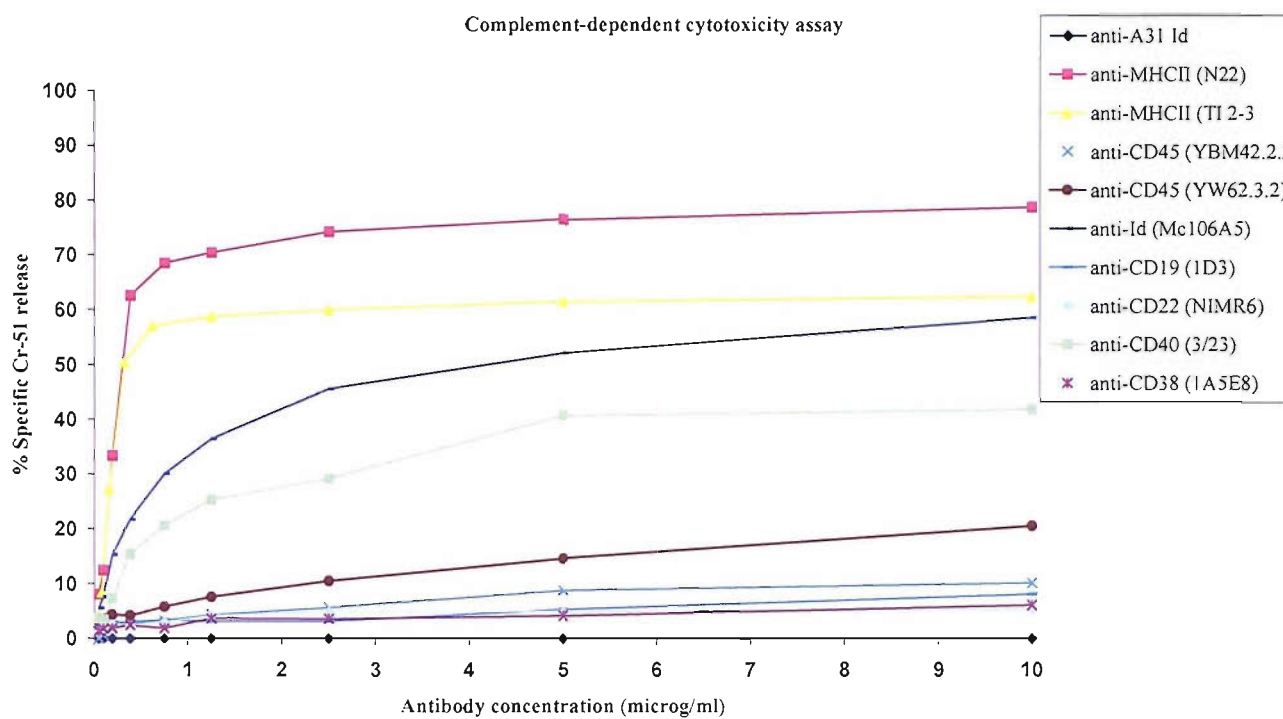


**Figure 5.3. Complement dependent cytotoxicity of BCL<sub>1</sub> cells.** <sup>51</sup>Cr labelled BCL<sub>1</sub> cells were mixed with mAb and fresh rat serum (final dilution, 1:3 with supplemented DMEM) and then warmed to 37°C. After 45 minutes the samples were centrifuged to sediment cells, and the specific <sup>51</sup>Cr release was assessed by counting supernatant. These results represent one of three similar experiments (see Appendix 5 for raw data). All samples were run in triplicate. The maximum release was calculated from the release of <sup>51</sup>Cr given when 1% Nonidet P-40 was added. Mc39-16 (Anti-A31 Id) mAb was used as a isotype-matched control which was nonlytic in these assays as the figure indicates.

The mAbs were also assessed in ADCC assay using human monocytes as effector cells. Figure 5.4 demonstrated that at the two mAb concentrations, the anti-MHCII antibodies (N22 and TI 2-3) were the most competent at cellular cytotoxicity, achieved about 20% cell lysis at lower mAb concentration (5  $\mu$ g/ml) and 25-30% cell lysis at higher concentration (10  $\mu$ g/ml). One of the two anti-CD45 mAb, YW62.3.2 also produced significant cell killing (15% cell lysis at the concentration of 5  $\mu$ g/ml and 20% cell lysis at the concentration of 10  $\mu$ g/ml). All of the other mAb demonstrated only moderate BCL<sub>1</sub> cytotoxicity activity of around 5-10% cell lysis.

**Figure 5.4**

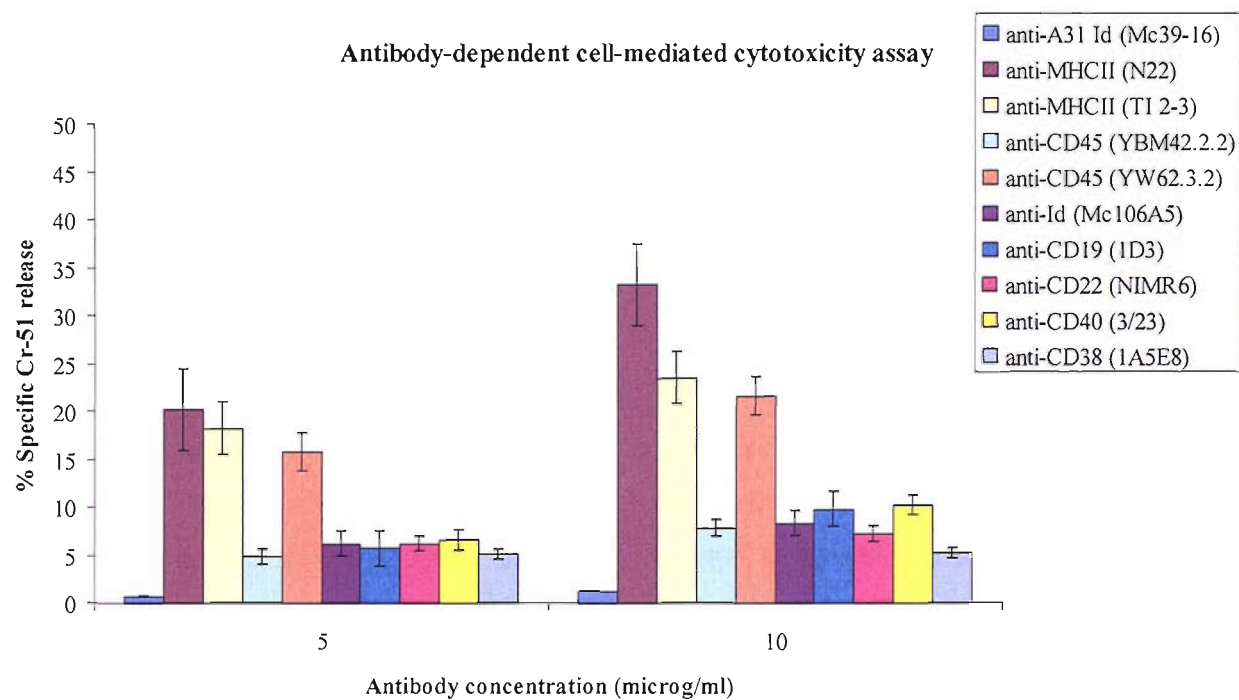


**Figure 5.4. Antibody dependent cell-mediated cytotoxicity of BCL<sub>1</sub> cells.** <sup>51</sup>Cr labelled BCL<sub>1</sub> cells were mixed with a panel of rat anti-mouse mAb at two concentrations (5 µg/ml and 10 µg/ml, respectively), and then human monocytes were added as effector cells at an Effector:Target cell ratio of 50:1. The cell mixture was incubated for 6 hours at 37°C, and then supernatants were harvested to estimate the <sup>51</sup>Cr release. The maximum release of radioactivity was calculated using target cells to which 100 µl of 1% Nonidet P-40 had been added. This figure shows the results of one of three similar experiments. Bar charts show the values of triplicates (mean +/- SD). Mc39-16 (anti-A31 Id) mAb was used as a control mAb.

### **5.3.3 Anti-CD45 mAb Demonstrated High Radiation Delivery Capability in Conventional Biodistribution Assays**

The cell binding experiments in the previous section have demonstrated that, the pan-leukocyte antigen CD45 has high levels of surface expression on BCL<sub>1</sub> cells with anti-CD45 mAb binding of around  $6 \times 10^5$  molecules per cell. This level is comparable to the anti-MHCII mAb binding ( $7.8 \times 10^5$  molecules per cell). Among the two anti-CD45 mAb, YW62.3.2 showed higher immunoreactivity, BCL<sub>1</sub> cell binding and ADCC activity. Therefore this mAb was chosen for subsequent biodistribution and RIT studies. As previously described in chapter 3, anti-MHCII mAb delivered more radiation to the splenic tumour than did anti-CD19 or anti-Id. As expected, similar biodistribution experiments confirmed that the anti-CD45 mAb (YW62.3.2) also delivered higher doses of radiation to splenic tumour. Figure 5.5 (A-D) showed the biodistribution of <sup>125</sup>I labelled anti-CD45 (figure 5.5C) in comparison with a panel of B-cell specific mAb (anti-CD19 and anti-MHCII) and an isotype matched control mAb given 10 days after tumour inoculation (BCL<sub>1</sub>,  $1 \times 10^5$ , iv.). At specific time points (as shown in Figure 5.5), over the next 4 days, the animals were sacrificed and the major organs removed to determine the percentage of injected radioactive dose (ID)/gram of organ tissue (g). Similar to anti-MHCII mAb, the superior ability of a single trace labeled (0.74 MBq <sup>125</sup>I) dose of 500 µg anti-CD45 to selectively target the splenic tumour is clearly shown while the anti-CD19 was again shown to be considerably poorer at delivering radiation to the spleen and in fact provided similar targeting of radiation (%ID/g) to that seen with an irrelevant isotype matched (control) mAb. Anti-CD45 mAb showed identical biodistribution pattern in both BCL<sub>1</sub> and A31 tumour models (data not shown).

**Figure 5.5**

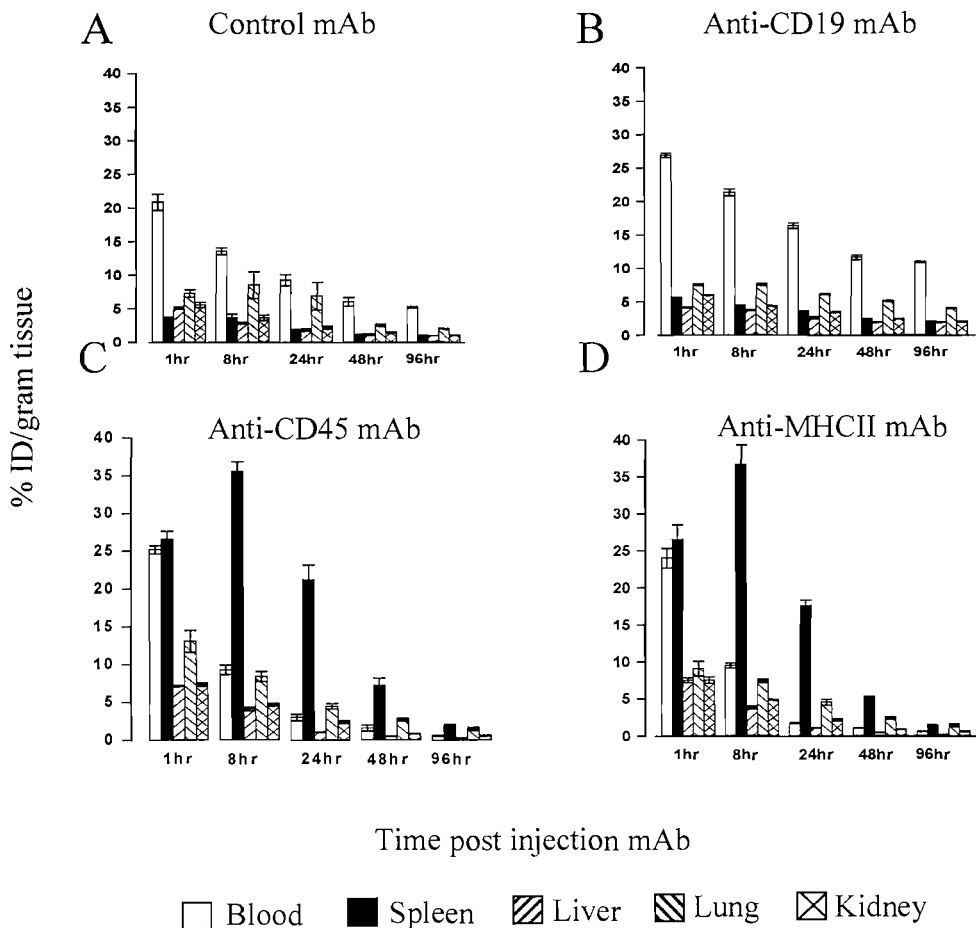


**Figure 5.5. Biodistribution of radiolabelled mAb in BCL<sub>1</sub> tumour models.** Groups of mice (18 for each group) were inoculated with 10<sup>5</sup> BCL<sub>1</sub> cells intravenously and then treated with <sup>125</sup>I labelled mAb (500 µg per mouse) 10 days later. At the time intervals indicated, animals were killed and samples of various organs were removed for weighing and estimation of radioactivity content. Results are expressed as the percentage of the injected dose of <sup>125</sup>I-mAb per gram of tissue (% ID/g). This experiment demonstrated that the anti-CD45 mAb has similar high radiation delivery capability to anti-MHCII mAb as shown in figure 5.5C and figure 5.5D. Each bar shows the mean and range of 3 animals investigated and the results shown were representative of 2 identical experiments.

Using the Medical Internal Radiation Dosimetry (MIRD) formulation, assuming total absorption of the non-penetrating radiation component of  $^{131}\text{I}$  with homogeneous distributions within each individual organ or whole body, the approximate radiation doses delivered by these mAb were calculated for whole body, lung, liver, kidney and the tumour bearing organ – spleen in early stage (10 days after intravenous inoculation of  $10^5$  BCL<sub>1</sub> cells) BCL<sub>1</sub> tumour models and the doses are presented below in Table 3.1.

The results confirmed the ability of anti-CD45 mAb to deliver high doses of radiation per MBq of radiolabelled mAb infused to the spleen and less non-specific irradiation to the whole body in a similar manner to anti-MHCII mAb. For an infusion of 18.5 MBq  $^{131}\text{I}$ -anti-CD45 mAb, the dose delivered to the spleen was estimated to be around 18.5 Gy in early stage tumour models, which was slightly higher than that delivered by anti-MHCII (18 Gy) and up to 3 – 6 times greater than that delivered by anti-CD19 (5.14 Gy) and the irrelevant (4.5 Gy) mAb (Figure 5.5 A, B, C, D).

Differing from the phenomena observed in clinical RIT studies using radiolabelled anti-CD45 mAb, in both BCL<sub>1</sub> and A31 models, anti-CD45 mAbs did not show high liver uptake. As shown in figure 5.5, the liver uptake (%ID/g) of radiolabelled anti-CD45 was actually lower than those of lung or kidney uptake.

**Table 5.1**

Organs	Radiation Dosimetry			
weight (g)	Anti-MHC II	Anti-CD45	Anti-CD19	Control
Whole body (22.45+/-0.34)	2.90+/-0.11	3.42+/-0.25	7.25+/-0.09	5.80+/-0.17
Spleen (0.15+/-0.02)	18.00+/-1.02	18.50+/-0.75	5.14+/-0.13	4.50+/-0.20
Liver (1.02+/-0.21)	1.82+/-0.17	2.74+/-0.33	6.05+/-0.44	3.04+/-0.07
Lung (0.15+/-0.03)	4.54+/-0.22	4.65+/-0.25	10.15+/-0.24	7.63+/-0.36
Kidney (0.45+/-0.03)	3.80+/-0.14	3.75+/-0.12	7.60+/-0.42	3.04+/-0.15

**Table 5.1 Internal radiation dosimetry of RIT treated mice with early stage tumour.** Based on the biodistribution data, the absorbed radiation doses of whole body and individual organs of RIT treated BALB/c mice were estimated according to the MRID formula. This table compared the dosimetry results of early stage tumour (10 days after the inoculation of  $1 \times 10^5$  BCL<sub>1</sub> tumours given by intravenous injection) when treated with 18.5 MBq <sup>131</sup>I labelled corresponding mAb. The absorbed radiation dose was measured as Gy (mean +/- range).

### 5.3.4 Anti-CD45 RIT Fails to Produce Long Term Survival

Having demonstrated that the anti-CD45 mAb delivered similar levels of radioactivity to the tumour bearing organ as anti-MHCII, the therapeutic efficacy of this radioimmunoconjugate was then investigated. Under conditions similar to that seen during the biodistribution studies, mice received  $10^5$  BCL<sub>1</sub> cells intravenously and were treated 10 days later with unlabeled or 9.25 MBq or 18.5 MBq  $^{131}\text{I}$  labeled anti-CD45 and anti-MHCII mAb in comparison. As reported in chapter 4, parallel groups of animals receiving additional unlabelled anti-Id (500  $\mu\text{g}$  / animal) were also included.

Figure 5.6 shows the results of one of three identical RIT studies. The anti-CD45 mAb like the anti-MHCII mAb had no therapeutic effect unlabelled. As previously reported in chapter 4, large doses (18.5 MBq) of  $^{131}\text{I}$ -labeled anti-MHCII plus unlabelled anti-Id produced 100% animal protection. In contrast, none of the animals treated with 18.5 MBq  $^{131}\text{I}$  labeled anti-CD45 and unlabelled anti-Id became long term survivors. Instead the animals treated in this group died of terminal tumour at around 55 to 65 days after inoculation which were similar to the level of tumour protection seen with 9.25 MBq  $^{131}\text{I}$  labelled anti-MHCII (data not shown). These therapeutic results could not be easily explained with conventional biodistribution studies which had demonstrated the ability of anti-CD45 to target similar doses of radiation to the spleen. We therefore hypothesised that these significant therapeutic results may be due to important difference in the tumour microdosimetry.

**Figure 5.6.**

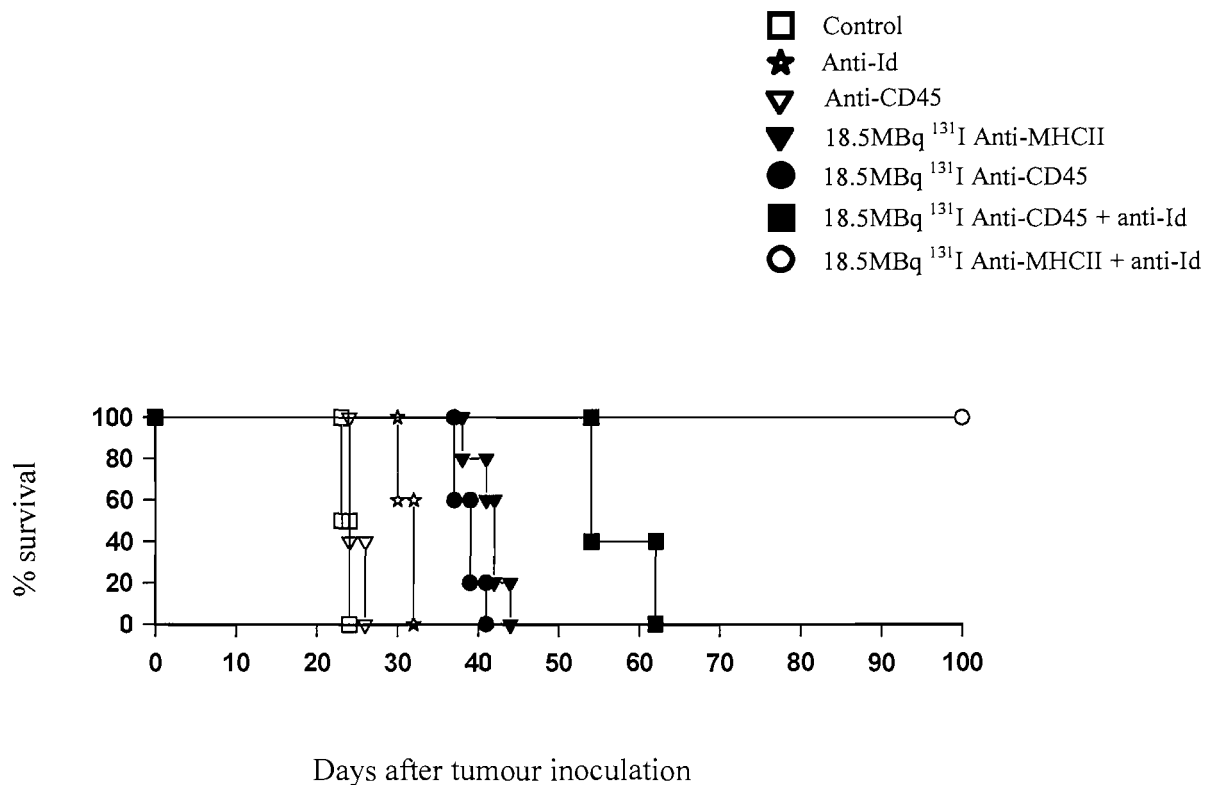


**Figure 5.6. RIT comparing the therapeutic effect of  $^{131}\text{I}$  labelled anti-CD45 and anti-MHCII mAb in BCL<sub>1</sub> lymphoma model.** In this experiment, groups of age and sex-matched BALB/c mice were inoculated by intravenous injection of  $10^5$  BCL<sub>1</sub> tumour cells and were treated 10 days later by intravenous injection of unlabelled anti-CD45 mAb, unlabelled anti-Id, 18.5 MBq  $^{131}\text{I}$  labelled anti-MHCII mAb and 18.5 MBq  $^{131}\text{I}$  labelled anti-CD45 mAb respectively (with and without the addition of unlabelled anti-Id). This experiment is representative of 3 identical experiments. The experiment demonstrated that similar to anti-MHCII, unlabelled anti-CD45 mAb had no therapeutic effect. Although 18.5 MBq  $^{131}\text{I}$  labelled anti-CD45 mAb provided approximately 15 days of protection which was similar to that provided by same amount of  $^{131}\text{I}$  labelled anti-MHCII mAb, the combination therapy (18.5 MBq  $^{131}\text{I}$  labelled anti-CD45 mAb plus unlabelled anti-Id) failed to achieve long term protection. The same figure shows that 100% of the animals treated with the combination of 18.5 MBq  $^{131}\text{I}$  labelled anti-MHCII mAb plus unlabelled anti-Id became long term survivors.

### 5.3.5 Intratumoural Localisation of mAb in RIT of BCL<sub>1</sub> Lymphoma

In order to study the intratumoural distribution of intravenously infused mAb, immunohistochemistry (IHC) studies were performed with BALB/c mice inoculated with BCL<sub>1</sub> tumour cells under identical conditions as those studied in biodistribution and RIT experiments. Figure 5.7 showed the difference of intratumoural distribution pattern of a panel of mAb on sequential GMA resin sections of BCL<sub>1</sub> inoculated BALB/c mouse spleen (day 10 after intravenous inoculation with 10<sup>5</sup> BCL<sub>1</sub> cells).

As demonstrated in biodistribution studies, the specific binding of intravenously injected mAb to target cells happened as early as 1 hour post injection and the peak accumulation was seen at 8 hours post injection. In this figure, the mouse spleen biopsy was taken 2 hours after the intravenous injection of 500 µg Mc106A5 (anti-BCL<sub>1</sub>-Id), fixed, processed and stained with mouse anti-rat mAb as the second antibody to locate the distribution of intravenously infused anti-Id. Figure 5.7A shows that a cluster of cells in the lower left edge of the view (arrowed in the picture) as well as some disseminated cells near the right edge of the view were stained positively indicating the selective binding of the intravenously administered anti-Id. Using the Zeiss KS400 imaging analysis package, about 3% of the cells were found to be stained positive. Figure 5.7B shows that the addition of a control mAb (Mc39-16, anti-A31-Id) prior to the application of mouse anti-rat antibody did not affect the staining. In figure 5.7C, to confirm that all BCL<sub>1</sub> cells had in fact been stained by the intravenously administered anti-Id mAb, additional anti-BCL<sub>1</sub>-Id was applied to the section prior to the mouse anti-rat antibody. This figure shows that apart from the cells positively stained in figure 5.7A, the additionally applied anti-Id failed to stain any additional tumour cells confirming that all the BCL<sub>1</sub> tumour cells were accurately targeted by the infused anti-Id mAb. In figure 5.7D, prior to the addition mouse anti-rat mAb as the second antibody, rat anti-mouse MHCII mAb (TI2-3) was applied to the section and the figure showed that as a mainly B-cell specific mAb, the anti-MHCII stained a large portion of the section mainly seen on the right side of the view in the same location as the BCL<sub>1</sub>

tumour cells. Approximately 35% of the cells were found to be stained positive. This suggested that the anti-MHCII mAb delivered the radiation in a more focused manner to the B-cell clusters where the tumour cells were localised. Figure 5.7E shows that the anti-CD3 mAb detected the T-cell areas that were not detected by the anti-MHCII mAb. Approximately 50% of the cells were found to stain positive by anti-CD3 mAb on this slide. Figure 5.7F shows that the anti-CD45 mAb stained the section homogeneously. Similar to those done with anti-Id as shown in figures 5.7A, B and C, for other mAbs, the staining patterns of intravenously infused and in vitro applied were also compared and the results showed no difference (data not shown).

In summary, these immunohistochemistry studies clearly demonstrate that the intratumoural localisation of these mAb used in biodistribution and RIT experiments were substantially different and that this difference could lead to a large variation in radiation microdosimetry. In contrast, using conventional biodistribution methodologies and assuming the homogeneous intratumoural distribution, this large radiation dosimetry variation was missed. We therefore hypothesise that it was the failure to detect these important differences in tumour dosimetry which failed to predict the poorer therapeutic efficacy of  $^{131}\text{I}$  labelled anti-CD45.

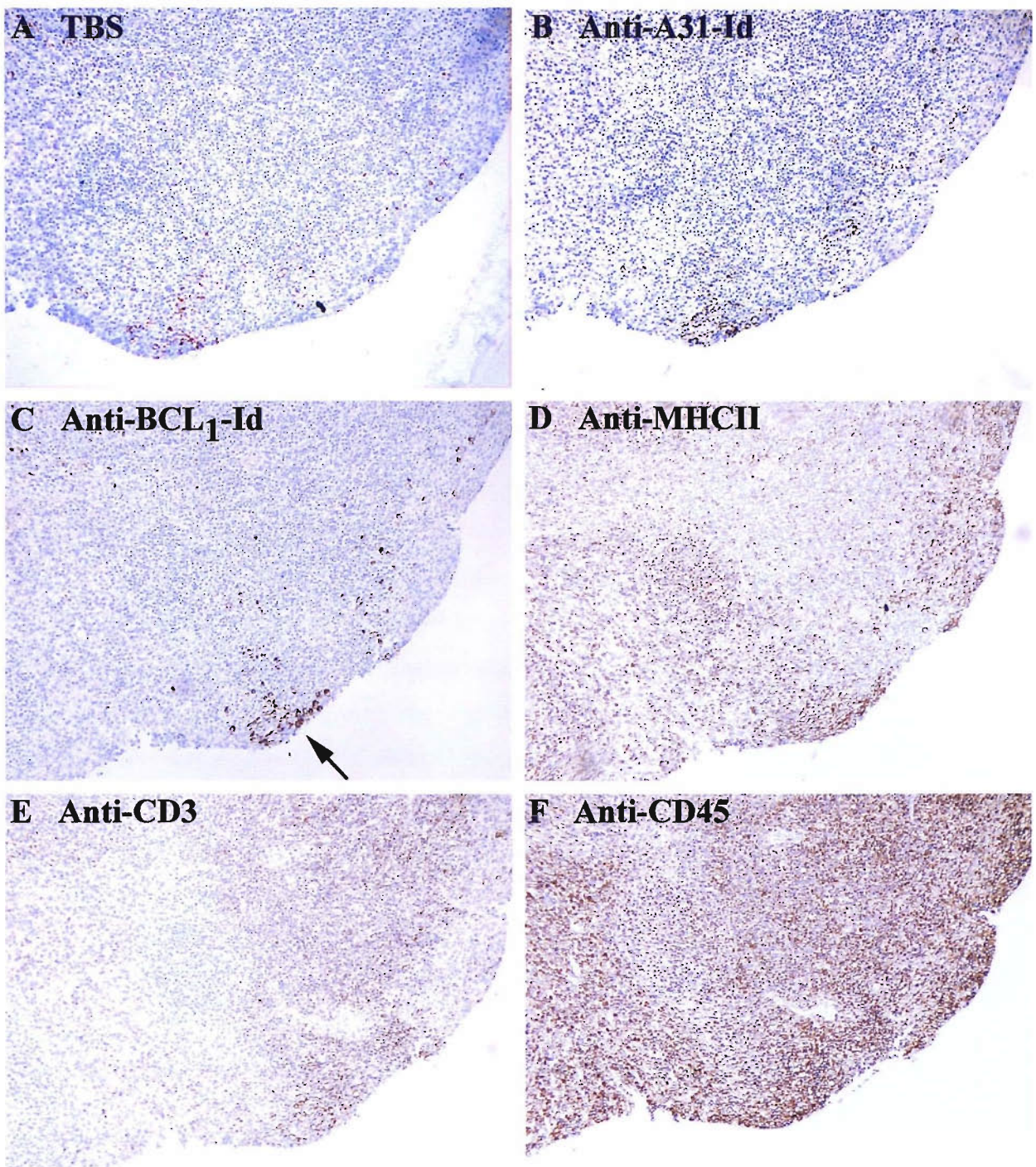


**Figure 5.7. Immunohistochemistry study revealed the micro-distribution of intravenously administered mAb in BCL<sub>1</sub> lymphoma.** Simultaneous to the biodistribution assays, parallel groups of age and sex-matched groups of mice were also inoculated with 10<sup>5</sup> BCL<sub>1</sub> cells intravenously and treated with <sup>125</sup>I labelled mAb (0.5mg/mouse) 10 days later. Animals were then sacrificed 4 hours after the intravenous injection of mAbs. Spleen biopsy samples were fixed and processed. Sequential slides were cut and stained with a panel of rat anti-mouse mAb as the first antibody and biotinylated mouse anti-rat antibody as secondary antibody. After exposing to DAB substrate, the slides were also counterstained with Mayer's haematoxylin. The different intratumoural distribution patterns of a panel of mAbs were shown in this figure with the tumour cell cluster stained positive as indicated by the black arrow in figure 5.7C. (Magnification: x 100)

The immunohistochemistry experiments performed in early stage BCL<sub>1</sub> tumours were then repeated with advanced stage tumour (day 18 post inoculation with tail vein injection of 10<sup>5</sup> BCL<sub>1</sub> cells). Figure 5.8A shows that anti-BCL<sub>1</sub>-Id positively stained a big cluster of cells with distinctive larger cell size mainly occupying the lower half of the view. The BCL<sub>1</sub> tumour cells comprised approximately 45% of the total splenocytes. Figures 5.8B shows the staining of anti-MHCII. The B-cell marginal zones were stained positively as well as the tumour cell clusters in the left half of the view on this section, whilst the germinal centre where the T-cells are predominantly located stained much less well with only a small number of positively stained cells scattering within negative cells. The anti-MHCII stained cells comprised approximately 65% of the total splenocytes indicating that with advanced BCL<sub>1</sub> tumour, the percentage of anti-MHCII positive cells increased substantially. Figure 5.8C shows staining with anti-CD3 mAb and revealed T-cells around the central arteriole, however the relative percentage of T-cells decreased to approximately 15% of total splenocytes. In figure 5.8D the anti-CD45 shows widespread B and T lymphocyte staining. This figure demonstrates that the micro-distribution patterns of these mAb are still markedly different in advanced stage tumours following intravenous infusion. Whereas the anti-Id mAb bound only to BCL<sub>1</sub> tumour cells, the anti-MHCII mAb distributed in accordance with the location of B lineage cells and the anti-CD45 mAb dispersed homogeneously within B and T-cells regions of the spleen.

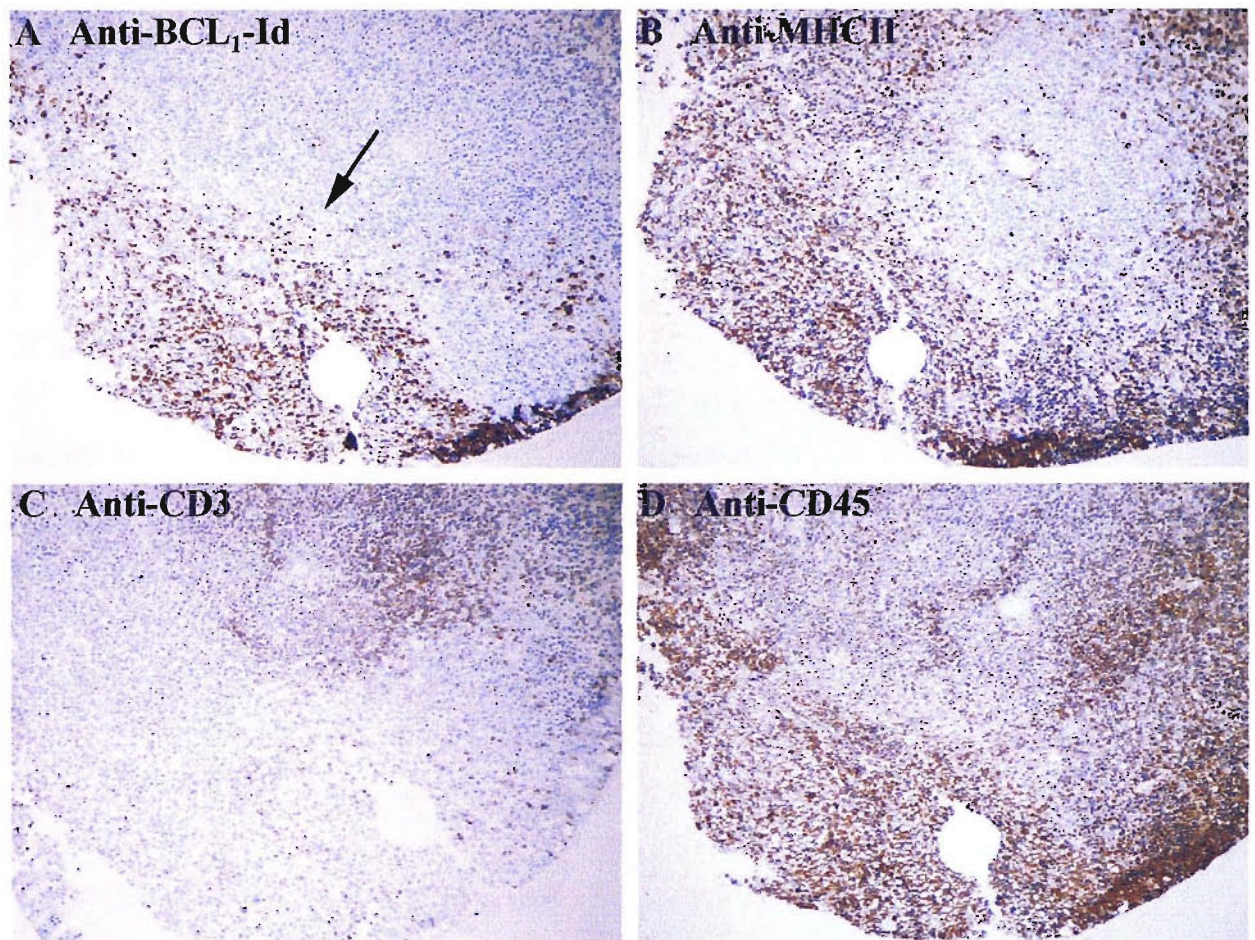


**Figure 5.8. Immunohistochemistry staining of advanced stage BCL<sub>1</sub> lymphoma.** Further to the immunohistochemistry studies on early stage BCL<sub>1</sub> tumours, the intratumoural distribution patterns of these mAbs were also investigated in BALB/c mice bearing advanced stage tumours. In this study, simultaneous to the corresponding biodistribution studies, parallel groups of mice were also inoculated with 10<sup>5</sup> BCL<sub>1</sub> cells by intravenous injection and treated with <sup>125</sup>I labelled mAb (0.5mg/mouse) 18 days later. Animals were sacrificed 2 hours post intravenous injection of mAbs. Spleen biopsy samples were fixed, processed, cut and stained as described previously. The different intratumoural distribution patterns of a panel of mAbs (anti-BCL<sub>1</sub>-Id, anti-MHCII, anti-CD3 and anti-CD45) on sequential sections were shown in this figure. A tumour nodule is seen in the lower part of the view which was stained positive by anti-BCL<sub>1</sub>-Id as indicated by the black arrow in figure 5.8A. (Magnification: x 100)

### **5.3.6 Long Term Survival is Achievable with Increased Doses of $^{131}\text{I}$ Labelled anti-CD45 mAb in RIT**

The immunohistochemistry studies revealed that the intravenously administered anti-MHCII mAb were concentrated within the B-cell zones around the BCL<sub>1</sub> tumour cells. This more targeted pattern of intratumoural distribution in early stage tumour model is likely to lead to a substantial increase in the absorbed tumour radiation dose. According to the measurement of the percentage of positively stained areas (35% on sections of early stage tumour), it is estimated that the actual tumour radiation dose delivered by anti-MHCII mAb could be as much as double the dose calculated from conventional biodistribution data in which the intratumoural distribution of infused mAb was assumed homogeneous and the radiation delivered to the tumour cells was substantially underestimated. However, CD45 is expressed on both T and B lymphocytes and as a result, the intratumoural distribution of intravenously administered anti-CD45 mAb was distributed homogeneously throughout the spleen as shown in figure 5.7. Therefore, the conventional biodistribution assay derived radiation dosimetry of  $^{131}\text{I}$  labelled anti-CD45 is likely to be a more accurate reflection of tumour dosimetry.

To confirm the importance of tumour micradosimetry and the reduced tumour radiation dose delivered by anti-CD45 relative to anti-MHCII, it was important to determine whether long term animal protection could be achieved with higher doses of  $^{131}\text{I}$  labelled anti-CD45 mAb in RIT. Figure 5.9 showed the results of a typical RIT study where some of the animals were given extremely high dose  $^{131}\text{I}$  (up to 37.0 MBq per mouse) labelled anti-CD45 mAb. Although 40% of the mice were lost due to radiation toxicity, in the group of mice treated with 37.0 MBq  $^{131}\text{I}$  labelled anti-CD45 plus unlabelled anti-Id, 60% of the mice became long term survivors. Notably, this kind of long term protection had never been achieved with lesser doses of  $^{131}\text{I}$  labelled anti-CD45 as shown previously in figure 5.6.

**Figure 5.9**

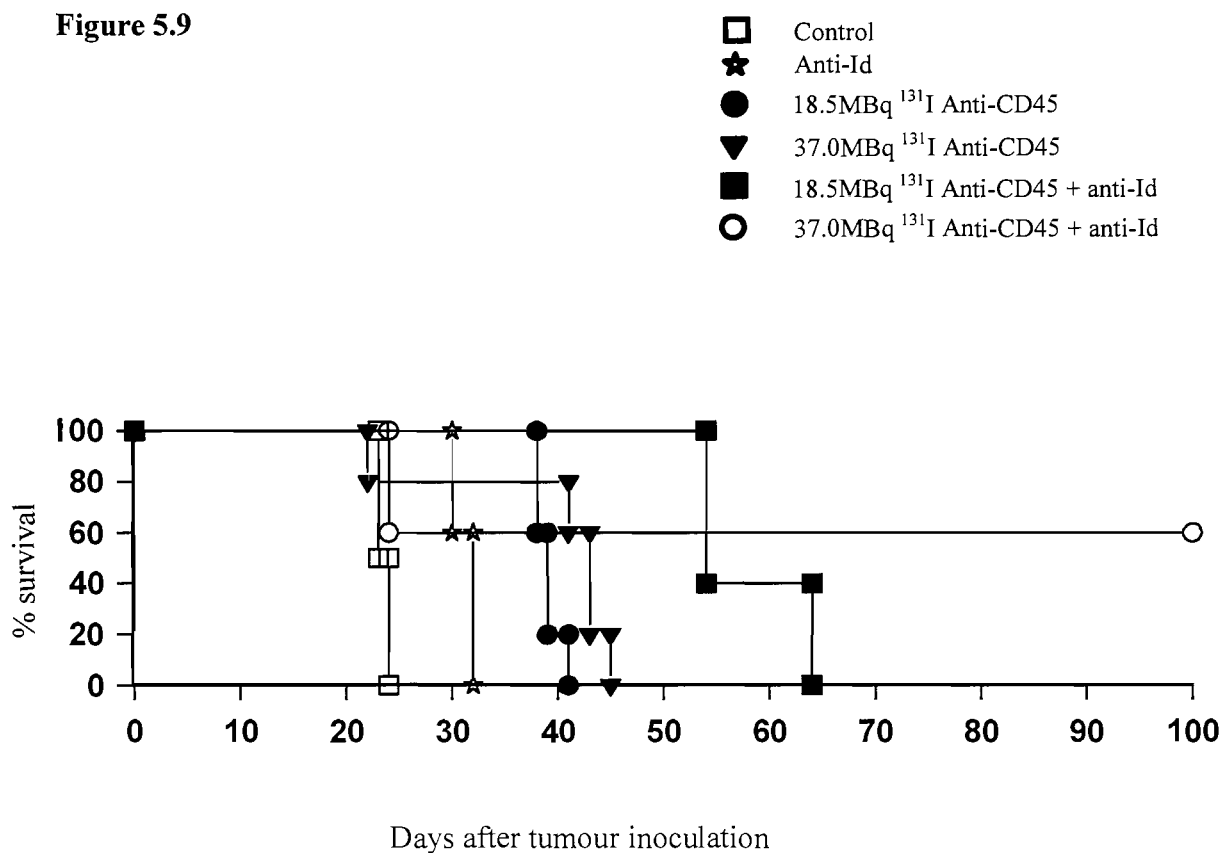


**Figure 5.9. Long term survival is achievable with double dose (37.0MBq)  $^{131}\text{I}$  labelled anti-CD45 mAb in RIT in BCL<sub>1</sub> lymphoma.** In this experiment, the RIT therapeutic effects of double dose (37.0 MBq)  $^{131}\text{I}$  labelled anti-CD45 mAb were compared to a standard dose (18.5 MBq)  $^{131}\text{I}$  labelled anti-CD45 mAb. Age and sex-matched BALB/c mice were inoculated with BCL<sub>1</sub> cells ( $10^5$  intravenously) on day 0, and RIT treatments were administered by intravenous injection 10 days later (500  $\mu\text{g}$  per mouse). While the combination of standard dose (18.5 MBq)  $^{131}\text{I}$  labelled anti-CD45 mAb and unlabelled anti-Id still failed to provide long term protection, 60% of animals treated with double dose (37.0 MBq)  $^{131}\text{I}$  labelled anti-CD45 mAb plus unlabelled anti-Id became long term survivors ( $P<0.01$ ). This figure also shows that 30% of animals treated with this double dose RIT died of radiation toxicity.

This experiment was then repeated and expanded with a reduced dose of  $^{131}\text{I}$  labelled anti-CD45 to try to avoid deaths due to radiation toxicity. From the previous experiment it was clear that 37.0 MBq was close to the maximal tolerated dose (MTD). Figure 5.10 shows the results of an RIT study where the anti-CD45 mAb was labelled with 30.0 MBq  $^{131}\text{I}$ . In this experiment, although the animals treated with 30.0 MBq  $^{131}\text{I}$  anti-CD45 mAb showed some acute irradiation related toxicity signs, such as fur loss and body weight loss, none of the animal died of toxicity and importantly 60% of the animals with 28.0 MBq  $^{131}\text{I}$  anti-CD45 plus unlabelled anti-Id became long term survivors. But in this experiment 40% of the animals died of developing tumour. In a separate study with the dose of  $^{131}\text{I}$  labelled anti-CD45 slightly increased to 34.0 MBq, 80% (4 out of 5 mice) of the animals achieved long term survival however one of the mice (20%) was lost secondary to irradiation toxicity (data not shown).

Within all these studies, in comparison, parallel groups of mice were also treated simultaneously with  $^{131}\text{I}$  labelled anti-MHCII mAb with the addition of unlabelled anti-Id and notably as reported previously, most (80-100%) of the animals under this treatment constantly achieved long term survival without significant irradiation toxicity related signs.

The results of these experiments further demonstrated that by increasing the radiation dose delivered to the tumour cells, long term protection is achievable, however severe radiation related toxicity was encountered.

**Figure 5.10**

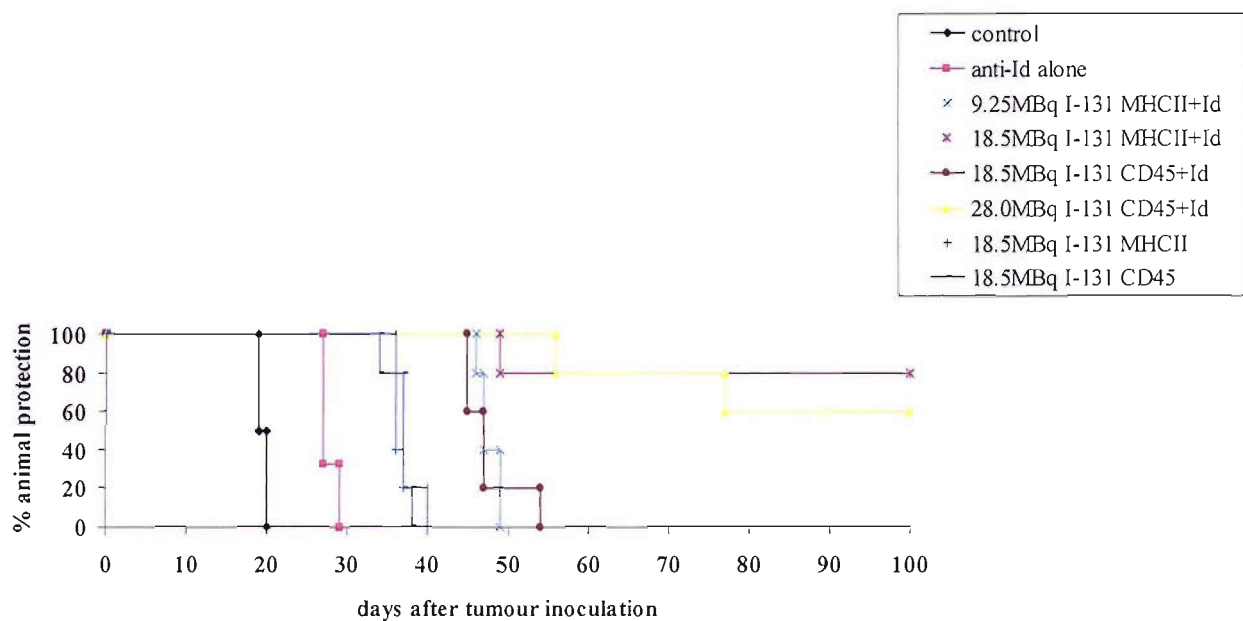


**Figure 5.10. Radiation dosimetry plays critical role in the success of RIT in BCL<sub>1</sub> lymphoma.** In this experiment, the RIT therapeutic effects of a reduced high dose (30.0 MBq) <sup>131</sup>I labelled anti-CD45 mAb were studied in comparison with standard dose (18.5 MBq) and half dose (9.25 MBq) <sup>131</sup>I labelled anti-CD45 mAb. Same to previous RIT experiments, groups of age and sex-matched BALB/c mice were inoculated with BCL<sub>1</sub> cells ( $10^5$  per animal, intravenously) on day 0, and RIT treatments were administered by intravenous injection 10 days later (500  $\mu$ g per mouse). Whilst the combination of standard dose (18.5 MBq) <sup>131</sup>I labelled anti-MHCII mAb with anti-Id provided long term protection to 80% mice, the high dose (30.0 MBq) <sup>131</sup>I labelled anti-CD45 mAb plus anti-Id also provided long term protection to 60% mice. Treated with this reduced high dose <sup>131</sup>I labelled anti-CD45 mAb, no animal was lost due to acute radiation toxicity. In the same study, none of the animals treated with lesser doses of <sup>131</sup>I labelled anti-CD45 mAb became long term survivor ( $P<0.01$ ).

## 5.4 Discussion

In this chapter, using both conventional biodistribution assessments and immunohistochemistry techniques, the therapeutic effects of  $^{131}\text{I}$  labelled mAbs were compared with the microscopic tumour dosimetry for the first time at cellular level in the same syngeneic B-cell lymphoma model. The important role of radiation microdosimetry in the successful clearance of lymphoma in RIT has been further clarified.

By comparing the dosimetry and RIT studies, as previously described in chapter 4 a radiation dose response was shown to exist for RIT of B-cell lymphoma in the presence of a signalling mAb. In this chapter, anti-CD45 mAb was found to deliver very similar doses of radiation as anti-MHCII mAb to the spleen. When 500  $\mu\text{g}$  of anti-CD45 was labelled with 18.5 MBq  $^{131}\text{I}$ , it delivered 18.5 Gy to the spleen whilst same amount of  $^{131}\text{I}$  labelled anti-MHCII delivered 18.0 Gy. It was therefore predicted that these two radioimmunoconjugates would deliver comparable therapeutic effects. However, comparison RIT studies persistently showed that the therapeutic effects of same amount of  $^{131}\text{I}$  radiolabelled anti-CD45 mAb to be inferior to that achieved by anti-MHCII.

The lack of correlation between the dosimetry data derived from conventional biodistribution assays and the therapeutic outcomes led to exploration of the potential microscopic dosimetry using immunohistochemistry studies of sequential biopsy sections. These studies revealed the different intratumoural distribution patterns of these mAbs. Whilst the anti-CD45 mAb dispersed homogeneously within the spleen, the anti-MHCII mAb specifically targeted the B-cell and tumour cell dominant regions. As a result, the dosimetry results derived from conventional biodistribution assays which assume the homogeneous distribution of mAb substantially underestimated the real radiation dose delivered to the tumour cells by anti-MHCII mAb. As such biodistribution assays assume homogeneous distribution of mAb, they are likely to estimate the radiation dose delivered by anti-CD45 more accurately than that with anti-MHCII. This is the first experimental data to indicate that rather than delivering less

than MIRD estimated radiation dose, some mAb targeting on tumour related antigens such as the anti-MHCII may deliver significantly higher radiation doses to the tumour cells than that determined from conventional dosimetry studies. This superior radiation delivery could lead to improved RIT therapeutic efficacy. However, in conventional biodistribution assay, by assuming the homogeneous intratumoural distribution, this large radiation dosimetry variation was missed. We believe these results not only highlighted the importance of radiation dosimetry in RIT, but also underpinned the fact that the current MIRD dosimetry has inadequacies in guiding the radiation dose evaluation in RIT.

Most recently, Dewaraja et al reported that in clinical settings the mismatch between tumour absorbed dose and RIT therapy response could also be due to the inaccuracies in activity quantification and dose estimation. With improved patient-specific, 3-dimensional, SPECT imaging based dosimetry method they found that the conventional MIRD based dosimetry method could have underestimated the tumour absorbed dose by up to 35% for smaller tumours of 7 ml in size and underestimate the absorbed dose by 12% for bigger tumours of 16 ml in size (Dewaraja, Wilderman et al. 2005).

Traditionally, the intratumoural distributions of mAb have been observed by autoradiography technology (Chung, Jang et al. 1994; Sato, Saga et al. 1999). But the poor spatial resolution of this technique restricted the observed magnification to around 2-4 fold which is far less than required to observe the real mAb localisation which should be at cellular level (Eklund and Williams 1991; Brown, Kaminski et al. 1997; Kinuya, Yokoyama et al. 1998). The recent introduction of radioluminography technique makes the observation of intratumoural distribution of radiolabelled mAb more convenient, but with a similar spatial resolution to autoradiography, still lack the high spatial resolution needed to observe localization of mAb at the cellular level (Flynn, Green et al. 1999; Kinuya, Yokoyama et al. 2000; Flynn, Boxer et al. 2001; Petrie, Flynn et al. 2002; Flynn, Pedley et al. 2003; Green, Flynn et al. 2004).

In this chapter, by taking biopsies simultaneously to the conventional biodistribution assays, although the immunohistochemistry images were not visualized directly through radiation exposure, it enabled us to observe the real intratumoural distribution of intravenously infused mAb at microscopic level. These studies demonstrated that the antigen-specificity of mAb determined their intratumoural distribution pattern which therefore determined their radiation delivery capability to the individual tumour cells located within the tissue.

This data strongly suggests that the dosimetric differences found at microscopic level may determine the RIT therapeutic efficacy of mAb. Rather than scattered heterogeneously in a random manner within the tissue as observed by conventional autoradiography technique, the radiolabelled mAb actually targeted onto the particular cells which express the target antigen. When the stained biopsy sections were observed under less magnification as for autoradiography, it also showed “heterogeneous” mAb distribution pattern. However, when the observation magnification was increased to cellular level, it was revealed that this heterogeneity was not random, but the mAb distribution was actually in accordance with the localisation of particular cell clusters within the tissue. Under certain magnification (x 100) as shown in figure 5.7 and figure 5.8, the intravenously injected mAb were clearly localised on the corresponding cells surface. Embedded in GMA resin, the immunohistochemistry technique reported in this chapter makes it possible to obtain extremely thin tissue sections of 1-2 $\mu$ m per section and technically enables us to get up to 6-7 sequential sections for each single tumour cell. This technique therefore enables us to compare the distribution patterns of a panel of mAb within even exactly same cell population.

By comparing the RIT therapies of double dose  $^{131}\text{I}$  labelled anti-CD45 mAb with that of the  $^{131}\text{I}$  labelled anti-MHCII, this study have also revealed that ultimate tumour killing could be achieved in this animal model using a radiolabelled less tumour specific mAb (anti-CD45), but with substantially escalated radiation toxicity. This result further underpinned the importance of antigen/antibody selection in RIT. Apart from the

emphasis of high antigen expression, the mAb specificity has been found extremely valuable.

## 5.5 Conclusions

In this chapter, by determining the intratumoural distribution of intravenously administered  $^{131}\text{I}$  labelled mAb, we observed at a cellular level the tumour dosimetry and the correlated RIT therapeutic effects of radioimmunoconjugates in the same BCL<sub>1</sub> syngeneic B-cell lymphoma model. It has been demonstrated that the different intratumoural biodistribution patterns of these mAbs lead to important differences in tumour radiation dosimetry which resulted in dramatically different therapeutic outcomes. This data suggests that the microdosimetry difference is only detectable at cellular level, and that conventional MIRD based dosimetry method is inadequate in providing accurate dosimetry evaluation in RIT and predicting response. Furthermore, this data confirms that the radiation dosimetry plays a critical role in the success of RIT and, the conventional dosimetry methods which assume the homogeneous intratumoural distribution of radiolabelled mAb could substantially underestimate the radiation dose delivered by mAb which targeting on tumour-related antigen in RIT.

Interestingly the high liver uptake of radiolabelled anti-CD45 mAb frequently observed in clinical studies was not seen in these murine B-cell lymphoma models. The reasons behind this discrepancy are not immediately apparent, but it is possible that the anti-CD45 used in the clinical studies may be binding non-specifically via the Fc arm and be taken up in the liver via the “bramble receptors” (Dr. Kim Orchard – personal communication). These differences do however highlight the need to be cautious when trying to extrapolate animal experimental results to the clinical situation.

## Chapter 6 Summary and Conclusions

Exciting progress has been made over the last several years in the development of RIT for NHL. The progress made during this time, in the clinic with radiolabelled anti-CD20 mAbs and with the use of “naked” anti-CD20 mAbs have surpassed anything previously achieved with mAbs over the whole of past 20 years. The commercial launch of “Rituximab”, a novel chimeric mAb that targets the B-cell specific CD20 antigen, in 1997 was the first, of perhaps many mAbs to gain a therapeutic license. Rituximab is now used worldwide not only for the treatment of B-cell lymphomas but many non-malignant conditions as well (Grillo-Lopez 2003; Weide, Heymanns et al. 2003; Edelbauer, Jungraithmayr et al. 2005; Maloney 2005). More recently, the two radiolabelled anti-CD20 mAbs, <sup>90</sup>Y labelled ibritumomab tiuxetan (Zevalin™, US FDA approval granted on February 19, 2002) and <sup>131</sup>I-tositumomab (Bexxar™, US FDA approval granted June 30, 2003), were granted approval for the treatment of refractory NHL in the US and <sup>90</sup>Y labelled ibritumomab tiuxetan (Zevalin™) was also approved in Europe in 2004. These approvals along with the increasing emergence of maturing clinical data has made it very likely that this new therapeutic modality will play an important role in the future management of NHL (Connors 2005; Hagenbeek 2005; Kaminski, Tuck et al. 2005; Marcus 2005; O'Connor O 2005; Wahl 2005).

Although we are seeing a welcomed increased optimism in the use of radiolabelled mAbs for the treatment of malignant diseases and in particular NHL, the mechanisms by which mAbs destroy cellular targets (Maloney 2005) and how RIT actually works as a treatment strategy are still poorly understood (Illidge and Johnson 2000). Despite extensive empirical clinical trial experience, the critical factors important in the mechanism of tumour cell kill by mAbs continue to be elusive and the subject of debate. The major immune mechanisms of action of mAbs include complement-dependent cytotoxicity and antibody-dependent cellular cytotoxicity. However a growing body of evidence reveals that some of the therapeutically useful mAbs, such as anti-idiotype and anti-CD20, may have an additional activity that involves transmembrane signalling and

the induction of apoptosis in these neoplastic cells (Shan, Ledbetter et al. 1998; Tutt, French et al. 1998; Maloney 2005).

The anti-tumour effects of RIT were assumed to be primarily due to the radioactivity of the radiolabelled antibody, which emits continuous low-dose-rate irradiation with heterogeneous dose deposition. In recent years, the intrinsic therapeutic effect of mAb has been gradually realised in RIT. However, the existence of radiation dose response in RIT of NHL remains controversial (Britton 2004). A substantial number of clinical trials failed to observe a radiation dose response in the treatment of NHL tumours and myelotoxicity. Some investigators therefore do not think dosimetric studies necessary for RIT (Wagner, Wiseman et al. 2002; Wiseman, Leigh et al. 2002; Wiseman, Kormmehl et al. 2003; Postema 2004; Goldenberg and Sharkey 2005). On the contrary, others do not share the same view and have reported that in their studies radiation dosimetry analysis had provided invaluable information to predict the therapeutic effect and toxicity (Wahl 2003; Britton 2004; Kaminski, Tuck et al. 2005). As a result, for the two US FDA approved RIT therapeutic regimens, Bexxar<sup>TM</sup> requires a dosimetric study prior to each therapeutic infusion to determine the optimal therapeutic dose (65-75cGy whole body dose) (Wahl 2003), but Zevalin<sup>TM</sup> dose not require such dosimetric studies (Wagner, Wiseman et al. 2002). Instead, the therapeutic dose of Zevalin<sup>TM</sup> is decided by the patient body weight (0.3 - 0.4 mCi/kg body weight dependent on the pre-treatment platelet count).

The clinical community although excited about the promising data emerged from RIT of B-cell lymphoma, remain uncertain as to how best to deliver this form of therapy. In order to clarify some of these important questions, syngeneic animal models are very helpful in testing a variety of treatment approaches. Therefore, the fundamental aims of the work described in this thesis was to explore whether radiation dose response exists in RIT of NHL and to determine the relative contribution of mAb and targeted radiation to the tumour killing in RIT.

An optimal Iodogen-Beads based radioiodination method was established and this method has been successfully used in both preclinical RIT studies and in clinical RIT trials (chapter 3). The in vitro characteristics as well as the in vivo biodistribution performance of a panel of radiolabelled B-cell related mAbs were described (chapter 3). These data further confirmed that irradiation would be better delivered by mAb which targets on highly expressed and non-internalising antigen, like anti-MHCII and anti-CD45 in this study. The dosimetric impact of pre-dosing was investigated in syngeneic BCL<sub>1</sub> model. Subsequently, based on the radiation dosimetry data abstracted from biodistribution studies, factors determining the successful clearance of tumour in RIT of B-cell lymphoma were explored (chapter 4). The relative contributions of mAb and irradiation were demonstrated both critical in successful RIT (chapter 4). Furthermore, for the first time, the existence of radiation dose response in the presence of a signalling mAb was observed (chapter 4).

Next in chapter 5, using both conventional biodistribution assessments and immunohistochemistry techniques, for the first time, the RIT therapeutic effects of <sup>131</sup>I labelled a panel of mAbs were compared with the microscopic tumour dosimetry at cellular level in the BCL<sub>1</sub> syngeneic B-cell lymphoma model (chapter 5). The important role of radiation microdosimetry in the successful clearance of lymphoma in RIT was demonstrated (chapter 5).

Based on the data obtained during the course of this study, I have published one first-authored research paper in the journal Blood (Du, Honeychurch et al. 2004) and another first-author paper focusing on the importance of intratumoural distribution of radiolabelled mAb is currently at a late stage of preparation to be submitted to Cancer Research. I have also been invited to present the work described in this thesis at several prestigious international meetings including an first author presentation at the Society of Nuclear Medicine (SNM) Annual Meeting (Du 2001), twice at the British Cancer Research Meeting (Du 2002; Bayne 2003; Du 2003), as well as the World Conference on Dosing of Antiinfectives and Antineoplasms (Du 2004) and the 8<sup>th</sup> Asia & Oceania Congress of Nuclear Medicine and Biology (Du 2004). Some of the data have also been

presented at an oral presentation of the American Society of Haematology (ASH) Annual Meeting (Illidge 2004).

Future clinical work involving tumour biopsies is planned to investigate whether the intratumoural microdosimetry of radiolabelled mAb also plays critical role in determining the clinical therapeutic effect of RIT in NHL. It is hoped that the work presented in this thesis has provided useful new insights into some of the important mechanisms that are operating in the successful clearance of tumour by RIT and will inform the future design and development of RIT for NHL to the benefit of patients who suffer with these diseases.

## Appendix 1

### mAb Binding (%) in Three Immunoreactivity Assays of Rat-anti-mouse mAb on BCL<sub>1</sub> Cells

No. of Cells (x 10 <sup>5</sup> )	anti-CD19	anti-CD22	anti-CD38	anti-Id	anti-MHCII	anti-A31Id
	0	0	0	0	0	0
7.8125	36.5	30.2	27.2	40.3	43.2	8.32
	33.7	27.9	29.4	37.2	40.3	7.35
	38	32.2	25.8	41.9	45.7	7.04
15.625	43.2	39.4	37	48.3	54.5	11.3
	45.8	43	38.4	46.2	51.2	10.65
	44.7	38.5	36.4	50.7	56.3	9.32
31.25	51.2	45.3	42.6	55.8	67.4	11.7
	48.4	44.3	40.3	52.4	64.5	10.6
	55.3	40.7	45.1	59.7	69	9.45
62.5	55.6	47.2	46.4	61	71.2	10.8
	53.4	48.4	43.7	57.9	74.8	11.5
	58.9	44.6	47.7	62.4	72.1	9.86
125	58.3	48.4	51.2	63.2	73.5	11.3
	60.2	52.5	47.5	60.1	72.8	12.4
	56.7	47.8	53.4	62.7	74.4	10.97

## Appendix 2

### BCL<sub>1</sub> Cell Binding [Molecules/cell (x 10<sup>5</sup>)] of Radioiodinated mAbs in 3 Experiments

Conc. of mAb ( $\mu$ g/ml)	anti-CD19	anti-CD22	anti-CD38	anti-Id	anti-MHCII	anti-A31Id
0	0	0	0	0	0	0
0.125	0.33	0.21	0.20	0.51	0.78	0.04
	0.27	0.17	0.14	0.47	0.75	0.07
	0.32	0.15	0.17	0.55	0.83	0.04
0.25	0.54	0.41	0.37	0.72	1.45	0.11
	0.43	0.43	0.34	0.62	1.52	0.15
	0.47	0.35	0.34	0.71	1.43	0.12
0.5	0.66	0.55	0.50	1.34	2.56	0.17
	0.72	0.47	0.43	1.25	2.45	0.16
	0.61	0.53	0.54	1.24	2.51	0.21
1	0.98	0.72	0.54	2.21	4.52	0.28
	0.84	0.64	0.57	2.19	4.58	0.25
	0.87	0.66	0.57	2.24	4.41	0.26
2	1.43	1.08	0.92	3.63	6.73	0.43
	1.31	1.15	0.95	3.51	6.48	0.34
	1.33	1.04	0.84	3.47	6.54	0.47
4	2.21	1.85	1.40	4.23	8.12	0.69
	2.30	1.74	1.33	4.11	7.83	0.66
	2.17	1.88	1.37	4.30	8.25	0.74

## Appendix 3

### mAb Binding (%) in Three Immunoreactivity Assays of Rat-anti-mouse mAb on BCL<sub>1</sub> Cells

No. of Cells (x 10 <sup>5</sup> )	anti-CD19	anti-CD452a	anti-CD452b	anti-Id	anti-MHCII	anti-A31Id
0	0	0	0	0	0	0
7.8125	32.5	33.2	36.2	41.3	40.2	9.42
	33.7	35.9	33.4	38.2	37.6	10.35
	30.8	31.2	37.8	42.7	45.8	11.03
15.625	43.2	41.4	44.7	46.3	54.8	11.37
	41.8	43	45.4	51.2	51.0	10.66
	42.7	44.5	47.4	50.7	56.7	12.32
31.25	46.2	46.3	51.6	58.8	68.1	13.07
	48.4	48.3	54.3	53.4	64.5	12.60
	45.3	45.7	53.1	56.7	69.9	12.44
62.5	48.6	52.2	52.4	62.5	71.4	13.08
	50.4	54.5	57.7	58.4	73.8	11.65
	51.2	52.6	55.1	64.1	70.1	12.86
125	50.3	52.4	54.2	63.3	73.5	14.33
	53.2	55.5	57.5	60.0	74.8	16.45
	53.7	57.8	59.4	64.7	71.4	13.97

## Appendix 4

### BCL<sub>1</sub> Cells Binding [Molecules/cell (x 10<sup>5</sup>)] of Radioiodinated mAbs in 3 experiments

Conc. of mAb ( $\mu$ g/ml)	anti-CD19	anti- CD452a	anti- CD452b	anti-Id	anti-MHCII	anti-A31Id
0	0	0	0	0	0	0
0.125	0.31	0.51	0.53	0.52	0.77	0.02
	0.26	0.55	0.57	0.47	0.84	0.05
	0.32	0.47	0.49	0.56	0.80	0.04
0.25	0.52	0.63	1.03	0.74	1.54	0.13
	0.43	0.68	0.98	0.63	1.47	0.15
	0.49	0.64	1.11	0.68	1.43	0.12
0.50	0.66	1.76	2.45	1.33	2.54	0.17
	0.71	1.83	2.43	1.46	2.35	0.16
	0.63	1.61	2.56	1.45	2.49	0.25
1.0	0.97	3.44	3.74	2.24	4.57	0.28
	0.86	3.67	3.63	2.19	4.44	0.35
	0.83	3.67	3.82	2.24	4.51	0.26
2.0	1.37	5.12	5.35	3.62	6.75	0.43
	1.32	4.85	5.07	3.53	6.68	0.34
	1.36	5.04	5.13	3.42	6.54	0.37
4.0	2.07	5.70	6.40	4.25	8.10	0.58
	2.35	5.91	6.71	4.22	8.11	0.63
	2.20	5.73	6.33	4.13	7.85	0.71

## Appendix 5

### Complement Dependent Cytotoxicity on BCL<sub>1</sub> Cells (% Specific <sup>51</sup>Cr release: Results of 3 Assays)

Conc. of mAb ( $\mu$ g/ml)	anti- CD19	anti- CD22	anti- CD38	anti- Id	anti- MHCII	anti- CD452a	anti- CD452b	anti- CD40	N22	anti- A31Id
0	0	0	0	0	0	0	0	0	0	0
0.0390625	2.11	1.22	1.44	5.64	3.75	0.05	3.52	3.71	8.13	0.001
	1.83	1.12	1.37	6.11	3.64	0.17	3.66	3.42	7.64	0.001
	2.05	1.27	1.40	5.35	3.90	0.06	3.17	3.47	8.20	0.001
0.078125	1.84	2.33	1.81	7.28	8.47	0.63	3.74	3.48	12.50	0.001
	2.07	1.84	1.75	7.03	8.17	0.69	3.83	3.51	13.12	0.001
	2.01	2.45	1.73	6.85	8.46	0.54	3.42	3.63	10.74	0.002
0.15625	2.52	2.61	1.92	14.58	27.25	2.11	4.43	7.32	33.47	0.001
	3.04	2.04	1.88	16.13	28.04	2.35	4.17	7.87	30.52	0.002
	3.10	2.27	1.79	15.04	26.77	1.86	4.45	6.94	38.04	0.001
0.3125	3.25	2.43	2.54	20.71	50.32	3.25	4.25	13.70	62.45	0.002
	3.07	2.75	2.31	22.13	52.47	3.76	4.61	14.13	58.70	0.002
	2.89	2.03	2.56	19.30	50.22	3.14	4.32	12.35	64.58	0.002
0.625	3.57	3.05	2.33	30.25	57.03	3.47	5.94	19.01	68.54	0.004
	3.02	3.34	2.87	33.04	58.96	4.02	6.21	21.12	71.20	0.003
	3.24	3.12	2.06	30.11	55.37	3.28	5.76	18.33	66.73	0.001
1.25	3.25	4.31	3.88	36.55	58.77	4.45	7.87	25.43	70.41	0.003
	3.41	4.54	3.71	39.42	61.32	4.50	7.60	23.72	72.15	0.002
	3.04	4.06	4.03	33.57	58.41	4.21	7.93	25.94	69.04	0.002
2.5	3.43	4.97	3.74	45.68	60.03	5.73	10.65	30.32	74.21	0.003
	3.17	4.33	3.49	48.01	62.37	5.96	11.32	29.35	71.72	0.003
	3.35	4.75	3.52	41.37	59.41	5.17	10.04	28.03	69.84	0.004
5.0	5.43	4.94	4.33	52.18	61.54	8.84	14.70	40.77	76.52	0.003
	4.86	5.23	4.52	54.32	62.38	9.03	15.12	39.30	77.43	0.004
	5.38	4.81	4.19	50.77	60.76	8.25	14.43	41.02	72.14	0.004
10.0	7.83	5.49	6.23	58.64	62.42	10.26	20.52	41.83	78.83	0.003
	8.30	5.63	5.94	59.73	64.07	11.77	22.31	43.06	79.32	0.005
	8.15	4.72	6.35	57.55	61.33	8.94	18.79	40.67	77.75	0.004

## References

Adam, T. (1989). "Radioiodination for therapy." Ann Clin Biochem **26** ( Pt 3): 244-5.

Aisenberg, A. C. (2000). "Historical review of lymphomas." Br J Haematol **109**(3): 466-76.

Amdur, R. J. and J. S. Bedford (1994). "Dose-rate effects between 0.3 and 30 Gy/h in a normal and a malignant human cell line." Int J Radiat Oncol Biol Phys **30**(1): 83-90.

Andersson, H., J. Elgqvist, et al. (2003). "Astatine-211-labeled antibodies for treatment of disseminated ovarian cancer: an overview of results in an ovarian tumor model." Clin Cancer Res **9**(10 Pt 2): 3914S-21S.

Antonescu, C., A. Bischof Delaloye, et al. (2005). "Repeated injections of (131)I-rituximab show patient-specific stable biodistribution and tissue kinetics." Eur J Nucl Med Mol Imaging.

Armitage, J. O. and D. D. Weisenburger (1998). "New approach to classifying non-Hodgkin's lymphomas: clinical features of the major histologic subtypes. Non-Hodgkin's Lymphoma Classification Project." J Clin Oncol **16**(8): 2780-95.

Avivi, I., S. Robinson, et al. (2003). "Clinical use of rituximab in haematological malignancies." Br J Cancer **89**(8): 1389-94.

Badger, C. C., J. Davis, et al. (1991). "Biodistribution and dosimetry following infusion of antibodies labeled with large amounts of 131I." Cancer Res **51**(21): 5921-8.

Bannerji, R., S. Kitada, et al. (2003). "Apoptotic-regulatory and complement-protecting protein expression in chronic lymphocytic leukemia: relationship to in vivo rituximab resistance." J Clin Oncol **21**(8): 1466-71.

Bayne, M., Zivanovic, M., Lewington, V., Du, Y., Harrison, C., Hodges, L., Johnson, P., Illidge, T. (2003). "Phase I/II study of fractionated radioimmunotherapy in relapsed low grade non-Hodgkin's lymphoma." British Journal of Cancer **88**(Suppl 1): S38.

Behr, T. M. (2002). "Is high-dose radioimmunotherapy needed in non-Hodgkin's lymphoma? For." Eur J Nucl Med Mol Imaging **29**(9): 1248-54.

Behr, T. M., M. Behe, et al. (2000). "Therapeutic advantages of Auger electron- over beta-emitting radiometals or radioiodine when conjugated to internalizing antibodies." Eur J Nucl Med **27**(7): 753-65.

Behr, T. M., M. Behe, et al. (2002). "Correlation of red marrow radiation dosimetry with myelotoxicity: empirical factors influencing the radiation-induced myelotoxicity of radiolabeled antibodies, fragments and peptides in pre-clinical and clinical settings." *Cancer Biother Radiopharm* **17**(4): 445-64.

Behr, T. M., R. D. Blumenthal, et al. (2000). "Cure of metastatic human colonic cancer in mice with radiolabeled monoclonal antibody fragments." *Clin Cancer Res* **6**(12): 4900-7.

Behr, T. M., D. M. Goldenberg, et al. (1997). "Radioimmunotherapy of solid tumors: a review "of mice and men"." *Hybridoma* **16**(1): 101-7.

Behr, T. M., M. Gotthardt, et al. (2002). "Radioiodination of monoclonal antibodies, proteins and peptides for diagnosis and therapy. A review of standardized, reliable and safe procedures for clinical grade levels kBq to GBq in the Gottingen/Marburg experience." *Nuklearmedizin* **41**(2): 71-9.

Behr, T. M., F. Griesinger, et al. (2002). "High-dose myeloablative radioimmunotherapy of mantle cell non-Hodgkin lymphoma with the iodine-131-labeled chimeric anti-CD20 antibody C2B8 and autologous stem cell support. Results of a pilot study." *Cancer* **94**(4 Suppl): 1363-72.

Behr, T. M., S. Memtsoudis, et al. (1998). "Experimental studies on the role of antibody fragments in cancer radio-immunotherapy: Influence of radiation dose and dose rate on toxicity and anti-tumor efficacy." *Int J Cancer* **77**(5): 787-95.

Behr, T. M., S. Memtsoudis, et al. (1999). "Radioimmunotherapy of colorectal cancer in small volume disease and in an adjuvant setting: preclinical evaluation in comparison to equitoxic chemotherapy and initial results of an ongoing phase-I/II clinical trial." *Anticancer Res* **19**(4A): 2427-32.

Behr, T. M., G. Sgouros, et al. (1998). "Therapeutic efficacy and dose-limiting toxicity of Auger-electron vs. beta emitters in radioimmunotherapy with internalizing antibodies: evaluation of 125I- vs. 131I-labeled CO17-1A in a human colorectal cancer model." *Int J Cancer* **76**(5): 738-48.

Behr, T. M., R. M. Sharkey, et al. (1997). "Variables influencing tumor dosimetry in radioimmunotherapy of CEA-expressing cancers with anti-CEA and antimucin monoclonal antibodies." *J Nucl Med* **38**(3): 409-18.

Behr, T. M., B. Wormann, et al. (1999). "Low- versus high-dose radioimmunotherapy with humanized anti-CD22 or chimeric anti-CD20 antibodies in a broad spectrum of B cell-associated malignancies." *Clin Cancer Res* **5**(10 Suppl): 3304s-3314s.

Bennett, J. M., M. S. Kaminski, et al. (2005). "Assessment of treatment-related myelodysplastic syndromes and acute myeloid leukemia in patients with non-Hodgkin lymphoma treated with tositumomab and iodine 131 tositumomab." Blood **105**(12): 4576-82.

Berinstein, N. L., A. J. Grillo-Lopez, et al. (1998). "Association of serum Rituximab (IDE-C2B8) concentration and anti-tumor response in the treatment of recurrent low-grade or follicular non-Hodgkin's lymphoma." Ann Oncol **9**(9): 995-1001.

Bhargava, K. K. and S. A. Acharya (1989). "Labeling of monoclonal antibodies with radionuclides." Semin Nucl Med **19**(3): 187-201.

Borchardt, P. E., R. R. Yuan, et al. (2003). "Targeted actinium-225 in vivo generators for therapy of ovarian cancer." Cancer Res **63**(16): 5084-90.

Britten, K. M., P. H. Howarth, et al. (1993). "Immunohistochemistry on resin sections: a comparison of resin embedding techniques for small mucosal biopsies." Biotech Histochem **68**(5): 271-80.

Britton, K. E. (2004). "Radioimmunotherapy of Non-Hodgkin's lymphoma." J Nucl Med **45**(5): 924-5.

Brown, R. S., M. S. Kaminski, et al. (1997). "Intratumoral microdistribution of [131I]MB-1 in patients with B-cell lymphoma following radioimmunotherapy." Nucl Med Biol **24**(7): 657-63.

Buchegger, F., A. Roth, et al. (2000). "Radioimmunotherapy of colorectal cancer liver metastases: combination with radiotherapy." Ann N Y Acad Sci **910**: 263-9; discussion 269-70.

Buchsbaum, D. J., P. G. Brubaker, et al. (1990). "Comparative binding and preclinical localization and therapy studies with radiolabeled human chimeric and murine 17-1A monoclonal antibodies." Cancer Res **50**(3 Suppl): 993s-999s.

Buchsbaum, D. J., V. K. Langmuir, et al. (1993). "Experimental radioimmunotherapy." Med Phys **20**(2 Pt 2): 551-67.

Buchsbaum, D. J., R. L. Wahl, et al. (1992). "Improved delivery of radiolabeled anti-B1 monoclonal antibody to Raji lymphoma xenografts by predosing with unlabeled anti-B1 monoclonal antibody." Cancer Res **52**(3): 637-42.

Buchsbaum, D. J., R. L. Wahl, et al. (1992). "Therapy with unlabeled and 131I-labeled pan-B-cell monoclonal antibodies in nude mice bearing Raji Burkitt's lymphoma xenografts." Cancer Res **52**(23): 6476-81.

Chan, H. T., D. Hughes, et al. (2003). "CD20-induced lymphoma cell death is independent of both caspases and its redistribution into triton X-100 insoluble membrane rafts." Cancer Res **63**(17): 5480-9.

Chaouchi, N., A. Vazquez, et al. (1995). "B cell antigen receptor-mediated apoptosis. Importance of accessory molecules CD19 and CD22, and of surface IgM cross-linking." J Immunol **154**(7): 3096-104.

Chung, J. K., J. J. Jang, et al. (1994). "Tumor concentration and distribution of carcinoembryonic antigen measured by in vitro quantitative autoradiography." J Nucl Med **35**(9): 1499-505.

Cobb, L. M., M. J. Glennie, et al. (1986). "Characterisation of a new murine B cell lymphoma." Br J Cancer **54**(5): 807-18.

Coiffier, B. (2004). "Effective immunochemotherapy for aggressive non-Hodgkin's lymphoma." Semin Oncol **31**(1 Suppl 2): 7-11.

Coiffier, B. (2005). "Monoclonal antibodies in the treatment of indolent lymphomas." Best Pract Res Clin Haematol **18**(1): 69-80.

Coiffier, B., E. Lepage, et al. (2002). "CHOP chemotherapy plus rituximab compared with CHOP alone in elderly patients with diffuse large-B-cell lymphoma." N Engl J Med **346**(4): 235-42.

Coleman M, M. S. K., Susan J. Knox, Andrew D. Zelenetz, Julie M. Vose (2003). [89] The BEXXAR Therapeutic Regimen (Tositumomab and Iodine I 131 Tositumomab) Produced Durable Complete Remissions in Heavily Pretreated Patients with Non-Hodgkins Lymphoma (NHL), Rituximab- Relapsed/Refractory Disease, and Rituximab-Naive Disease. Session Type: Oral Session. American Society of Haematology 45th Annual Meeting, San Diego.

Connors, J. M. (2005). "Radioimmunotherapy--hot new treatment for lymphoma." N Engl J Med **352**(5): 496-8.

Cragg, M. S., M. B. Bayne, et al. (2004). "A new anti-idiotype antibody capable of binding rituximab on the surface of lymphoma cells." Blood **104**(8): 2540-2.

Cragg, M. S., R. R. French, et al. (1999). "Signaling antibodies in cancer therapy." Curr Opin Immunol **11**(5): 541-7.

Cragg, M. S. and M. J. Glennie (2003). "Antibody specificity controls in vivo effector mechanisms of anti-CD20 reagents." Blood.

Cragg, M. S., S. M. Morgan, et al. (2003). "Complement-mediated lysis by anti-CD20 mAb correlates with segregation into lipid rafts." Blood **101**(3): 1045-52.

Cragg, M. S., L. Zhang, et al. (1999). "Analysis of the interaction of monoclonal antibodies with surface IgM on neoplastic B-cells." Br J Cancer **79**(5-6): 850-7.

Davis, T. A., M. S. Kaminski, et al. (2004). "The radioisotope contributes significantly to the activity of radioimmunotherapy." Clin Cancer Res **10**(23): 7792-8.

Dechant, M., J. Bruenke, et al. (2003). "HLA class II antibodies in the treatment of hematologic malignancies." Semin Oncol **30**(4): 465-75.

Del Vecchio, S., J. C. Reynolds, et al. (1989). "Local distribution and concentration of intravenously injected  $^{131}\text{I}$ -9.2.27 monoclonal antibody in human malignant melanoma." Cancer Res **49**(10): 2783-9.

DeNardo, G. L., S. J. DeNardo, et al. (1998). "Maximum-tolerated dose, toxicity, and efficacy of  $^{131}\text{I}$ -Lym-1 antibody for fractionated radioimmunotherapy of non-Hodgkin's lymphoma." J Clin Oncol **16**(10): 3246-56.

DeNardo, G. L., S. J. DeNardo, et al. (1998). "Low-dose, fractionated radioimmunotherapy for B-cell malignancies using  $^{131}\text{I}$ -Lym-1 antibody." Cancer Biother Radiopharm **13**(4): 239-54.

DeNardo, G. L., S. J. DeNardo, et al. (1990). "Fractionated radioimmunotherapy of B-cell malignancies with  $^{131}\text{I}$ -Lym-1." Cancer Res **50**(3 Suppl): 1014s-1016s.

DeNardo, G. L., S. J. DeNardo, et al. (2000). " $^{131}\text{I}$ -Lym-1 in mice implanted with human Burkitt's lymphoma (Raji) tumors: loss of tumor specificity due to radiolysis." Cancer Biother Radiopharm **15**(6): 547-60.

DeNardo, G. L., D. L. Kukis, et al. (1999). "67Cu-versus  $^{131}\text{I}$ -labeled Lym-1 antibody: comparative pharmacokinetics and dosimetry in patients with non-Hodgkin's lymphoma." Clin Cancer Res **5**(3): 533-41.

DeNardo, G. L., J. P. Lewis, et al. (1994). "Effect of Lym-1 radioimmunoconjugate on refractory chronic lymphocytic leukemia." Cancer **73**(5): 1425-32.

DeNardo, G. L., G. R. Mirick, et al. (2003). "Characterization of human IgG antimouse antibody in patients with B-cell malignancies." Clin Cancer Res **9**(10 Pt 2): 4013S-21S.

DeNardo, G. L., R. T. O'Donnell, et al. (2000). "Radiation dosimetry for  $^{90}\text{Y}$ -2IT-BAD-Lym-1 extrapolated from pharmacokinetics using  $^{111}\text{In}$ -2IT-BAD-Lym-1 in patients with non-Hodgkin's lymphoma." J Nucl Med **41**(5): 952-8.

DeNardo, G. L., C. L. Siantar, et al. (2002). "Radiation dosimetry for radionuclide therapy in a nonmyeloablative strategy." Cancer Biother Radiopharm **17**(1): 107-18.

DeNardo, S. J. (2000). "Tumor-targeted radionuclide therapy: trial design driven by patient dosimetry." J Nucl Med **41**(1): 104-6.

DeNardo, S. J., G. L. DeNardo, et al. (1988). "Treatment of B cell malignancies with  $^{131}\text{I}$  Lym-1 monoclonal antibodies." Int J Cancer Suppl **3**: 96-101.

Denardo, S. J., C. M. Richman, et al. (1998). "Synergistic therapy of breast cancer with Y-90-chimeric L6 and paclitaxel in the xenografted mouse model: development of a clinical protocol." Anticancer Res **18**(6A): 4011-8.

Denkers, E. Y., C. C. Badger, et al. (1985). "Influence of antibody isotype on passive serotherapy of lymphoma." J Immunol **135**(3): 2183-6.

DeVita, V. T., Jr., G. P. Canellos, et al. (1975). "Advanced diffuse histiocytic lymphoma, a potentially curable disease." Lancet **1**(7901): 248-50.

Dewaraja, Y. K., S. J. Wilderman, et al. (2005). "Accurate Dosimetry in  $^{131}\text{I}$  Radionuclide Therapy Using Patient-Specific, 3-Dimensional Methods for SPECT Reconstruction and Absorbed Dose Calculation." J Nucl Med **46**(5): 840-9.

Donjerkovic, D. and D. W. Scott (2000). "Activation-induced cell death in B lymphocytes." Cell Res **10**(3): 179-92.

Du, Y., J. Honeychurch, et al. (2004). "Antibody-induced intracellular signaling works in combination with radiation to eradicate lymphoma in radioimmunotherapy." Blood **103**(4): 1485-94.

Du, Y., Honeychurch, J., Johnson, PW, Glennie, MJ, Illidge, TM (2002). A radiation dose response exists for radioimmunotherapy of B-cell lymphoma only in the presence of signalling monoclonal antibody. British Cancer Research Meeting 2002, Glasgow, UK, British Journal of Cancer.

Du, Y., Honeychurch, J., Johnson, PW, Glennie, MJ, Illidge, TM (2003). "Long term clearance of tumour in radioimmunotherapy of B-cell lymphoma requires targeted radiation and monoclonal antibody induced cell surface signalling." British Journal of Cancer **88**(Suppl 1): S38.

Du, Y., Honeychurch, J., Johnson, PW, Illidge, TM (2001). Low dose rate irradiation and antibody can be synergistic in action and both are critical to successful radioimmunotherapy in B-cell lymphoma. Proceedings of the SNM 48th Annual Meeting, Toronto, Canada, Journal of Nuclear Medicine.

Du, Y., Jia SQ (1995). Radioiodination of monoclonal antibodies using N-bromosuccinimide: laboratory and clinical study. the First China-Japan Nuclear Medicine Conference, Beijing, China.

Du, Y., Johnson, PW, Glennie, MJ, Illidge, TM (2004). Microdosimetry and intratumoural localisation of intravenously administered I-131 labelled monoclonal antibodies are critical to successful radioimmunotherapy of lymphoma. World Conference on Antiinfectives and Antineoplasms, Nuremberg, Germany.

Du, Y., Johnson, PW, Glennie, MJ, Illidge, TM (2004). Targeted radiation and signalling antibody synergise in eradicating tumour cells in the radioimmunotherapy of B-cell lymphoma. 8th Asia & Oceania Congress of Nuclear Medicine and Biology, Beijing, China, Proceedings of the 8th Asia & Oceania Congress of Nuclear Medicine and Biology.

Dyer, M. J., G. Hale, et al. (1989). "Effects of CAMPATH-1 antibodies in vivo in patients with lymphoid malignancies: influence of antibody isotype." Blood **73**(6): 1431-9.

Edelbauer, M., T. Jungraithmayr, et al. (2005). "Rituximab in childhood systemic lupus erythematosus refractory to conventional immunosuppression: case report." Pediatr Nephrol **20**(6): 811-3.

Eklund, K. E. and J. R. Williams (1991). "A method for quantitative autoradiography over stained sections of tumors exposed in vivo to radiolabeled antibodies." Int J Radiat Oncol Biol Phys **21**(6): 1635-42.

Elliott, T. J., M. J. Glennie, et al. (1987). "Analysis of the interaction of antibodies with immunoglobulin idiotypes on neoplastic B lymphocytes: implications for immunotherapy." J Immunol **138**(3): 981-8.

Fisher, D. R. (1994). "Radiation dosimetry for radioimmunotherapy. An overview of current capabilities and limitations." Cancer **73**(3 Suppl): 905-11.

Fisher, D. R. (2000). "Internal dosimetry for systemic radiation therapy." Semin Radiat Oncol **10**(2): 123-32.

Fisher, R. I. (2000). "Current therapeutic paradigm for the treatment of non-Hodgkin's lymphoma." Semin Oncol **27**(6 Suppl 12): 2-8.

Fisher, R. I. (2003). "Overview of non-Hodgkin's lymphoma: biology, staging, and treatment." Semin Oncol **30**(2 Suppl 4): 3-9.

Fisher, R. I., E. R. Gaynor, et al. (1993). "Comparison of a standard regimen (CHOP) with three intensive chemotherapy regimens for advanced non-Hodgkin's lymphoma." N Engl J Med **328**(14): 1002-6.

Fisher, R. I., T. P. Miller, et al. (1998). "New REAL clinical entities." Cancer J Sci Am **4 Suppl 2**: S5-12.

Fisher, R. I. and M. M. Oken (1995). "Clinical practice guidelines: non-Hodgkin's lymphomas." Cleve Clin J Med **62 Suppl 1**: SI6-42, quiz SI43-5.

Flynn, A. A., G. M. Boxer, et al. (2001). "Relationship between tumour morphology, antigen and antibody distribution measured by fusion of digital phosphor and photographic images." Cancer Immunol Immunother **50**(2): 77-81.

Flynn, A. A., A. J. Green, et al. (1999). "A novel technique, using radioluminography, for the measurement of uniformity of radiolabelled antibody distribution in a colorectal cancer xenograft model." Int J Radiat Oncol Biol Phys **43**(1): 183-9.

Flynn, A. A., R. B. Pedley, et al. (2003). "The nonuniformity of antibody distribution in the kidney and its influence on dosimetry." Radiat Res **159**(2): 182-9.

Forero, A., P. L. Weiden, et al. (2004). "Phase I trial of a novel anti-CD20 fusion protein in pretargeted radioimmunotherapy for B-cell non-Hodgkin's lymphoma." Blood.

Friedberg, J. W. and R. I. Fisher (2004). "Iodine-131 tositumomab (Bexxar(R)): radioimmunoconjugate therapy for indolent and transformed B-cell non-Hodgkin's lymphoma." Expert Rev Anticancer Ther **4**(1): 18-26.

Fung H, S. J. F., A. Nademanee, A. Molina, D. Yamauchi, R. Speilberger, N. Kogut, F. Sahebi, P. Parker, R. Rodriguez, A. Krishnan, L. Popplewell, J. Wong, A. Raubitschek (2003). A New Preparative Regimen for Older Patients with Aggressive CD 20-Positive B-Cell Lymphoma Utilizing Standard-Dose Yttrium-90 Ibritumomab Tiuxetan (Zevalin) Radioimmunotherapy (RIT) Combined with High-Dose BEAM Followed by Autologous Hematopoietic Cell Transplantation (AHCT): Targeted Intensification without Increased Transplant-Related Toxicity. ASH, San Diego.

Garber, K. (2002). "For Bexxar, FDA meeting offers long-awaited chance at approval." J Natl Cancer Inst **94**(23): 1738-9.

George, A. J., H. M. McBride, et al. (1991). "Monoclonal antibodies raised against the idiotype of the murine B cell lymphoma, BCL1 act primarily with heavy chain determinants." Hybridoma **10**(2): 219-27.

Glennie, M. J. and P. W. Johnson (2000). "Clinical trials of antibody therapy." Immunol Today **21**(8): 403-10.

Glennie, M. J. and J. G. van de Winkel (2003). "Renaissance of cancer therapeutic antibodies." Drug Discov Today **8**(11): 503-10.

Goldenberg, D. M. (2001). "The role of radiolabeled antibodies in the treatment of non-Hodgkin's lymphoma: the coming of age of radioimmunotherapy." Crit Rev Oncol Hematol **39**(1-2): 195-201.

Goldenberg, D. M., J. A. Horowitz, et al. (1991). "Targeting, dosimetry, and radioimmunotherapy of B-cell lymphomas with iodine-131-labeled LL2 monoclonal antibody." J Clin Oncol **9**(4): 548-64.

Goldenberg, D. M. and R. M. Sharkey (2005). "Radioimmunotherapy of non-Hodgkin's lymphoma revisited." J Nucl Med **46**(2): 383-4.

Gopal, A. K., T. A. Gooley, et al. (2003). "High-dose radioimmunotherapy versus conventional high-dose therapy and autologous hematopoietic stem cell transplantation for relapsed follicular non-Hodgkin's lymphoma: a multivariable cohort analysis." Blood.

Gopal, A. K., J. G. Rajendran, et al. (2002). "High-dose chemo-radioimmunotherapy with autologous stem cell support for relapsed mantle cell lymphoma." Blood **99**(9): 3158-62.

Gordon, L. I., T. E. Witzig, et al. (2002). "Yttrium 90 ibritumomab tiuxetan radioimmunotherapy for relapsed or refractory low-grade non-Hodgkin's lymphoma." Semin Oncol **29**(1 Suppl 2): 87-92.

Gordon, L. I. W., T.E. Emmanouilides, C, et al: (2002). "90Y ibritumomab tiuxetan in aggressive NHL: Analysis of response and toxicity." Proc Am Soc Clin Oncol **21**: 266a.

Green, A., A. Flynn, et al. (2004). "Nonuniform absorbed dose distribution in the kidney: the influence of organ architecture." Cancer Biother Radiopharm **19**(3): 371-7.

Gregory, S., Kaminski, M., Zelenetz, A., Jain, V., (2002). "Characteristics of Patients with Relapsed and Refractory Low Grade Non-Hodgkin's Lymphoma Who Sustained Durable Responses Following Treatment with Tositumomab and Iodine I 131 Tositumomab (Bexxar®)." Blood **100**(11 part2): Abstract 4791.

Grillo-Lopez, A. J. (2003). "Rituximab (Rituxan/MabThera): the first decade (1993-2003)." Expert Rev Anticancer Ther **3**(6): 767-79.

Grossbard, M. L., O. W. Press, et al. (1992). "Monoclonal antibody-based therapies of leukemia and lymphoma." Blood **80**(4): 863-78.

Hagenbeek, A. (2005). "Future trends in radioimmunotherapy." Semin Oncol **32**(1 Suppl 1): S57-62.

Hajjar, G., S. R. M., et al. (2001). "Interim results of a phase I/II radioimmunotherapy trial in relapsed/ refractory non-Hodgkin's lymphoma (NHL) patients given Y-90 labeled anti-CD22 humanised monoclonal antibodies." Blood (ASH abst. 2560): 611a.

Harris, N. L., E. S. Jaffe, et al. (1999). "World Health Organization classification of neoplastic diseases of the hematopoietic and lymphoid tissues: report of the Clinical Advisory Committee meeting-Airlie House, Virginia, November 1997." J Clin Oncol **17**(12): 3835-49.

Hekman, A., A. Honselaar, et al. (1991). "Initial experience with treatment of human B cell lymphoma with anti-CD19 monoclonal antibody." Cancer Immunol Immunother **32**(6): 364-72.

Hennigan, T. W., R. H. Begent, et al. (1991). "Histamine, leukotriene C4 and interleukin-2 increase antibody uptake into a human carcinoma xenograft model." Br J Cancer **64**(5): 872-4.

Hiddemann, W., D. L. Longo, et al. (1996). "Lymphoma classification--the gap between biology and clinical management is closing." Blood **88**(11): 4085-9.

Hindorf, C., O. Linden, et al. (2003). "Change in tumor-absorbed dose due to decrease in mass during fractionated radioimmunotherapy in lymphoma patients." Clin Cancer Res **9**(10 Pt 2): 4003S-6S.

Hohenstein, M. A., S. C. Augustine, et al. (2003). "Establishing an institutional model for the administration of tositumomab and iodine I 131 tositumomab." Semin Oncol **30**(2 Suppl 4): 39-49.

Honeychurch, J., M. J. Glennie, et al. (2003). "Anti-CD40 monoclonal antibody therapy in combination with irradiation results in a CD8 T-cell-dependent immunity to B-cell lymphoma." Blood.

Honeychurch, J., M. J. Glennie, et al. (2003). "Anti-CD40 monoclonal antibody therapy in combination with irradiation results in a CD8 T-cell-dependent immunity to B-cell lymphoma." Blood **102**(4): 1449-57.

Horning, S., Younes, A., Lucas, J., Podoloff, D., Jain, V., (2002). "Rituximab Treatment Failures: Tositumomab and Iodine I 131 Tositumomab [Bexxar®]

Can Produce Meaningful Durable Responses." Blood **100**(11 part1): Abstract 1385.

Horning, S. J. (2003). "Future directions in radioimmunotherapy for B-cell lymphoma." Semin Oncol **30**(6 Suppl 17): 29-34.

Huber, R., C. Seidl, et al. (2003). "Locoregional alpha-radioimmunotherapy of intraperitoneal tumor cell dissemination using a tumor-specific monoclonal antibody." Clin Cancer Res **9**(10 Pt 2): 3922S-8S.

Hui, T. E., D. R. Fisher, et al. (1992). "Localized beta dosimetry of <sup>131</sup>I-labeled antibodies in follicular lymphoma." Med Phys **19**(1): 97-104.

Illidge, T., Bayne MC, Zivanovic M, Du Y, Lewington V, Johnson PW (2004). "Phase I/II study of fractionated radioimmunotherapy in relapsed low grade non-Hodgkin's lymphoma." Blood **104**(11): #131.

Illidge, T., J. Honeychurch, et al. (2000). "A new in vivo and in vitro B cell lymphoma model, pi-BCL1." Cancer Biother Radiopharm **15**(6): 571-80.

Illidge, T., J. Honeychurch, et al. (2000). "Radioimmunotherapy in the pi-BCL1 B cell lymphoma model: efficacy depends on more than targeted irradiation alone." Cancer Biother Radiopharm **15**(6): 581-91.

Illidge, T. M. (1998). "Radiation-induced apoptosis." Clin Oncol (R Coll Radiol) **10**(1): 3-13.

Illidge, T. M. and M. C. Bayne (2001). "Antibody therapy of lymphoma." Expert Opin Pharmacother **2**(6): 953-61.

Illidge, T. M., M. S. Cragg, et al. (1999). "The importance of antibody-specificity in determining successful radioimmunotherapy of B-cell lymphoma." Blood **94**(1): 233-43.

Illidge, T. M. and P. W. Johnson (2000). "The emerging role of radioimmunotherapy in haematological malignancies." Br J Haematol **108**(4): 679-88.

Janssen, M. L., W. Pels, et al. (2003). "Intraperitoneal radioimmunotherapy in an ovarian carcinoma mouse model: Effect of the radionuclide." Int J Gynecol Cancer **13**(5): 607-13.

Jhanwar, Y. S. and C. Divgi (2005). "Current status of therapy of solid tumors." J Nucl Med **46** Suppl 1: 141S-50S.

Jurcic, J. G., S. M. Larson, et al. (2002). "Targeted alpha particle immunotherapy for myeloid leukemia." Blood **100**(4): 1233-9.

Juveid, M. E., E. Stadtmauer, et al. (1999). "Pharmacokinetics, dosimetry, and initial therapeutic results with  $^{131}\text{I}$ - and  $(^{111}\text{In})/^{90}\text{Y}$ -labeled humanized LL2 anti-CD22 monoclonal antibody in patients with relapsed, refractory non-Hodgkin's lymphoma." Clin Cancer Res **5**(10 Suppl): 3292s-3303s.

Kaminski, M., Zelenetz, A., Leonard, J., Saleh, M., Jain, V., (2002). "Bexxar® Radioimmunotherapy Produces a Substantial Number of Durable Complete Responses in Patients with Multiply Relapsed or Refractory Low Grade or Transformed Low Grade Non-Hodgkin's Lymphoma." Blood **100**(11 part1): Abstract1382.

Kaminski, M. S., L. M. Fig, et al. (1992). "Imaging, dosimetry, and radioimmunotherapy with iodine 131-labeled anti-CD37 antibody in B-cell lymphoma." J Clin Oncol **10**(11): 1696-711.

Kaminski, M. S., K. Kitamura, et al. (1986). "Importance of antibody isotype in monoclonal anti-idiotype therapy of a murine B cell lymphoma. A study of hybridoma class switch variants." J Immunol **136**(3): 1123-30.

Kaminski, M. S., M. Tuck, et al. (2005). "131I-tositumomab therapy as initial treatment for follicular lymphoma." N Engl J Med **352**(5): 441-9.

Kaminski, M. S., Tuck, M., Regan, D., Kison, P., Wahl, R., (2002). "High Response Rates and Durable Remissions in Patients with Previously Untreated, Advanced-Stage, Follicular Lymphoma Treated with Tositumomab and Iodine I-131 Tositumomab (Bexxar®)." Blood **100**(11 part1): Abstract1381.

Kaminski, M. S., K. R. Zasadny, et al. (1996). "Iodine-131-anti-B1 radioimmunotherapy for B-cell lymphoma." J Clin Oncol **14**(7): 1974-81.

Kaminski, M. S., K. R. Zasadny, et al. (1993). "Radioimmunotherapy of B-cell lymphoma with  $[^{131}\text{I}]$ anti-B1 (anti-CD20) antibody." N Engl J Med **329**(7): 459-65.

Kaminski, M. S., A. D. Zelenetz, et al. (2001). "Pivotal study of iodine I 131 tositumomab for chemotherapy-refractory low-grade or transformed low-grade B-cell non-Hodgkin's lymphomas." J Clin Oncol **19**(19): 3918-28.

Kassis, A. I. and S. J. Adelstein (2005). "Radiobiologic principles in radionuclide therapy." J Nucl Med **46** Suppl 1: 4S-12S.

Khazaeli, M. B., R. M. Conry, et al. (1994). "Human immune response to monoclonal antibodies." J Immunother **15**(1): 42-52.

Kinuya, S., X. F. Li, et al. (2003). "Intraperitoneal radioimmunotherapy in treating peritoneal carcinomatosis of colon cancer in mice compared with systemic radioimmunotherapy." *Cancer Sci* **94**(7): 650-4.

Kinuya, S., K. Yokoyama, et al. (2000). "Optimal timing of administration of hyperthermia in combined radioimmunotherapy." *Cancer Biother Radiopharm* **15**(4): 373-9.

Kinuya, S., K. Yokoyama, et al. (2000). "Enhanced efficacy of radioimmunotherapy combined with systemic chemotherapy and local hyperthermia in xenograft model." *Jpn J Cancer Res* **91**(5): 573-8.

Kinuya, S., K. Yokoyama, et al. (1998). "Persistent distension and enhanced diffusive extravasation of tumor vessels improved uniform tumor targeting of radioimmunoconjugate in mice administered with angiotensin II and kininase inhibitor." *Oncol Res* **10**(11-12): 551-9.

Knox, S. J. (1995). "Overview of studies on experimental radioimmunotherapy." *Cancer Res* **55**(23 Suppl): 5832s-5836s.

Knox, S. J., R. Levy, et al. (1990). "Determinants of the antitumor effect of radiolabeled monoclonal antibodies." *Cancer Res* **50**(16): 4935-40.

Knox, S. J. and R. F. Meredith (2000). "Clinical radioimmunotherapy." *Semin Radiat Oncol* **10**(2): 73-93.

Kohler, G. and C. Milstein (1975). "Continuous cultures of fused cells secreting antibody of predefined specificity." *Nature* **256**(5517): 495-7.

Koral, K. F., Y. Dewaraja, et al. (2003). "Update on hybrid conjugate-view SPECT tumor dosimetry and response in 131I-tositumomab therapy of previously untreated lymphoma patients." *J Nucl Med* **44**(3): 457-64.

Koral, K. F., M. S. Kaminski, et al. (2003). "Correlation of tumor radiation-absorbed dose with response is easier to find in previously untreated patients." *J Nucl Med* **44**(9): 1541-3; author reply 1543.

Kotzin, B. L. and S. Strober (1980). "Role of the spleen in the growth of a murine B cell leukemia." *Science* **208**(4439): 59-61.

Kraeber-Bodere, F., C. Sai-Maurel, et al. (2002). "Enhanced antitumor activity of combined pretargeted radioimmunotherapy and paclitaxel in medullary thyroid cancer xenograft." *Mol Cancer Ther* **1**(4): 267-74.

Krop, I., A. R. de Fougerolles, et al. (1996). "Self-renewal of B-1 lymphocytes is dependent on CD19." *Eur J Immunol* **26**(1): 238-42.

Kurosaki, T., S. A. Johnson, et al. (1995). "Role of the Syk autophosphorylation site and SH2 domains in B cell antigen receptor signaling." J Exp Med **182**(6): 1815-23.

L. I. Gordon, T. E. W., J. L. Murray, (2003). "Yttrium-90 ibritumomab tiuxetan radioimmunotherapy produces high response rates and durable remissions in patients with relapsed or refractory low grade, follicular or transformed B-cell NHL: Final results of a randomized controlled trial." Proc of the Am Soc Clin Onc: 2315a.

Langmuir, V. K., R. W. Atcher, et al. (1990). "Iodine-125-NRLU-10 kinetic studies and bismuth-212-NRLU-10 toxicity in LS174T multicell spheroids." J Nucl Med **31**(9): 1527-33.

Langmuir, V. K., H. L. Mendonca, et al. (1992). "Comparisons of the efficacy of 186Re- and 131I-labeled antibody in multicell spheroids." Int J Radiat Oncol Biol Phys **24**(1): 127-32.

Langmuir, V. K., H. L. Mendonca, et al. (1992). "Comparisons between two monoclonal antibodies that bind to the same antigen but have differing affinities: uptake kinetics and 125I-antibody therapy efficacy in multicell spheroids." Cancer Res **52**(17): 4728-34.

Le Doussal, J. M., J. Barbet, et al. (1992). "Bispecific-antibody-mediated targeting of radiolabeled bivalent haptens: theoretical, experimental and clinical results." Int J Cancer Suppl **7**: 58-62.

Lee, D. S. and B. W. Griffiths (1984). "Comparative studies of Iodo-bead and chloramine-T methods for the radioiodination of human alpha-fetoprotein." J Immunol Methods **74**(1): 181-9.

Ling, C. C., I. J. Spiro, et al. (1984). "Dose-rate effect between 1 and 10 Gy/min in mammalian cell culture." Br J Radiol **57**(680): 723-8.

Liu, S. Y., J. F. Eary, et al. (1998). "Follow-up of relapsed B-cell lymphoma patients treated with iodine-131-labeled anti-CD20 antibody and autologous stem-cell rescue." J Clin Oncol **16**(10): 3270-8.

Loevinger (1988). MIRD Primer for Absorbed Dose Calculations. New York, The Society of Nuclear Medicine Inc.

Loevinger, R. (1988). MIRD primer for absorbed dose calculation. New York, The Society of Nuclear Medicine, Inc.

Longo, D. L., P. L. Duffey, et al. (2000). "Combination chemotherapy followed by an immunotoxin (anti-B4-blocked ricin) in patients with indolent lymphoma: results of a phase II study." Cancer J **6**(3): 146-50.

Looney, R. J., J. H. Anolik, et al. (2004). "B cell depletion as a novel treatment for systemic lupus erythematosus: a phase I/II dose-escalation trial of rituximab." Arthritis Rheum **50**(8): 2580-9.

Ma, D., M. R. McDevitt, et al. (2002). "Radioimmunotherapy for model B cell malignancies using 90Y-labeled anti-CD19 and anti-CD20 monoclonal antibodies." Leukemia **16**(1): 60-6.

Maloney, D. G. (2005). "Concepts in radiotherapy and immunotherapy: anti-CD20 mechanisms of action and targets." Semin Oncol **32**(1 Suppl 1): S19-26.

Marches, R., E. Racila, et al. (1995). "Tumour dormancy and cell signalling--III: Role of hypercrosslinking of IgM and CD40 on the induction of cell cycle arrest and apoptosis in B lymphoma cells." Ther Immunol **2**(3): 125-36.

Marcus, R. (2005). "Use of 90Y-ibritumomab tiuxetan in non-Hodgkin's lymphoma." Semin Oncol **32**(1 Suppl 1): S36-43.

Marcus, R., K. Imrie, et al. (2005). "CVP chemotherapy plus Rituximab compared with CVP as first-line treatment for advanced follicular lymphoma." Blood **105**(4): 1417-23.

Mather, S. J. and B. G. Ward (1987). "High efficiency iodination of monoclonal antibodies for radiotherapy." J Nucl Med **28**(6): 1034-6.

Matthews, D. C., F. R. Appelbaum, et al. (1999). "Phase I study of (131)I-anti-CD45 antibody plus cyclophosphamide and total body irradiation for advanced acute leukemia and myelodysplastic syndrome." Blood **94**(4): 1237-47.

Matthews, D. C., F. R. Appelbaum, et al. (1997). "The use of radiolabeled antibodies in bone marrow transplantation for hematologic malignancies." Cancer Treat Res **77**: 121-39.

McDevitt, M. R., G. Sgouros, et al. (1998). "Radioimmunotherapy with alpha-emitting nuclides." Eur J Nucl Med **25**(9): 1341-51.

McLaughlin, P. (2001). "Rituximab: perspective on single agent experience, and future directions in combination trials." Crit Rev Oncol Hematol **40**(1): 3-16.

Meeker, T. C., J. Lowder, et al. (1985). "A clinical trial of anti-idiotype therapy for B cell malignancy." Blood **65**(6): 1349-63.

Michel, R. B., A. V. Rosario, et al. (2003). "Experimental therapy of disseminated B-Cell lymphoma xenografts with 213Bi-labeled anti-CD74." Nucl Med Biol **30**(7): 715-23.

Milenic, D. E. (2000). "Radioimmunotherapy: designer molecules to potentiate effective therapy." Semin Radiat Oncol **10**(2): 139-55.

Miller, R. A., D. G. Maloney, et al. (1982). "Treatment of B-cell lymphoma with monoclonal anti-idiotype antibody." N Engl J Med **306**(9): 517-22.

Nemecek, E. R., D. K. Hamlin, et al. (2005). "Biodistribution of yttrium-90-labeled anti-CD45 antibody in a nonhuman primate model." Clin Cancer Res **11**(2 Pt 1): 787-94.

Nemecek, E. R. and D. C. Matthews (2003). "Use of radiolabeled antibodies in the treatment of childhood acute leukemia." Pediatr Transplant **7 Suppl 3**: 89-94.

Ng, B., E. Kramer, et al. (2001). "Radiosensitization of tumor-targeted radioimmunotherapy with prolonged topotecan infusion in human breast cancer xenografts." Cancer Res **61**(7): 2996-3001.

Niilo, H. and E. A. Clark (2002). "Regulation of B-cell fate by antigen-receptor signals." Nat Rev Immunol **2**(12): 945-56.

O'Connor O, A. (2005). "Developing new drugs for the treatment of lymphoma." Eur J Haematol **75 Suppl 66**: 150-8.

Oh, P., Y. Li, et al. (2004). "Subtractive proteomic mapping of the endothelial surface in lung and solid tumours for tissue-specific therapy." Nature **429**(6992): 629-35.

Paganelli, G., Chinol, M, Stoldt, H. S., Aftab, F, Geraghty, J and Siccardi, A. G. (1998). Radioimmunological therapy. Clinical Nuclear Medicine. M. N. Maisey, Britton, K. E. and Collier, B. D., Chapman & Hall Medical: 39-52.

Pagel, J. M., N. Hedin, et al. (2003). "Comparison of anti-CD20 and anti-CD45 antibodies for conventional and pretargeted radioimmunotherapy of B-cell lymphomas." Blood **101**(6): 2340-8.

Pandit-Taskar, N., P. A. Hamlin, et al. (2003). "New strategies in radioimmunotherapy for lymphoma." Curr Oncol Rep **5**(5): 364-71.

Parker, B. A., A. B. Vassos, et al. (1990). "Radioimmunotherapy of human B-cell lymphoma with 90Y-conjugated antiidiotype monoclonal antibody." Cancer Res **50**(3 Suppl): 1022s-1028s.

Pedley, R. B., S. A. Hill, et al. (2001). "Eradication of colorectal xenografts by combined radioimmunotherapy and combretastatin a-4 3-O-phosphate." Cancer Res **61**(12): 4716-22.

Peto, R. (1974). "Editorial: Guidelines on the analysis of tumour rates and death rates in experimental animals." Br J Cancer **29**(2): 101-5.

Petrie, I. A., A. A. Flynn, et al. (2002). "Spatial accuracy of 3D reconstructed radioluminographs of serial tissue sections and resultant absorbed dose estimates." Phys Med Biol **47**(20): 3651-61.

Pfreundschuh, M., L. Trumper, et al. (2004). "Two-weekly or 3-weekly CHOP chemotherapy with or without etoposide for the treatment of elderly patients with aggressive lymphomas: results of the NHL-B2 trial of the DSHNHL." Blood **104**(3): 634-41.

Pfreundschuh, M., L. Trumper, et al. (2004). "Two-weekly or 3-weekly CHOP chemotherapy with or without etoposide for the treatment of young patients with good-prognosis (normal LDH) aggressive lymphomas: results of the NHL-B1 trial of the DSHNHL." Blood **104**(3): 626-33.

Piro, L. D., C. A. White, et al. (1999). "Extended Rituximab (anti-CD20 monoclonal antibody) therapy for relapsed or refractory low-grade or follicular non-Hodgkin's lymphoma." Ann Oncol **10**(6): 655-61.

Postema, E. J. (2004). "Dosimetry and radioimmunotherapy of non-Hodgkin's lymphoma." J Nucl Med **45**(12): 2126-7; author reply 2127.

Press, O. W. (2003). "Radioimmunotherapy for non-Hodgkin's lymphomas: a historical perspective." Semin Oncol **30**(2 Suppl 4): 10-21.

Press, O. W., F. R. Appelbaum, et al. (1995). "Radiolabeled antibody therapy of lymphomas." Important Adv Oncol: 157-71.

Press, O. W., M. Corcoran, et al. (2001). "A comparative evaluation of conventional and pretargeted radioimmunotherapy of CD20-expressing lymphoma xenografts." Blood **98**(8): 2535-43.

Press, O. W., J. F. Eary, et al. (1993). "Radiolabeled-antibody therapy of B-cell lymphoma with autologous bone marrow support." N Engl J Med **329**(17): 1219-24.

Press, O. W., J. F. Eary, et al. (1995). "Phase II trial of 131I-B1 (anti-CD20) antibody therapy with autologous stem cell transplantation for relapsed B cell lymphomas." Lancet **346**(8971): 336-40.

Press, O. W., A. G. Farr, et al. (1989). "Endocytosis and degradation of monoclonal antibodies targeting human B-cell malignancies." Cancer Res **49**(17): 4906-12.

Press, O. W., J. P. Leonard, et al. (2001). "Immunotherapy of Non-Hodgkin's lymphomas." Hematology (Am Soc Hematol Educ Program): 221-40.

Press, O. W. and J. Rasey (2000). "Principles of radioimmunotherapy for hematologists and oncologists." Semin Oncol **27**(6 Suppl 12): 62-73.

Press, O. W., D. Shan, et al. (1996). "Comparative metabolism and retention of iodine-125, yttrium-90, and indium-111 radioimmunoconjugates by cancer cells." Cancer Res **56**(9): 2123-9.

Ruffner, K. L. and D. C. Matthews (2000). "Current uses of monoclonal antibodies in the treatment of acute leukemia." Semin Oncol **27**(5): 531-9.

Safavy, A., D. J. Buchsbaum, et al. (1993). "Synthesis of N-[tris[2-[[N-(benzyloxy)amino]carbonyl]ethyl]methyl]succinamic acid, trisuccin. Hydroxamic acid derivatives as a new class of bifunctional chelating agents." Bioconjug Chem **4**(3): 194-8.

Saga, T., H. Sakahara, et al. (2001). "Enhancement of the therapeutic outcome of radioimmunotherapy by combination with whole-body mild hyperthermia." Eur J Cancer **37**(11): 1429-34.

Saga, T., H. Sakahara, et al. (1999). "Radioimmunotherapy for liver micrometastases in mice: pharmacokinetics, dose estimation, and long-term effect." Jpn J Cancer Res **90**(3): 342-8.

Saga, T., J. N. Weinstein, et al. (1994). "Two-step targeting of experimental lung metastases with biotinylated antibody and radiolabeled streptavidin." Cancer Res **54**(8): 2160-5.

Salako, Q. A., R. T. O'Donnell, et al. (1998). "Effects of radiolysis on yttrium-90-labeled Lym-1 antibody preparations." J Nucl Med **39**(4): 667-70.

Sato, N., T. Saga, et al. (1999). "Intratumoral distribution of radiolabeled antibody and radioimmunotherapy in experimental liver metastases model of nude mouse." J Nucl Med **40**(4): 685-92.

Schaffland, A. O., F. Buchegger, et al. (2004). "131I-rituximab: relationship between immunoreactivity and specific activity." J Nucl Med **45**(10): 1784-90.

Schlom, J., K. Siler, et al. (1991). "Monoclonal antibody-based therapy of a human tumor xenograft with a 177lutetium-labeled immunoconjugate." Cancer Res **51**(11): 2889-96.

Sgouros, G., S. Squeri, et al. (2003). "Patient-Specific, 3-Dimensional Dosimetry in Non-Hodgkin's Lymphoma Patients Treated with  $^{131}\text{I}$ -anti-B1 Antibody: Assessment of Tumor Dose-Response." J Nucl Med **44**(2): 260-268.

Shan, D., J. A. Ledbetter, et al. (1998). "Apoptosis of malignant human B cells by ligation of CD20 with monoclonal antibodies." Blood **91**(5): 1644-52.

Shan, D., J. A. Ledbetter, et al. (2000). "Signaling events involved in anti-CD20-induced apoptosis of malignant human B cells." Cancer Immunol Immunother **48**(12): 673-83.

Shan, D. and O. W. Press (1995). "Constitutive endocytosis and degradation of CD22 by human B cells." J Immunol **154**(9): 4466-75.

Shani, J., W. Wolf, et al. (1986). "Labeling and comparative biodistribution of the monoclonal antibody KS1/4 in nude mice bearing human lung adenocarcinoma." Int J Rad Appl Instrum B **13**(4): 379-82.

Sharkey, R. M., T. M. Behr, et al. (1997). "Advantage of residualizing radiolabels for an internalizing antibody against the B-cell lymphoma antigen, CD22." Cancer Immunol Immunother **44**(3): 179-88.

Sharkey, R. M., R. D. Blumenthal, et al. (1990). "Biological considerations for radioimmunotherapy." Cancer Res **50**(3 Suppl): 964s-969s.

Sharkey, R. M., A. Brenner, et al. (2003). "Radioimmunotherapy of non-Hodgkin's lymphoma with  $^{90}\text{Y}$ -DOTA humanized anti-CD22 IgG ( $^{90}\text{Y}$ -Epratuzumab): do tumor targeting and dosimetry predict therapeutic response?" J Nucl Med **44**(12): 2000-18.

Sharkey, R. M. and D. M. Goldenberg (2005). "Perspectives on cancer therapy with radiolabeled monoclonal antibodies." J Nucl Med **46 Suppl 1**: 115S-27S.

Sharkey, R. M., H. Karacay, et al. (2005). "Improved therapy of non-Hodgkin's lymphoma xenografts using radionuclides pretargeted with a new anti-CD20 bispecific antibody." Leukemia.

Sharkey, R. M., H. Karacay, et al. (2003). "Optimizing bispecific antibody pretargeting for use in radioimmunotherapy." Clin Cancer Res **9**(10 Pt 2): 3897S-913S.

Sharkey, R. M., W. J. McBride, et al. (2003). "A universal pretargeting system for cancer detection and therapy using bispecific antibody." Cancer Res **63**(2): 354-63.

Slavin, S. and S. Strober (1978). "Spontaneous murine B-cell leukaemia." Nature **272**(5654): 624-6.

Smith-Jones, P. M., S. Vallabhajosula, et al. (2003). "Radiolabeled monoclonal antibodies specific to the extracellular domain of prostate-specific membrane antigen: preclinical studies in nude mice bearing LNCaP human prostate tumor." J Nucl Med **44**(4): 610-7.

Steffens, M. G., O. C. Boerman, et al. (1999). "Intratumoral distribution of two consecutive injections of chimeric antibody G250 in primary renal cell carcinoma: implications for fractionated dose radioimmunotherapy." Cancer Res **59**(7): 1615-9.

Stein, R., S. Chen, et al. (1997). "Advantage of yttrium-90-labeled over iodine-131-labeled monoclonal antibodies in the treatment of a human lung carcinoma xenograft." Cancer **80**(12 Suppl): 2636-41.

Surfus, J. E., J. A. Hank, et al. (1996). "Anti-renal-cell carcinoma chimeric antibody G250 facilitates antibody-dependent cellular cytotoxicity with in vitro and in vivo interleukin-2-activated effectors." J Immunother Emphasis Tumor Immunol **19**(3): 184-91.

Teeling, J. L., R. R. French, et al. (2004). "Characterization of new human CD20 monoclonal antibodies with potent cytolytic activity against non-Hodgkin lymphomas." Blood **104**(6): 1793-800.

Thieblemont, C. and B. Coiffier (2002). "Combination of chemotherapy and monoclonal antibodies for the treatment of lymphoma." Int J Hematol **76**(5): 394-400.

Thomas, G. D., M. J. Chappell, et al. (1989). "Effect of dose, molecular size, affinity, and protein binding on tumor uptake of antibody or ligand: a biomathematical model." Cancer Res **49**(12): 3290-6.

Torres, R. M., C. L. Law, et al. (1992). "Identification and characterization of the murine homologue of CD22, a B lymphocyte-restricted adhesion molecule." J Immunol **149**(8): 2641-9.

Tutt, A. L., R. R. French, et al. (1998). "Monoclonal antibody therapy of B cell lymphoma: signaling activity on tumor cells appears more important than recruitment of effectors." J Immunol **161**(6): 3176-85.

van der Jagt, R. H., C. C. Badger, et al. (1992). "Localization of radiolabeled antimyeloid antibodies in a human acute leukemia xenograft tumor model." Cancer Res **52**(1): 89-94.

Vervoordeldonk, S. F., P. A. Merle, et al. (1994). "Preclinical studies with radiolabeled monoclonal antibodies for treatment of patients with B-cell malignancies." Cancer **73**(3 Suppl): 1006-11.

von Schilling, C. (2002). "Is high-dose radioimmunotherapy needed in non-Hodgkin's lymphoma? Against." Eur J Nucl Med Mol Imaging **29**(9): 1254-6.

Vriesendorp, H. M., S. M. Quadri, et al. (1992). "Selection of reagents for human radioimmunotherapy." Int J Radiat Oncol Biol Phys **22**(1): 37-45.

Vuist, W. M., R. Levy, et al. (1994). "Lymphoma regression induced by monoclonal anti-idiotypic antibodies correlates with their ability to induce Ig signal transduction and is not prevented by tumor expression of high levels of bcl-2 protein." Blood **83**(4): 899-906.

Wagner, H. N., Jr., G. A. Wiseman, et al. (2002). "Administration guidelines for radioimmunotherapy of non-Hodgkin's lymphoma with (90)Y-labeled anti-CD20 monoclonal antibody." J Nucl Med **43**(2): 267-72.

Wahl, R. L. (1994). "Experimental radioimmunotherapy. A brief overview." Cancer **73**(3 Suppl): 989-92.

Wahl, R. L. (1998). Lymphoma. Clinical Nuclear Medicine. K. E. B. a. B. D. C. M. N. Maisey, Chapman & Hall Medical: 53 - 63.

Wahl, R. L. (2003). "The clinical importance of dosimetry in radioimmunotherapy with tositumomab and iodine I 131 tositumomab." Semin Oncol **30**(2 Suppl 4): 31-8.

Wahl, R. L. (2005). "Tositumomab and (131)I therapy in non-Hodgkin's lymphoma." J Nucl Med **46** Suppl 1: 128S-40S.

Weide, R., J. Heymanns, et al. (2003). "Successful long-term treatment of systemic lupus erythematosus with rituximab maintenance therapy." Lupus **12**(10): 779-82.

Weir, H. K., M. J. Thun, et al. (2003). "Annual report to the nation on the status of cancer, 1975-2000, featuring the uses of surveillance data for cancer prevention and control." J Natl Cancer Inst **95**(17): 1276-99.

White, C. A., S. E. Halpern, et al. (1996). "Radioimmunotherapy of relapsed B-cell lymphoma with yttrium 90 anti-idiotype monoclonal antibodies." Blood **87**(9): 3640-9.

Wilder, R. B., G. L. DeNardo, et al. (1996). "Radioimmunotherapy: recent results and future directions." J Clin Oncol **14**(4): 1383-400.

Wingo, P. A., L. A. Ries, et al. (1998). "Cancer incidence and mortality, 1973-1995: a report card for the U.S." Cancer **82**(6): 1197-207.

Wingo, P. A., T. Tong, et al. (1995). "Cancer statistics, 1995." CA Cancer J Clin **45**(1): 8-30.

Winter, G. and C. Milstein (1991). "Man-made antibodies." Nature **349**(6307): 293-9.

Wiseman, G. A., E. Kormmehl, et al. (2003). "Radiation dosimetry results and safety correlations from 90Y-ibritumomab tiuxetan radioimmunotherapy for relapsed or refractory non-Hodgkin's lymphoma: combined data from 4 clinical trials." J Nucl Med **44**(3): 465-74.

Wiseman, G. A., B. Leigh, et al. (2002). "Radiation dosimetry results for Zevalin radioimmunotherapy of rituximab-refractory non-Hodgkin lymphoma." Cancer **94**(4 Suppl): 1349-57.

Witzig, T. E., L. I. Gordon, et al. (2002). "Randomized controlled trial of yttrium-90-labeled ibritumomab tiuxetan radioimmunotherapy versus rituximab immunotherapy for patients with relapsed or refractory low-grade, follicular, or transformed B-cell non-Hodgkin's lymphoma." J Clin Oncol **20**(10): 2453-63.

Witzig, T. E., C. A. White, et al. (2003). "Safety of yttrium-90 ibritumomab tiuxetan radioimmunotherapy for relapsed low-grade, follicular, or transformed non-hodgkin's lymphoma." J Clin Oncol **21**(7): 1263-70.

Witzig, T. E., C. A. White, et al. (1999). "Phase I/II trial of IDEC-Y2B8 radioimmunotherapy for treatment of relapsed or refractory CD20(+) B-cell non-Hodgkin's lymphoma." J Clin Oncol **17**(12): 3793-803.

Woltanski, K. P., W. Besch, et al. (1990). "Radioiodination of peptide hormones and immunoglobulin preparations: comparison of the chloramine T and iodogen method." Exp Clin Endocrinol **95**(1): 39-46.

Yang, F. E., R. S. Brown, et al. (1992). "Quantitative autoradiographic evaluation of the influence of protein dose on monoclonal antibody distribution in human ovarian adenocarcinoma xenografts." Cancer Immunol Immunother **35**(6): 365-72.

Yao, Z., M. Zhang, et al. (2002). "Radioimmunotherapy of A431 xenografted mice with pretargeted B3 antibody-streptavidin and (90)Y-labeled 1,4,7,10-tetraazacyclododecane-N,N',N",N"-tetraacetic acid (DOTA)-biotin." Cancer Res **62**(20): 5755-60.

Yao, Z., M. Zhang, et al. (2004). "Pretargeted alpha emitting radioimmunotherapy using (213)Bi 1,4,7,10-tetraazacyclododecane-N,N',N",N"-tetraacetic acid-biotin." Clin Cancer Res **10**(9): 3137-46.

Yokota, T., D. E. Milenic, et al. (1992). "Rapid tumor penetration of a single-chain Fv and comparison with other immunoglobulin forms." Cancer Res **52**(12): 3402-8.

Zalutsky, M. R., M. A. Noska, et al. (1989). "Enhanced tumor localization and in vivo stability of a monoclonal antibody radioiodinated using N-succinimidyl 3-(tri-n-butylstanny)benzoate." Cancer Res **49**(20): 5543-9.

Zelenetz, A. D. (1999). "Radioimmunotherapy for lymphoma." Curr Opin Oncol **11**(5): 375-80.

Zelenetz, A. D. (2003). "A clinical and scientific overview of tositumomab and iodine I 131 tositumomab." Semin Oncol **30**(2 Suppl 4): 22-30.

Zhang, M., Z. Yao, et al. (2002). "Pretargeting radioimmunotherapy of a murine model of adult T-cell leukemia with the alpha-emitting radionuclide, bismuth 213." Blood **100**(1): 208-16.

Zhang, M., Z. Yao, et al. (1998). "Improved intratumoral penetration of radiolabeled streptavidin in intraperitoneal tumors pretargeted with biotinylated antibody." J Nucl Med **39**(1): 30-3.

Zhang, M., Z. Zhang, et al. (2003). "Pretarget radiotherapy with an anti-CD25 antibody-streptavidin fusion protein was effective in therapy of leukemia/lymphoma xenografts." Proc Natl Acad Sci U S A **100**(4): 1891-5.